Essays on Portfolio Allocation and Derivatives Pricing with Lévy Processes

Thesis

Submitted to the University of Warwick
for the degree of
Doctor of Philosophy

by
KUN ZHANG

supervised by
Dr. Xing Jin
Dr. Xue-Mei Li

5 May, 2014

To my wife and my family

Acknowledgment

A large number of people contributed directly and indirectly to the accomplishment of this thesis. Most of all, I want to thank my supervisor Dr. Xing Jin. He introduced me to the subject of my research work and gave me the opportunity that conducted to this thesis. His support and contagious enthusiasm was absolutely essential for me. I also thank Dr. Xue-Mei Li who not only supported me a lot academically but also gave warm care for my life in the UK.

I have to express my thankfulness to Dr. Hening Liu and Dr. Alexander Stremme. I thank these two gentlemen for the help, guidance and for being my thesis examiners. All the valuable suggestions and corrections, useful comments and instructive feedback greatly helped me to improve this thesis in various aspects. My heartfelt appreciation goes to Professor Michael Mol, as he literally and selflessly crossed the ocean to help me out.

My special thanks should be delivered to the whole Finance group at Warwick Business school for the insightful and detailed discussions that helped the accomplishment of my thesis. Especially, I would particularly like to thank Professor Andrea Gamba and

Professor Michael Moore.

Last but not least, I would like to thank my wife, Yan Wang, for her love, kindness and support she has shown during the past four years. I might be able to finalize this thesis without her, but she did make me a better man. Deepest thanks go to my children Yadong and Keyi who caused the delay of this thesis but brought me countless happiness and endless joy. I own special thanks to my friends who helped me at Warwick Business School and kept reminding me that there are other interesting things to do in the UK besides working. Particularly, I want to thank Nicki Pegg who has been easing my life during my hard working days at the business school. I take pleasure in thanking Warwick Business School that supported me both financially and academically.

Declarations

The work submitted in this thesis is the result of my own investigation, except where otherwise stated. It has not already been accepted for any degree at another university, and is also not being concurrently submitted for any other degree at another university.

Contents

List of Figures

List of Tables

Abstract

This thesis studies the use of Lévy processes for option pricing and portfolio allocation problem. First, a new Geometric Lévy model is proposed to capture the volatility smirk exhibited by index options. To solve the new model, an efficient numerical algorithm is adopted, which can be applied to any time-changed Lévy model. It is the first attempt to model multi-scale volatility along with the leverage effect, based on pure jump processes. Calibration results show that the proposed model exhibits excellent performance. Second, the dynamic portfolio choice problem in a jump-diffusion model is considered, where an investor may face constraints on her portfolio weights. With several examples, the impact of no-short-selling and/or no-borrowing constraints on the performance of optimal portfolio strategies is examined. Last, the portfolio allocation problem is reconsidered with a new multi-variate jump-diffusion model, while the effect of asymmetric correlation is taken into account Empirical results show that the new model fits asymmetric correlations well. By allowing investment constraints, the economic loss of ignoring asymmetric dependence is evaluated. An explanation for the under-diversification problem is provided, concerning the risk caused by asymmetric correlations.

Chapter 1

General Introduction

Lévy processes have been popular in the world of mathematics and statistics for a very long time, and are also playing an important role in many other fields of science, such as physics. However, the history of using Lévy processes in mathematical finance is not very long. Nowadays, the rapid development of financial engineering has encouraged both academic researchers and market participants to borrow ideas from probability theory and stochastic analysis. Lévy processes have been used to model financial returns for equities, equity options, credit derivatives and so on. The applications of Lévy processes for finance and financial engineering theory are still open and growing rapidly.

A Lévy process that is named after the French mathematician Paul Lévy, is a stochastic process with independent and stationary increments. A Lévy process might be understood as the continuous-time analog of a random walk. Although researchers focus on pure-jump processes while dealing with Lévy processes, the most well known example of Lévy

processes is Brownian motion. Brownian motion is the only process that has continuous paths. The sum of any two Lévy processes is still a Lévy process. Indeed, Lévy processes cover almost all the stochastic processes adopted for portfolio allocation problem and derivative pricing problem.

In reality, since large movements of financial return can be observed from both the international and domestic markets, diffusion models apparently fail to provide accurate estimation of financial returns. For instance, in the original setting of Merton's portfolio problem, no jump is considered. Research has continued to extend the original framework by allowing jumps, such as the compound Poisson jump. This is a simple case of Lévy processes. The history of using jumps for derivative pricing dates back to an even earlier time. Many Geometric Lévy models have been widely used for option pricing and credit derivatives pricing.

In this thesis, three topics associated with portfolio allocation problem and option pricing are discussed with the use of Lévy processes. The research work includes not only developing a new Geometric Lévy model but also using existing Lévy processes to solve some existing problems of finance and economics.

In chapter 2, a multi-dimensional stochastic volatility model is developed, using time-changed Lévy processes, in order to capture the implied volatility smirk exhibited by index options. Substantial empirical literature has suggested that the index dynamics should be free of diffusion components, which supports the important use of infinite-activity jumps in modelling. The proposed model is of pure jumps only, and provides a

non-Gaussian innovation. This new model admits stochastic volatility by randomizing the business time with a stochastic time-change. Due to the inexistence of explicit solution of European option prices, an efficient numerical algorithm known as the COS expansion is adopted. The numerical pricing framework can be applied to all time-changed Lévy models, and the computation time is comparable to that of the traditional Carr-Madan FFT method. It is the first attempt to model both long-run and short-run volatility components with pure jump processes. It is also the first Lévy model that is of the leverage effect. Calibration results based on real market data show that the proposed model exhibits excellent performance, compared with several benchmark models, such as the celebrated Heston model.

In chapter 3, the dynamic portfolio choice problem in a jump-diffusion model is considered, where an investor may face constraints on her portfolio weights: for instance, no-short-selling constraints. It is a daunting task to use standard numerical methods to solve a constrained portfolio choice problem, especially when there is a large number of state variables. By suitably embedding the constrained problem in an appropriate family of unconstrained ones, we provide some equivalent optimality conditions for the indirect value function and optimal portfolio weights. These results simplify and help to solve the constrained optimal portfolio choice problem in jump-diffusion models. Finally, we apply our theoretical results to several examples, to examine the impact of no-short-selling and/or no-borrowing constraints on the performance of optimal portfolio strategies.

In chapter 4, the portfolio allocation problem is reconsidered while the effect of asymmetric

correlation is taken into account. In recent years, asymmetric correlation has been widely reported and investigated in the literature, which is that correlations between asset returns are significantly bigger during a bearish time. Great efforts have been made to measure and explain this phenomenon. It is suggested that asymmetric dependence can reduce the economic value of portfolio diversification, and underestimating asymmetry might cause large biases in hedging practice. In this chapter, we develop a multi-dimensional jump-diffusion framework with stochastic volatility which can capture asymmetry, even given a large number of state variables. Based on several statistic measures for asymmetry, our framework outperforms benchmark models, such as regime-switching models and copula models, which are specially designed for capturing asymmetry. The asset allocation problem is solved in this framework, allowing investment constraints i.e. no-short-selling constraint. We quantify the economic loss for a suboptimal portfolio allocation if asymmetric dependence is ignored and provide an explanation for under diversification, which indicates how asymmetry affects investment decisions.

Chapter 5 concludes the thesis and discusses future research.

Chapter 2

Option pricing and calibration with time-changed Lévy processes

2.1 Introduction

Option pricing has been deeply investigated for more than forty years. Black and Scholes (1973) have laid the foundation of using Brownian motion in option pricing theory. This was the first time that market participants could convert their financial intuition into actual prices in a quantitative sense. As spurred on market observations, Merton (1976) brings the Compound Poisson jump into modelling, which provides more flexility for the distribution of innovation. However, the Black-Scholes model and its succeeding extended work only solve the pricing problem in a qualitative sense, and produce biases documented by an extensive empirical literature. Nevertheless, the continuous-time model has also

been criticised for its inflexibility, compared to discrete-time models which can easily be embedded with different distributions. Only normals or mixtures of normals keep the tractability for continuous-time models before the advent of Lévy models.

Stochastic volatility models boom the research on modelling derivatives, and these have mainly been inspired by the stylized feature known as volatility smile or smirk. Many models have been proposed, in order to enhance the performance of option pricing via trying to capture this feature. Heston (1993) develops a decent model that employs a CIR process to model the latent movement of volatility. It is a reliable model that can be used to price equity options, index options and even currency and commodity derivatives. It also admits the leverage effect, namely the fact that increasing stock prices are accompanied by declining volatility and vice versa, by adopting a negative correlation between stock return and its variance. The leverage effect is even more important when pricing index options. This is because the leverage effect can produce negative skewness in stock returns so as to generate the so-called volatility smirk.

Many literature has contributed to investigating the empirical performance of stochastic volatility models (See Bates (2000), Duffie et al. (2000) and Huang and Wu (2004)). Although it is suggested that stochastic volatility models can outperform the Black-Scholes model, these models are still short of pricing accuracy. It has been recently revealed that volatility has multi-scale components, that is the long-run and short-run components. Engle and Lee (1999) and Heston and Nandi (2000), meanwhile, explore the possibility of modelling volatility with a persistent long-run component and a volatile short-run com-

ponent. Christoffersen et al. (2009) extend the original Heston model with an additional mean-reverting variance dynamics, and use the extended Heston model to capture the index option smirk. It is shown that the shape of the smile is largely independent of the volatility level, and single-factor stochastic volatility models cannot capture this feature. Fouque et al. (2011) discuss the fast and slow time-scale of volatility, and provide an informative review of developing multi-scale stochastic volatility models. The multi-scale stochastic volatility models can fit the market well; however, due to the complexity and redundant size of parameter space, it has not been welcomed either by market participants or academic researchers.

Jump is another aspect that plays an important role when trying to explain some stylized market features. For example, only the existence of jumps can explain why the skew is so steep for short term derivatives. Looking back on all the financial crises that we have experienced, it is hard to resist the idea of introducing jumps into modelling. Merton (1976) starts using jumps by introducing the Compound Poisson jump, in order to capture rare and large movements of return series. A more general choice is using a Lévy process. Lévy processes are related to Infinitely Divisible distribution, which can provide a variety of non-Gaussian distributions. Nowadays, Lévy processes have become a popular alternative to diffusion, especially in derivative pricing. Lévy processes have drawn even more attentions with the occurrence of the credit crunch that took place in 2007. Jump risk that represents the sudden loss in the market cannot be modelled by diffusion models. Imitating the Black-Scholes model, many Geometric Lévy models have

been proposed, such as the Variance Gamma (VG) model (see Madan et al. (1998)) and the CGMY model (see Carr et al. (2002)). Lévy models can only capture the volatility smile in the short term, so introducing stochastic volatility into Geometric Lévy models is in demand.

Carr et al. (2003) investigate how to use the stochastic time-change technique and show how to randomize the business time. Time-change stochastic models can exhibit stochastic volatility. The idea is intuitive. If the business time does not run with a constant intensity, the trading volumes will become non-constant as well. Stochastic volatility comes from stochastic trading activities. Nevertheless, an important feature is still missing for those time-changed models, that is the leverage effect. Unlike the Heston model, time-changed Lévy models cannot easily incorporate dependence between return and variance, due to discontinuity. This might be the main reason why existing time-change Lévy models cannot perform as well as the Heston model. Existing time-changed Lévy models are developed via using the pricing framework introducers in Carr et al. (2003); however it only allows independent time-change, otherwise no explicit solution can be obtained.

A combination of diffusions and jumps has been considered to improve the performance of the Heston model. The so-called SVJ models show good performance, which are stochastic volatility models with jumps in the spot price only. For example, the Heston model with jumps does enhance the pricing accuracy, despite the difficulty of hedging incurred. It is straightforward to apply the same idea to the volatility process. Apparently investors observe jumps in volatility market. However, Gatheral (2006) states that SVJ models can

outperform SVJJ models which allow jumps in both spot price and volatility. Empirical experiments show that SVJJ models are even worse than pure diffusion models. This is really a puzzle. A possible explanation is that SVJJ models exhibit less leverage effect than SVJ models. This sheds light on the importance of taking into account the leverage effect, which also interprets the main contribution of this chapter.

Carr and Wu (2004) develop a brilliant idea to overcome the drawback and embed the leverage effect into time-changed Lévy models. They use a complex measure change to disentangle the connection between the time-change and the spot price. The explicit form of the characteristic function of log prices can be obtained by solving some ODEs. A simple example is that the Heston model can be derived via randomizing the business time of the Black-Scholes model with a correlated CIR process. Nevertheless, the innovative framework is not quite practical. This is because it depends on whether we can solve some ODEs explicitly. And the answer is NO for most of the existing models. Carr and Wu (2004) argue that the method can be implemented by numerically solving ODEs; however, the numerical work is not affordable. The standard pricing procedure is using the Carr-Madan formula with the Fast Fourier Transform (FFT) method. At least 4096 sampling points are required to provide accurate prices. Hence, each option price requires solving 4096 ODEs simultaneously. It will require enormous computation to finish one round of searching for the calibration procedure.

Tractability is a crucial criteria when developing new models. Although the Monte Carlo simulation technique can be used to solve the pricing problem, it is too time-consuming.

Daily Calibration requires the pricing work be done within a very short time. Carr and Madan (1999) show how FFT can be used to speed up the calculation when pricing European derivatives. It has become a standard approach for solving affine models and Lévy models. After this, many numerical approaches have been introduced to solve European option prices, given explicit characteristic functions. Attari (2004) obtains an efficient formula and uses direct integration method to solve option prices. Chourdakis (2004) develops a fractional FFT algorithm to speed up the traditional FFT method and reduces the number of sampling points. Lord et al. (2008) reformulate the well-known risk-neutral valuation formula by using convolution, and achieve almost linear complexity based on the FFT method. Fang and Oosterlee (2008) use the COS expansion method to recover the characteristic function of log returns, and introduce a new pricing formula of European option. Haslip and Kaishev (2013) present an efficient and robust pricing method based on the B-spline interpolation, aiming to price European-style derivatives.

A comprehensive framework is developed in this chapter in which the COS expansion method is employed, combined with the Runge-Kutta scheme for solving ODEs. With this framework, European option prices can be obtained by numerically solving the characteristic functions of log returns. Experiments demonstrate that computation time is comparable to that of the Carr-Madan method. This framework allows to incorporate any kind of Lévy process time-changed by any Subordinator. Hence, for the purpose of option pricing, it is possible to investigate and compare the performance of complicated stochastic time-changed Lévy models.

Finding an appropriate Lévy process is a basic, but difficult work. Since Lévy processes provide us with a variety of choices concerning the innovation distribution, it is not clear which process should be used for modelling. Different Lévy models have very different behaviours. There is no universal process working under all circumstances. Carr and Wu (2003) state that S&P 500 index option prices exhibit a different pattern against other financial derivatives. For instance, we observe volatility smirk in index option markets rather than volatility smile. Volatility smirk is a market phenomenon that implied volatilities for in-the-money calls are much higher than those of out-of-the-money calls. This emerges after the US market Crash of 1987. In this chapter, we focus on pricing European index options and propose a model that is specifically designed to capture the movements of stock indices.

The contributions of this chapter can be understood in three aspects. First, it provides a numerical pricing framework to generate model prices in a very short time for any time-changed Lévy model. Indeed, it serves to extends Carr and Wu (2003)'s work and demonstrates that it is possible and practical to provide accurate option prices via the complex leverage-measure-change method. Second, it inspires researchers to investigate potential Lévy models by developing a new multi-scale stochastic volatility model equipped with the time-change technique. In particular, the leverage effect is incorporated in this new model as there is dependence imposed between the return and the variance. To the best of our knowledge, this is the first pure-jump stochastic volatility model that admits the leverage effect. Numerical results show that our model is capable of fitting the special pat-

tern of index options well. Finally, the effect of considering both long-run and short-run volatility components is discussed in this chapter. Based on numerical experiments, the benefit of decomposing the volatility is verified by comparing the performance between our model and six benchmark models.

The rest of this chapter is organized as follows. Section 2.2 describes the model proposed in this chapter and shows how to derive the characteristic function of log returns. Section 2.3 shows how to solve time-changed Lévy models numerically with the leverage-measure method introduced in Carr and Wu (2004). In section 2.4, the accuracy of option prices generated by the numerical pricing framework is shown and compared with the traditional FFT method. Daily calibration is implemented with real data of the S&P 500 index options. To show the performance of our model, a comparison with benchmark models is provided. Section 2.5 concludes this chapter and discusses future research.

2.2 A Geometric Stochastic Lévy Model

Lévy processes have been widely used to model financial returns. Lévy processes can generate a variety of distributions at a fixed time horizon. The underlying Lévy process used in this chapter is a special case of the α-processes, which has been introduced in Carr and Wu (2003). It is known as the Finite Moment Log Stable process (FMLS). In this chapter, we refer to it as the LS process. The LS process only admits negative jumps with a positive drift.

Considering a complete probability space $(\Omega, \mathcal{F}, \mathbb{P})$ endowed with a standard complete filtration $\{\mathcal{F}_t\}$ satisfying the usual conditions, a one-dimensional real-valued stochastic process $\{L_t\}_{t\geq 0}$ with $L_0 = 0$ is said to be a Lévy process if the following conditions are satisfied.

- $L_0 = 0$, a.s.
- $L_t - L_s \perp L_s$, for any $t > s$
- $L_t - L_s$ is equal in distribution to L_{t-s}, for any $t > s$

The above three conditions can be concluded as the property of "independent stationary increment". If one more condition that $L_{t-s} \sim N(0, t-s)$ is imposed, $\{L_t\}_{0\leq t\leq T}$ will be a Brownian motion. By the Lévy-Khintchine Theorem, if we define the characteristic function of L_t as

$$\Phi(u) = \mathbb{E}\left[e^{iuL_t}\right] = e^{-t\Psi(u)}, \qquad t \geq 0 \tag{2.1}$$

where $\Psi(u)$ is called the characteristic exponent, then $\Psi(u)$ has the form of

$$\Psi(u) = -iu\mu + \frac{1}{2}u^2\sigma^2 + \int_{\mathbb{R}\setminus\{0\}} (1 - e^{iux} + iux\mathbf{1}_{|x|<1})\pi(x)dx \tag{2.2}$$

with $\int_{\mathbb{R}\setminus\{0\}}(x^2 \wedge 1)\pi(x)dx < \infty$, where $\mu \in \mathbb{R}$ is the constant drift, $\sigma > 0$ is the volatility parameter, and $\pi(x)$ is the Lévy measure which describes the arrival rate of jumps with all sizes. The triplet (μ, σ, π) is known as the Lévy triplet, which can fully characterize the Lévy process.

Lévy processes are closely related to the Infinitely Divisible Distribution. For any arbitrary distribution with infinite divisibility, a unique Lévy process can be defined correspondingly. Hence, there are many available choices for modelling financial returns. Popular Lévy processes include the Poisson process, Variance Gamma process, NIG process and so on. The characteristic function defined in (2.1) usually has the support of $\mathbb{R}$, but it can also be extended to a complex domain.

Based on jump frequency, Lévy processes can be categorized into two types: jumps with finite activity and jumps with infinite activity. A pure jump Lévy process is said to be of finite activity if

$$\int_{\mathbb{R}\setminus\{0\}} \pi(x)dx = \lambda < \infty \tag{2.3}$$

where λ measures the mean arrival rate of jumps. A jump process that is of finite activity can only generate a finite number of jumps within any finite time interval. When λ in (2.3) is not finite, it is said to be of infinite activity. In any finite time interval, there are infinitely many jumps if the jump process is of infinite activity. Infinite activity jumps can capture frequent small movements, while finite activity jumps are suitable to model infrequent large movements. It is believed that the diffusion component may not be needed if an infinite activity jump process is employed.

Brownian motion and Compound Poisson jump are two popular cases of Lévy processes. In this section, we choose a special case of α-stable processes. A stochastic process $\{L_t, 0 \leq t \leq T\}$ is said to be an α-stable process if its characteristic function has the form

of

$$\Phi(u) = \exp\left(-iu\theta + |\sigma u|^{\alpha}\left(1 - i\beta sgn(u)\tan\frac{\pi\alpha}{2}\right)\right), \qquad u \in \mathbb{R} \tag{2.4}$$

where $\alpha \in (0,1) \cup (1,2]$, $\theta \in \mathbb{R}$, $\sigma > 0$ and $\beta \in [-1,1]$. The corresponding Lévy measure is absolutely continuous with respect to the Lebesgue measure, with density

$$\pi(dx) = \begin{cases} c^{+}x^{-\alpha-1} & \text{if} \quad x > 0 \\ \\ c^{-}(-x)^{-\alpha-1} & \text{if} \quad x < 0 \end{cases}$$

where c^{+} and c^{-} are two nonnegative real constants. The process L_t is symmetric if $c^{+} = c^{-}$. We can also derive $\beta = (c^{+} - c^{-})/(c^{+} - c^{-})$. L_t only has one-side jumps if either c^{-} or c^{+} is zero. In this chapter, we set $c^{-} = 0$ and the process only has negative jumps; this does not imply that it only generates negative returns. Indeed, when $c^{-} = 0$ the process has a positive drift with negative jumps. This process is the FMLS process mentioned in Carr and Wu (2003), where β is set to be -1.

Lévy processes can be used to model financial returns because of the property of "independent stationary increment". This coincides with the implication of the Efficient Market Hypothesis (see Fama (1970)). Constructing a Lévy model is easy and straightforward. Suppose that the log return follows a Log Stable (LS) process, the spot price is governed as

$$S_t = S_0 \exp\left((r - \xi)t + \sigma L_t\right), \qquad \alpha \in (1,2], \quad t \in [0,T] \tag{2.5}$$

where r is the constant risk-free rate, σ is the volatility parameter and ξ is the martingale correction. Actually, L_t can degenerate to Brownian motion by setting $\alpha = 2$, which

makes (2.5) equivalent to the Black-Scholes model. An arbitrary α-stable distribution of L_t does not guarantee stationary option prices, because only the case of $\beta = -1$ provides finite moments of all orders. A detailed discussion can be found in Carr and Wu (2003). The model presented in (2.5) is proposed in Carr and Wu (2003) and exhibits excellent performance on pricing index options, compared with the VG model and the Merton Jump-diffusion (MJD) model. However, it does not admit stochastic volatility.

The time-change technique can be applied to Lévy processes to generate stochastic volatility. The intuition is that we can randomize the clock on which the stochastic process is run. Hence, the number of transactions in a given time interval is also random. Since a high number of transactions causes high return volatility, time-changed Lévy processes can produce stochastic volatility. There are many choices for randomizing the business time, such as the Ornstein-Uhlenbeck process and the CIR process. Lévy subordinators are also good candidates.

Let $t \to T_t (t \geq 0)$ be an increasing càdlàg process satisfying the usual conditions; a new process can be generated by evaluating L at T:

$$Y_t = L_{T_t}, \qquad t \geq 0 \tag{2.6}$$

As proved by Monroe (1978), every semimartingale can be represented by a time-change Brownian motion. Hence, Y_t is a very general specification for financial modelling. The random time T_t must be a nondecreasing process, and can be represented by

$$T_t = \int_0^t v_{s-} ds \tag{2.7}$$

where v_t is the instantaneous activity rate. An important point is that we want to impose dependence between the return innovations in L_t and the activity rate v_t, which can generate the leverage effect. Heston (1993) demonstrates how to incorporate stochastic volatility while pricing options and bonds. The Heston model can also be represented as a time-changed Black-Scholes model with a CIR activity rate process. Since we have abandoned the diffusion component, there will be no dependence between L_t and v_t if v_t follows a pure-diffusion process. Similarly, if v_t is driven by another pure-jump process, L_t and v_t are still independent to each other.

The multi-scale effect of volatility is another aspect that can not be ignored. Generally speaking, the time-series of volatility exhibit different time scales. Usually, we can decompose the one-dimensional volatility into a long-run component and a short-run component. The long-run volatility is heavily correlated with return series while the short-run volatility is more likely to be volatile. Hence, we can employ a randomness to drive both the return and the long-run volatility, such that there exists dependence between the two. The short-run volatility will have an independent innovation. The new Geometric time-changed Lévy model is represented as

$$\begin{aligned}
S_t &= S_0 \exp\left(rt + L_{T_t}^{\alpha_1,-1} - \xi T_t\right) \\
T_t &= T_t^1 + T_t^2 = \int_0^t v_s^1 ds + \int_0^t v_s^2 ds \\
dv_t^1 &= \kappa_1(a_1 - v_t^1)dt + \beta_1^{1/\alpha_1} dL_{T_t^1}^{\alpha_1,1} \\
dv_t^2 &= \kappa_2(a_2 - v_t^2)dt + \beta_2^{1/\alpha_2} dL_{T_t^2}^{\alpha_2,1}
\end{aligned} \tag{2.8}$$

where r is the risk-free rate, and ξ is the martingale correction. T_t is the stochastic time

that has two independent activity rates v_t^1 and v_t^2. $L_t^{\alpha_1,1}$ is a mirror image of $L_t^{\alpha_1,-1}$, which means that a negative jump happening in S_t will bring a positive jump in v_t^1 at the same time. v_t^i seems to follow a non-Gaussian Ornstein-Uhlenbeck (OU) process with mean-reverting speed κ^i and volatility of volatility β_i; it is governed by a non-Gaussian "square-root" process as the activity process v_t^i is incorporated with time-change itself. We can rewrite v_t^i as

$$dv_t^i = \kappa_i(a_i - v_t^i)dt + (\beta v_t^i)^{1/\alpha_i} dL_t^{\alpha_i,1} \tag{2.9}$$

When $\alpha_i = 2$, (2.9) becomes a CIR process. As expected, the model (2.8) is of stochastic volatility and multi-scale volatility components. We will also investigate how the dependence between S_t and T_t can affect the pricing performance.

Carr and Wu (2004) have suggested the idea that can be seen as a simple version of model (2.8) that only has one activity process. The idea of introducing an additional activity process is simple but very powerful. The benefits of doing this are not only that variance has both long-run and short-run effects but also that the leverage effect is obtained. This comprehensive model shown in (2.8) is of infinite activity jumps, so it can capture both small-but-frequent and large-but-rare movements. The dependence structure between the return and the volatility is also stochastic, which results in stochastic correlations.

Unfortunately, there is no explicit solution to the characteristic function of log return for this new model. As T_t is not independent of L_t, it is impossible to use the iteration rule to work out the expectation $\mathbb{E}[\exp(iuL_{T_t})]$. Although many time-changed Lévy models have been introduced such as the VGSV model and the CGMYSV model (see Carr et al.

(2002)), none of these models admits the leverage effect. The reason why existing time-changed Lévy models do not admits the leverage effect is straightforward. This is because explicit solutions exists only when T_t is independent of L_t. Carr and Wu (2004) firstly solve this problem by introducing a Leverage-measure. The dependence of the time-changed process can be disentangled under the new measure. Deriving the characteristic function of log return is converted into how to solve the Laplace transform of the activity rate processes.

2.3 Combining the Leverage-measure with the COS expansion method

In this section, we present how to use the Leverage-measure method to solve the characteristic function of log return numerically.

2.3.1 Leverage-measure change

Solving the present model defined in (2.8) is extremely hard, especially due to the dependence between L_t and T_t. According to Theorem 1 in Carr and Wu (2004), under a probability measure $\mathbb{P}$ a time-changed Lévy process $Y_t = L_{T_t}$ has a representation of the characteristic function:

$$\phi_Y(u) = \mathbb{E}\left[e^{iuY_t}\right] = \mathbb{E}^Q\left[e^{-T_t\Psi(u)}\right] = L_{T_t}\left(\Psi(u)\right) \tag{2.10}$$

where $\mathbb{E}[\cdot]$ and $\mathbb{E}^{\mathbb{Q}}[\cdot]$ denote expectations under measures $\mathbb{P}$ and $\mathbb{Q}$, $\Psi(\cdot)$ is the characteristic exponent of L_t, and $L_{T_t}(\cdot)$ is the Laplace transform of T_t. The associated Radon−Nikodým derivative is

$$\left.\frac{d\mathbb{Q}}{d\mathbb{P}}\right|_t = M_t(u) = \exp\left(iuY_t + T_t\Psi(u)\right)$$

With (2.10), the characteristic function $\phi_Y(u)$ is the composition of the characteristic exponent $\Psi(\cdot)$ and the Laplace transform of T_t. In another word, the dependence has been disentangled. For Lévy process, $\Psi(\cdot)$ always has explicit solutions. Deriving the Laplace transform $L_{T_t}(\cdot)$ is a familiar course to researchers of fixed income derivatives. With the activity rate v_t, we have

$$L_{T_t}(u) = \mathbb{E}\left[\exp\left(-u\int_0^t v_s ds\right)\right] \tag{2.11}$$

which can be seen as the bond price if uv_s is regarded as the short rate. As $\Psi(\cdot)$ is known explicitly, the pricing problem relies on whether (2.11) can be solved explicitly.

According to Filipović (2001) and Carr and Wu (2004), for any Feller process v_t with the infinitesimal generator

$$\begin{aligned}\mathcal{A}f(x) =& \frac{1}{2}\sigma^2 x f''(x) + (a' - \kappa x)f'(x) + \\ & \int_{\mathbb{R}} (f(x+y) - f(x) - f'(x)(1\wedge y))(m(dy) + x\mu(dy)),\end{aligned} \tag{2.12}$$

the Laplace transform of the random time T_t is exponentially affine with respect to the initial rate v_0, namely

$$L_{T_t}(u) = \exp\left(-b(t)v_0 - c(t)\right) \tag{2.13}$$

where the functions $b(t)$ and $c(t)$ are the solutions to the following ordinary differential equations (ODEs):

$$\begin{aligned} b'(t) &= u - \kappa b(t) - \frac{1}{2}\sigma^2 b(t)^2 + \int_{\mathbb{R}\setminus 0} \left(1 - \exp(-yb(t)) - b(t)(1 \wedge y)\right) \mu(dy) \\ c'(t) &= ab(t) + \int_{\mathbb{R}} \left(1 - \exp(-yb(t))\right) m(dy) \end{aligned} \tag{2.14}$$

with the boundary conditions: $b(0) = 0$ and $c(0) = 0$.

To construct a geometric martingale under the risk-neutral measure, the underlying process X_t needs to satisfy

$$\mathbb{E}[\exp(X_t)] = 1 \qquad a.s.$$

For example, $X_t = \frac{t}{2} - W_t$. Suppose we have a Lévy process $(X_t)_{t\geq 0}$ which has the Lévy triplet (a, σ^2, π). According to Lévy-Khintchine representation, we know

$$\Phi(u) = \mathbb{E}[\exp(iuX_t)] = \exp\left(iuat - \frac{1}{2}\sigma^2 u^2 t + t\int_{\mathbb{R}\setminus\{0\}} \left(e^{iux} - 1 - iux\mathbf{1}_{|x|<1}\right) \pi(dx)\right)$$

where $\Phi(u)$ is the corresponding characteristic function of X_t. Based on $(X_t)_{t\geq 0}$, we want to construct a 'new' process $(L_t)_{t\geq 0}$ such that

$$\mathbb{E}[\exp(L_t)] = 1 \qquad a.s.$$

where $L_t = X_t - \xi t$. It is easy to derive $\xi = \frac{1}{t}\log\Phi(-i) = -\Psi(-i)$. Hence, L has the Lévy triplet of $(a + \Psi(-i), \sigma^2, \pi)$. We then can apply time-change to L_t.

For the present model defined in (2.8), the infinitesimal generator of v_t^i is

$$\mathcal{A}f(x) = (a - (\kappa + \delta)x)\, f'(x) + \beta x \int_{\mathbb{R}\setminus\{0\}} (f(x + y) - f(x) - f'(x)(1 \wedge y))\pi(dy) \tag{2.15}$$

with

$$b(t) = u - \kappa b(t) + \beta \int_{\mathbb{R}^+} (1 - \exp(-b(t)x))\mu(dx)$$

$$c(t) = ab(t) \tag{2.16}$$

where $\pi(dy) = c|y|^{-\alpha-1}dy$, $c = -\sec\frac{\pi\alpha}{2\Gamma(-\alpha)}$, and $\delta = \frac{c}{\alpha-1}$. Finally, the Laplace transform of T_t is

$$L_{T_t}(u) = \mathbb{E}[\exp(-uT_t)] = \mathbb{E}[\exp(-uT_t^1)\exp(-uT_t^2)] = L_{T_t^1}(u) * L_{T_t^2}(u) \tag{2.17}$$

Thus far, the pricing problem seems quite easy as far as we are able to solve (2.16). However, unless $\alpha = 2$ there is no explicit solution to (2.16). This turns out to be very tricky. Only diffusion models can be solved explicitly with the leverage-measure method, but it is not necessary to do so. While we need to solve (2.16) for an arbitrary Lévy process, $b(t)$ and $c(t)$ cannot be solved explicitly. For this reason, we need to try to find numerical solutions.

2.3.2 Solving ODEs: $b(t)$ and $c(t)$

Using numerical methods, we focus on solving $b(t)$ and $c(t)$. Note that $c(t)$ only relies on $b(t)$. $b(t)$ and $c(t)$ cannot be solved separately. Only first-order ODEs are considered here. Given

$$y'(t) = f(t, y), \qquad y(t_0) = y0,$$

the aim is to solve y(T), starting from t_0. The time interval is discretized as $[t_0 : h : T]$, where $h = \frac{T-t_0}{n}$ given the step number n. A common fourth-order Runge-Kutta method can be represented as:

$$y(n+1) = y(n) + \frac{h}{6}(k_1 + 3k_2 + 2k_3 + k_4) \tag{2.18}$$

where

$$\begin{aligned} k_1 &= f(t_n, y(n)) \\ k_2 &= f(t_n + \frac{1}{2}h, y(n) + \frac{h}{2}k_1) \\ k_3 &= f(t_n + \frac{1}{2}h, y(n) + \frac{h}{2}k_2) \\ k_4 &= f(t_n + h, y(n) + hk_1) \end{aligned}$$

and $t_{n+1} = t_n + h$. It is straightforward to solve $b(t)$ with (2.18). The fourth-order Runge-Kutta method is an efficient method for numerically solving non-stiff initial value problems. Solving $c(t)$ requires the whole information of $b(t)$, so the Simpson's 3/8 rule is adopted to compute the integral. Given

$$c'(t) = f(t), \qquad c(t_0) = c_0, \tag{2.19}$$

we solve it as:

$$\begin{aligned} c(t_1) &= c(t_0) + \frac{h}{2}\left(f(t_0) + f(t_1)\right) \\ c(t_2) &= c(t_0) + \frac{h}{3}\left(f(t_0) + 4f(t_1) + f(t_2)\right) \\ c(t_n) &= c(t_{n-3}) + \frac{3h}{8}\left(f(t_{n-3}) + 3f(t_{n-2}) + 3f(t_{n-1}) + f(t_n)\right), \qquad n \geq 3 \end{aligned} \tag{2.20}$$

We can simply apply (2.18) and (2.20) together to the following ODEs:

$$b'(t) = \Psi(u) - \kappa b(t) + \beta \int_{\mathbb{R}_0^+} (1 - e^{-b(t)x}) \mu^u(dx)$$

$$= \Psi(u) - \kappa b(t) + \sec \frac{\pi\alpha}{2} \beta \left[(b(t) + iu)^\alpha - (iu)^\alpha \right] \tag{2.21}$$

$$c'(t) = ab(t) \tag{2.22}$$

2.3.3 COS Expansion method

After the Carr-Madan formula has been proposed, many amended algorithms are introduced in order to speed up the calculation and enhance efficiency and stability. For example, Chourdakis (2004) uses the fractional FFT method to reduce the computation time by one-half, and Kilin (2011) shows how caching technique can accelerate the calculation. Several new approaches have been developed, which do not depend on the Carr-Madan formula. For example, Lord et al. (2008) use a Convolution method to price not only European options but also early-exercise options, which is also based on the FFT method. All the methods above require a large number of sampling points, which means these methods are not suitable to be combined with the Runge-Kutta method. Fang and Oosterlee (2008) introduce a COS expansion method which is based on the Fourier-cosine expansion. This method is fast and only needs a very limited number of sampling points. Another crucial advantage of the COS method is that it can price many options with different strikes simultaneously while only computing the characteristic function once. This is very important, as our framework relies numerical solutions of characteristic functions.

Hence, the COS method can dramatically reduce the pricing and calibration time.

This general idea of the COS method is very simple. Considering an arbitrary function $f(\theta)$ supported on $[0, \pi]$, the cosine expansion of $f(\theta)$ can be expressed as:

$$f(\theta) = \sum\nolimits_{k=0}^{\prime\infty} A_k \cos(k\theta) \qquad \text{with} \qquad A_k = \frac{2}{\pi} \int_0^{\pi} f(\theta) \cos(k\theta) d\theta \tag{2.23}$$

where $\sum'$ represents a corrected summation in which the first term is weighted by one-half. The support of $f(\theta)$ can be extended to any finite interval $[a, b] \in \mathbb{R}$. For example, we can define $\theta = \frac{x-a}{b-a}$ and $x = \frac{b-a}{\pi}\theta + a$, and have

$$f(x) = \sum\nolimits_{k=0}^{\prime\infty} A_k \cos\left(\frac{x-a}{b-a} k\pi\right) \tag{2.24}$$

with

$$A_k = \frac{2}{b-a} \int_a^b f(x) \cos\left(\frac{x-a}{b-a} k\pi\right) dx \tag{2.25}$$

Based on the cosine expansion we want to use the corresponding characteristic function to recover $f(\theta)$, because most commonly used financial models have explicit characteristic functions while density functions are unknown. Firstly, we use a truncated function $\phi_1(u)$ to approximate the true characteristic function $\phi(u)$:

$$\phi_1(u) = \int_a^b e^{iux} f(x) dx \simeq \phi(u) \tag{2.26}$$

If the truncation is chosen appropriately, the approximation (2.26) is numerically interchangeable with $\phi(u)$. Since A_k can be rewritten as:

$$A_k = \frac{2}{b-a} Re\left\{\phi_1\left(\frac{k\pi}{b-a}\right) \exp\left(-i\frac{ak\pi}{b-a}\right)\right\} \tag{2.27}$$

As with (2.26), we can have

$$F_k = \frac{2}{b-a} Re\left\{\phi\left(\frac{k\pi}{b-a}\right)\exp\left(-i\frac{ak\pi}{b-a}\right)\right\}, \tag{2.28}$$

and we get $A_k \simeq F_k$. The implication of this is that we can obtain an approximation of $f(x)$:

$$f_1(x) = {\sum}'^{\infty}_{k=0} F_k \cos\left(\frac{x-a}{b-a}k\pi\right) \tag{2.29}$$

Then, we truncate (2.29) and obtain

$$f_2(x) = {\sum}'^{N-1}_{k=0} F_k \cos\left(\frac{x-a}{b-a}k\pi\right) \tag{2.30}$$

Apparently, (2.30) shows that the corresponding characteristic function can be used to recover the whole information of $f(x)$ approximately. Suppose there is a European option with strike price K and spot price S_0. Denote $x = \log(S_0/K)$ and $y = \log(S_t/K)$. Let the payoff function be $g(y)$. The option price with the time to maturity t is

$$\begin{aligned}
C(x,t) &= \mathbb{E}[e^{-rt}g(y)] \\
&\simeq e^{-rt}\int_a^b g(y)f(y|x)dy \\
&= e^{-rt}\int_a^b g(y){\sum}'^{\infty}_{k=0} A_k(x)\cos\left(\frac{y-a}{b-a}k\pi\right)dy \\
&= \frac{b-a}{2}e^{-rt}{\sum}'^{\infty}_{k=0} A_k(x)\frac{2}{b-a}\int_a^b g(y)\cos\left(\frac{y-a}{b-a}k\pi\right)dy \\
&= \frac{b-a}{2}e^{-rt}{\sum}'^{\infty}_{k=0} A_k(x)V_k
\end{aligned} \tag{2.31}$$

where $f(y|x)$ is the conditional density function, $[a,b]$ is the truncation boundary, and $V_k = \frac{2}{b-a}\int_a^b g(y)\cos\left(\frac{y-a}{b-a}k\pi\right)dy$. Applying truncation to (2.31), we can have

$$C_2(x,t) = \frac{b-a}{2}e^{-rt}{\sum}'^{N-1}_{k=0} A_k(x)V_k \tag{2.32}$$

We can also replace A_k with F_k and have a further approximation:

$$\begin{aligned} C_3(x,t) &= \frac{b-a}{2} e^{-rt} \sum\nolimits_{k=0}^{\prime N-1} F_k(x) V_k \\ &= e^{-rt} \sum\nolimits_{k=0}^{\prime N-1} Re \left\{ \phi\left(\frac{k\pi}{b-a}\right) \exp\left(-i\frac{ak\pi}{b-a}\right) \right\} V_k \end{aligned} \tag{2.33}$$

(2.33) is a very general representation for any model which has an explicitly characteristic function of log-return. With finite number N, we can compute $C_3(x,t)$ given V_k. As it turns out, V_k can be solved analytically for most of the cases. For European options,

$$V_k = \frac{2}{b-a} K \left(\chi_k(0,b) - \psi(0,b) \right) \tag{2.34}$$

where $\chi_k(\cdot)$ and $\psi_k(\cdot)$ are simple functions defined as:

$$\begin{aligned} \chi_k(c,d) &= \int_c^d e^y \cos\left(k\pi \frac{y-a}{b-a}\right) dy \\ \psi(c,d) &= \int_c^d \cos\left(k\pi \frac{y-a}{b-a}\right) dy \end{aligned}$$

where $[c,d] \in [a,b]$. The choice of truncation boundary $[a,b]$ is also crucial to the precision. There are several choices of truncating the domain. Cumulants are used in Fang and Oosterlee (2008). In our experiment, we follow the same procedure.

2.4 Empirical Performance

In this section, we use the market data to test the empirical performance of the present model. The data set chosen is a sample of S&P 500 index option prices. We also select several benchmark models with particular reasons, including the Variance Gamma (VG)

model (see Madan et al. (1998)) and the Heston model (see Heston (1993)). The VG model is a pure-jump model that is of infinite activity and provides non-Gaussian innovation. The Heston model is a celebrated stochastic volatility model. The selection of benchmark models will cover most of aspects of derivative pricing. Details can be found in the next subsection.

2.4.1 Benchmark models

To compare the performance, we select six benchmark models including the Heston model, the Double Heston model, the Variance Gamma(VG) model, the time-changed VG (VGSV) model, the finite moment Log Stable (LS) model, the one-dimensional time-changed LS (LSSV1) model. Our new model is named as the two-dimensional time-changed LS (LSSV2) model. The first five benchmark models all have explicit solutions of characteristic function of log returns, so it is straightforward to compute option prices with the FFT method. The last two models need to be solved numerically, based on the algorithm introduced in this chapter. The reasons why the six benchmark models are chosen are various, since we want to test the benefits of adding up stochastic volatility, multi-scale volatility components and the leverage effect. These benchmark models have different characteristics that we want to test with. The categorized information is presented in Table 2.1.

Compared with benchmark models, we can investigate the benefits of introducing stochastic multi-scale volatility and incorporating the leverage effect. The comparison will be

Table 2.1: *The category table of benchmark models*

	Heston	Double Heston	VG	VGSV	LS	LSSV1	LSSV2
Stochastic Volatility (SV)	Yes	Yes	No	Yes	No	Yes	Yes
Multi-scale SV	No	Yes	N/A	No	N/A	No	Yes
Leverage Effect	Yes	Yes	N/A	No	N/A	Yes	Yes
Explicit Solution	Yes	Yes	Yes	Yes	Yes	No	No

done based on the results of daily calibration. Before applying the pricing framework, we need to show that the framework is reliable and able to provide good accuracy. Moreover, the computational time has to be relatively small, in order to keep the tractability. Characteristic functions of all benchmark models are provided in Appendix A.1.

2.4.2 Comparison of pricing accuracy

The numerical framework is of approximation when solving ODEs, so it needs to be proved that numerically generated prices are accurate and reliable. To demonstrate this, we firstly use the Heston model as the only benchmark model in this subsection. The Heston model has an explicit characteristic function and can also be obtained via using the leverage-measure change. Hence, we can compare the results given by both methods. Suppose we have a drifted Brownian motion

$$X_t = W_t - \frac{1}{2}t \quad ,$$

and define a CIR process

$$dv_t = (a - \kappa v_t)dt + \eta\sqrt{v_t}dZ_t$$

where $\mathbb{E}[dW_t dZt] = \rho dt$. Then, we can define a time-changed Lévy model as

$$\begin{aligned} S_t &= S_0 \exp\left((r-q)t + X_{T_t}\right) \\ T_t &= \int_0^t v_s ds \end{aligned} \tag{2.35}$$

We can modify the Heston model and rewrite it as

$$\begin{aligned} S_t &= S_0 \exp\left((r-q)t + \int_0^t \sqrt{v_s} dW_s - \frac{1}{2}\int_0^t v_s ds\right) \\ dv_t &= (a - \kappa v_t)dt + \eta\sqrt{v_t} dZ_t \end{aligned} \tag{2.36}$$

Apparently, (2.35) and (2.36) refer to the same model. Applying the numerical method proposed in this chapter to (2.35), we can obtain numerical solutions to option prices. We can then compare with semi-closed solutions based on (2.36) as explicit characteristic functions are known. Details of solving (2.35) can be found in Appendix A.2.

We use the FFT method and the COS method to produce option prices one after another. A comparison of results is provided in Table 2.2, Table 2.3 and Table 2.4. Given different maturities and moneyness, we assess the accuracy of our numerical method. A little surprisingly, we find that our numerical method is even faster than the FFT method, given the same accuracy. For example, the COS method gets a good accuracy of 1.33E−06 with 15.735 milliseconds while the FFT method only achieves 5.46E−06 with 37.038 milliseconds, for pricing short-term ATM options. Similar situations can be observed for both the ITM options and the OTM options. The advantage of the COS method is less for long-term options. For the long-term ITM option shown in Table 2.3, the COS method needs 47.124 milliseconds to get 1.04E−06. The FFT method costs only

18.613 milliseconds to have a similar accuracy. This is because the long-term options need more steps to solve the corresponding ODEs, which results in more computational time. On the whole, the COS method does not require more computational time, even it involves numerically solving ODEs. This is not counter-intuitive. If only a medium level of accuracy is required, the FFT method is faster as it can compute the characterization function directly. If a very good level of accuracy is required, the COS method can provide prices even faster than the FFT method.

The above experiment demonstrates the accuracy and fast speed of our pricing framework. We also provide an additional test on how it performs with our new model. Unlike the Heston model, neither the LSSV1 nor the LSSV2 model has an explicit solution. Hence, it is hard to evaluate the accuracy of option prices. However, with the Heston case, it is believed that our numerical method is able to provide accurate prices.

Despite the huge computation time, we can use Monte Carlo simulation to compute option prices. The first thing that should be confirmed is how to sample a specific distribution. The infinitely divisible distribution we have is the α-stable distribution. The sampling algorithm is given in Appendix A.3. We simply use the Euler scheme in the simulation. The simulation of the time-change can be easily done with the fact that X_t and $t^{1/\alpha}X_1$ have the same distribution. If $\alpha = 0.5$, it becomes the familiar case of Brownian motion.

Table 2.5 shows the comparison of pricing results between the simulation method and the COS method. LSSV1 and LSSV2 models are used in the comparison, as both of them do not have explicit characteristic functions. It is suggested that the COS method can

Table 2.2: *The comparison of pricing accuracy of the Heston model (At-the-Money)*

The upper panel presents the pricing errors of a short-term European call with the maturity $T = 1$. The lower panel depicts the pricing errors of a long-term European call with the maturity $T = 10$. Both options have the same spot price $S_0 = 100$ and strike price $K = 100$. The reference option values are 5.785155450 and 22.318945574, respectively. Reference values are obtained by using the FFT method with $N = 2^{20}$. Computational times are presented in milliseconds (msec.). 20 steps are used to solve ODEs for the COS method. Parameters of the Heston model are $\kappa = 1.5768$, $a = 0.0628$, $\eta = 0.5751$, $\rho = -0.5711$ and $v_0 = 0.0175$.

COS			FFT		
N	error	time(msec.)	N	error	time(msec.)
64	0.001415	11.051	4096	0.001433	5.699
96	1.95E-05	13.281	8192	7.15E-05	10.634
128	3.87E-06	13.768	16384	3.36E-05	11.207
160	1.33E-06	15.735	32768	1.48E-05	19.285
192	1.32E-06	35.077	65536	5.46E-06	37.038
N	error	time(msec.)	N	error	time(msec.)
64	0.0049	36.825	4096	3.25E-04	5.698
96	4.96E-04	40.675	8192	1.59E-05	10.248
128	1.66E-05	44.219	16384	7.39E-06	11.193
160	1.13E-07	32.141	32768	3.14E-06	18.402
192	1.13E-07	52.428	65536	1.02E-06	37.060

Table 2.3: *The comparison of pricing accuracy of the Heston model (In-the-Money)*

The upper panel presents the pricing errors of a short-term European call with the maturity $T = 1$. The lower panel depicts the pricing errors of a long-term European call with the maturity $T = 10$. Both options have the same spot price $S_0 = 100$ and strike price $K = 90$. The reference option values are 12.70953156 and 27.084936345, respectively. Reference values are obtained by using the FFT method with $N = 2^{20}$. Computational times are presented in milliseconds (msec.). 20 steps are used to solve ODEs for the COS method, expect for those with numbers shown in brackets. Parameters of the Heston model are $\kappa = 1.5768$, $a = 0.0628$, $\eta = 0.5751$, $\rho = -0.5711$ and $v_0 = 0.0175$.

	COS			FFT	
N	error	time(msec.)	N	error	time(msec.)
64	2.26E-04	10.518	4096	5.38E-04	0.527
96	3.67E-05	11.183	8192	1.20E-04	10.399
128	1.32E-06	13.175	16384	3.56E-05	12.321
160	2.99E-06	15.427	32768	4.91E-06	18.644
192(40)	5.31E-07	20.466	65536	1.99E-06	36.740
N	error	time(msec.)	N	error	time(msec.)
64	0.012	35.016	4096	2.56E-04	5.569
96	7.43E-04	38.929	8192	5.74E-05	10.376
128	1.67E-05	43.377	16384	1.70E-05	10.211
160	1.04E-06	47.124	32768	2.35E-06	18.613
192	1.35E-07	55.703	65536	9.49E-07	38.553

Table 2.4: *The comparison of pricing accuracy of the Heston model (Out-of-the-Money)*

The upper panel presents the pricing errors of a short-term European call with the maturity $T = 1$. The lower panel depicts the pricing errors of a long-term European call with the maturity $T = 10$. Both options have the same spot price $S_0 = 100$ and strike price $K = 110$. The reference option values are 1.787134785 and 18.243849718, respectively. Reference values are obtained by using the FFT method with $N = 2^{20}$. Computational times are presented in milliseconds (msec.). 20 steps are used to solve ODEs for the COS method, expect for those with numbers shown in brackets. Parameters of the Heston model are $\kappa = 1.5768$, $a = 0.0628$, $\eta = 0.5751$, $\rho = -0.5711$ and $v_0 = 0.0175$.

COS			FFT		
N	error	time(msec.)	N	error	time(msec.)
64	4.18E-04	10.749	4096	3.59E-04	5.401
96	4.64E-05	11.729	8192	1.70E-04	10.716
128	4.36E-05	13.585	16384	7.37E-05	11.721
160(40)	1.73E-05	19.417	32768	2.55E-05	23.441
192(40)	1.72E-05	28.134	65536	1.28E-06	37.079
N	error	time(msec.)	N	error	time(msec.)
64	0.0063	35.034	4096	8.10E-05	5.607
96	5.86E-04	38.839	8192	3.79E-05	10.361
128	1.24E-05	42.772	16384	1.64E-05	11.876
160	6.93E-07	46.478	32768	5.66E-06	18.425
192	4.52E-07	51.415	65536	2.84E-07	38.005

provide accurate option prices across different moneyness.

Table 2.5: *The comparison of the Monte Carlo method against the COS method: LSSV1 and LSSV2*

The upper panel presents the European call prices of the LSSV1 model given by the MC method and the COS method. The lower panel depicts the European call prices of the LSSV2 model. The spot price is 10. The risk-free rate is 0.03, and the dividend rate is 0.04. The maturity is 2 years. The strikes for ITM, ATM and OTM are 8, 10 and 12, respectively. Parameters of the LSSV1 model are $\kappa = 3.2523$, $a = 0.1415$, $\alpha = 1.8323$, $\beta = 0.2252$ and $v_0 = 0.0499$. Parameters of the LSSV2 model are $\kappa_1 = 3.2523$, $\kappa_2 = 0.5326$, $a_1 = 0.1115$, $a_2 = 0.0235$, $\alpha_1 = 1.6323$, $\alpha_2 = 1.4382$, $\beta_1 = 0.2252$, $\beta_2 = 0.5323$, $v_0^1 = 0.0369$ and $v_0^2 = 0.0445$. The number of sample paths in each MC trial is 10^6 and the number of steps is 100. The COS method uses 128 points in all computation work.Numbers reported in brackets are the corresponding standard errors.

LSSV1	MC	COS
ITM	2.3218 (0.0023)	2.3226
ATM	1.1398 (0.0016)	1.1393
OTM	0.3923 (0.0008)	0.3942
LSSV2	MC	COS
ITM	2.4268 (0.0054)	2.4332
ATM	1.2758 (0.0050)	1.2698
OTM	0.5625 (0.0049)	0.5638

2.4.3 Comparison of daily calibration

Having demonstrated the good accuracy of the numerical pricing framework, we can now focus on the calibration problem to show the empirical performance of our new model. We employ a daily calibration procedure, as it has been widely used by many academic research. To measure the distance between the model prices and market prices, we use the weighted sum of squared pricing errors (WSSE). Data filtering is also important to investigate the empirical performance. The idea of data filtering is that we want to abandon prices which show too much noise.

For the empirical study we propose, European S&P 500 options data are collected from 1998 to 2003 from OptionMetrics. We use implied volatilities to backout the corresponding option prices. Considering the trading volume, only out-of-the-money options are selected, which means that either call options or put options are adopted according to the moneyness. Each quoted option price was matched with the underlying index price which has been adjusted for dividends and splits. The risk-free rates come from T-bill rates and the whole term-structure is generated by interpolation. Data sets are selected carefully from the original data as data filtering also has an impact on evaluating the performance. Option prices with extreme small maturities and moneyness are abandoned as well as those that violate the put-call parity.

Daily implied volatilities of the S&P 500 index options across a variety of strike prices and maturities are chosen as the dataset used in this experiment. The sample period is from January 7, 1998 to December 29, 2003. The corresponding interest rates are obtained from

Bloomberg. The implied volatilities are computed based on standard European options on the S&P 500 index (SPX) which is the most liquid European options traded.

Following Bakshi et al. (1997a) and Huang and Wu (2004), similar data-filtering rules are applied to trim the raw implied volatility data. First, only Wednesday prices are used to reduce the impact of the day-of-the-week effect. This is widely applied by many empirical literature. Second, options with very short maturity, say seven business days, are eliminated. Third, implied volatilities that are either larger than 70% or option prices that are less than 0.05 dollar are all discarded. After trimming the raw data, there are 361 days of volatility surface data left and 81380 option quotes. Finally, only out-of-the-money option prices are selected, because of the better liquidity.

A comparison of computation time used for different methods is shown in Table 2.6. The reason why we compare the computation time in this subsection is because our framework has a special advantage of accelerating the calibration procedure. The FFT method can generate a series of prices with different strikes simultaneously, which is a quite useful benefit for calibration. Our framework admits the same thing. By randomly selecting one trading day in our dataset, we proceed the calibration with both the FFT method and the COS method. We even "force" the FFT method to solve the LSSV1 model and the LSSV2 model. Although the computational time will be extremely large, we just provide it for illustrative purpose. With Table 2.6, the Heston model is said to be the fastest model despite the method used. For the LSSV1 model, it causes about two times more to produce option prices. The LSSV2 model requires 425 seconds to finish the

calibration, which is about fifteen time larger than that of the Heston model. Since the LSSV2 model has a large dimension of parameter space, it is not surprising to have more computational time. For example, the LSSV2 model uses 525 times of search to find the optimal parameter set while the Heston model only searches 373 times.

Table 2.6: *A Comparison of computational time of daily calibration for the COS method and the FFT method*

The computational time is measured in seconds. The Number of search means how many times the calibration costs to find the optimal parameter set. The FFT method uses 4096 sampling points, and the COS method uses 128 sampling points.

	Heston		LSSV1		LSSV2	
	Time (sec.)	Number of search	Time (sec.)	Number of search	Time (sec.)	Number of search
COS	2.765	373	8.909	320	43.235	525
FFT	2.331	374	8.33E4	321	6.36E5	532

A summary of the implied volatility data is provided in Table 2.7 and Table 2.8. According to Table 2.7, the number of OTM put quotes is a little more than that of OTM call quotes. The most active trades centralize at prices with maturity within $(30, 90)$ and maturity larger than 180 days. Table 2.8 shows the volatility smirk exhibited commonly in index option markets.

The calibration procedure is implemented by minimizing the weighted sum of squared pricing errors for each benchmark model. Let Θ denote the optimal parameter set, and

Table 2.7: *Numbers of implied volatilities categorized by moneyness and days to maturity*

	DTM< 30	30 <DTM< 90	90 <DTM< 180	DTM> 180	ALL
S/X < 0.975	4492	9601	5757	17139	36989
0.975 <S/X< 1	1100	1943	541	1551	5135
1 <S/X< 1.025	1049	1853	523	1481	4906
1.025 <S/X< 1.05	847	1482	482	1335	4146
1.05 <S/X< 1.075	598	1196	446	1319	3559
S/X > 1.075	2272	6925	4203	13245	26645
ALL	10358	23000	11952	36070	81380

Table 2.8: *Average implied volatility categorized by moneyness and days to maturity*

	DTM< 30	30 <DTM< 90	90 <DTM< 180	DTM> 180	ALL
S/X < 0.975	0.3173	0.2290	0.2006	0.1908	0.2344
0.975 <S/X< 1	0.1959	0.1999	0.2089	0.2152	0.2050
1 <S/X< 1.025	0.2141	0.2109	0.2185	0.2215	0.2163
1.025 <S/X< 1.05	0.2363	0.2266	0.2259	0.2266	0.2289
1.05 <S/X< 1.075	0.2648	0.2415	0.2346	0.2308	0.2429
S/X > 1.075	0.5905	0.3647	0.3150	0.2774	0.3869
ALL	0.3032	0.2454	0.2339	0.2270	0.2524

it should be implemented as

$$\Theta = \arg\min \sum_{i=1}^{N} wmse_i$$

where N is the number of maturities, $wmse_i$ is the weighted sum of squared pricing errors given the i-th maturity. $wmse_i$ is computed as:

$$wmse_t = \min \frac{1}{N_i} \sum_{i=1} \omega_{ij} e_{ij}^2$$

where N_i is the number of prices with the same maturity T_i, ω_{ij} is the weighting coefficient of the j-th option data, and e_{ij} is the j-th pricing error. For each trading day, all trimmed data of the current volatility surface are used for calibration. To minimize the weighted sum of squared pricing errors, a global search algorithm is employed. The weighting matrix is essential to calibration results. Most related literature chooses the identity matrix in calibration. A concern should be raised, as with the identity matrix OTM options take less weights in the calibration; however, OTM options should play an important role because of the good liquidity. Weighting matrix can also balance the contributions of different maturities. There are many possible choices on the weighting matrix. If the pricing error is measured by implied volatility, an identity weighting matrix will work; however, calculating implied volatilities is time-consuming. Some research focus on deriving asymptotic implied volatility, which can be applied to enhance the calibration performance. In this section, we use a weighting matrix obtained by using regression with maturity and moneyness. The calibration procedure aims to find the equivalent measure that best fits the current volatility surface. To speed up the calibration, the calibrated parameters are used as the initial guess for the calibration of the successive trading day.

Table 2.9 presents the calibration results of all models. For each calendar year, the sum of WSS errors are reported for each model. Obviously, the Heston model and LSSV2 model are the two candidates of the winner. It is surprised to see that the Double Heston model does not provide a better performance. In principle, a model with more parameters should outperform its simplification; however, the calibration procedure involves a numerical search in the parameter space. For example, the Double Heston model has 10 parameters while the Heston model only has 5 parameters. It is much harder to search in a 10-dimensional space than in the 5-dimensional space. The Double Heston model might have the potential to better fit the volatility surface. However it needs more care to implement the calibration. In our experiment, we do not set up a particular search method for the Double Heston model. The high pricing errors of the Double Heston might be due to that the corresponding calibration stops with a local minimization. Our LSSV2 model should suffer from the same problem.

Compared with the VG model and the VGSV model, it is suggested that introducing stochastic volatility can significantly reduce the pricing errors. The average pricing errors of the VGSV model is about 60% of those of the VG model. The LS model also exhibits good performance, which coincides with the results in Carr and Wu (2003). With a parsimonious model that only has two parameters, the pricing error is only about two times that of the Heston model. The benefit of introducing stochastic volatility for the LS model is not very large, as the improvements from LSSV1 and LS are only medium. This might be explained by the restricted dependence imposed by the LSSV1 model. Although

the LSSV1 model admits stochastic volatility, there is only one source of innovation. Compared with the LSSV2 model, the enhancement is very impressive. Apparently, introducing another dynamics is obviously useful as the LSSV2 model always significantly outperforms the LSSV1 model.

Table 2.9: *Daily calibration results of all models*

	Heston	Double Heston	VG	VGSV	LS	LSSV1	LSSV2
1998	0.2652	0.8402	0.8545	0.4444	0.4554	0.3589	0.2572
1999	0.2865	0.6050	0.8188	0.4205	0.4831	0.3790	0.2983
2000	0.3489	0.7609	1.0065	0.4355	0.3789	0.4712	0.2622
2001	0.1563	0.7388	0.9115	0.5125	0.2901	0.2783	0.2097
2002	0.2959	0.2536	0.8369	0.4979	0.4242	0.3835	0.2274
2003	0.2798	0.4566	0.8749	0.5039	0.3820	0.3602	0.3047

Except for comparing the pricing error, the stability of calibrated parameter set is another crucial criterion. In Table 2.10, we can compare the optimal parameter sets of all models. Along with the optimal parameters reported, we also provide the corresponding standard deviations in brackets. For example. the Heston model shows very good stability. Only the long-run mean κ has a large standard deviation of 1.269. The Double Heston model is derived in order to decompose the volatility and capture the multi-variate volatility components. As expected, the mean-reverting speeds should be different. The effect of a long-run and a short-run should imply that either κ_1 or κ_2 is large with a small counterpart; however, we do not observe such an expectation from Table 2.10. For the LSSV2 model, the mean-reverting speed parameters κ_1 and κ_2 are 3.325 and 1.805. Observing

the average variance parameters, we have $a_1 = 0.067$ and $a_2 = 0.002$. This coincides with our assumption of the large long-run volatility component and the small short-run volatility component. In all, the weighted pricing errors of the Heston model is 0.2721, which is slightly more than 0.2599 for the LSSV2 model. This does not suggest that the new model can outperform the Heston model, as the pricing errors are in the same level; the stability of LSSV2 is better according to Table 2.9. From the example of the Double Heston model, the calibration result can be expected to improve because of its large parameter space. If some ad-hoc calibration technique is used, the LSSV2 model has the potential to achieve a better result.

The proposed model exhibits better potentials to explain an important stylized features observed from the market. It is suggested by empirical studies that volatility has multiple components such as long-run and short-run effects. The evolution of volatility is a composition of long-run stable process and a short-run volatile process. Many literature have tried to propose multi-dimensional processes to capture such a feature. For example, the double-Heston model employs two CIR processes and splits the multiple components of volatility in a qualitative sense. Looking at the optimal parameter set of the LSSV2 model, it is believed that the intuition of the modelling has been realized by the model. For example, the αs of v_t^1 and v_t^2 are very different. α_1 is 1.812, which suggests that the short-run volatility is more smooth and of less large movements; α_2 is 1.183, which indicates that the long-run volatility has more frequent jumps. As expected, the long-run volatility has large mean-reverting speed, small volatility of volatility and the short-run

volatility has small mean-reverting speed with large volatility of volatility. The Double Heston model does not exhibit such a performance while it is hard to tell the difference between the variance processes v_t^1 and v_t^2.

2.5 Conclusion

In this chapter, we develop a sophisticated numerical pricing framework that can be applied to any time-changed Lévy model. The random time process is allowed to be dependent on the spot price process so that the leverage effect is incorporated. The numerical framework provides accurate option prices within relatively short computational time. With the numerical pricing framework, a time-change Lévy model is proposed which is of multi-scale stochastic volatility and leverage effect. Based on real option data, numerical experiments of calibration are implemented to show the outstanding performance of the present model.

Table 2.10: *Calibrated parameters of all models*

The optimal parameter set of models is obtained by minimizing the weighted sum of squared pricing errors. For each trading day, the calibration is run individually. The calibrated parameter set is used as the initial guess for the successive daily calibration.

Model Specification													
Θ	Heston	Θ	Double Heston	Θ	VG	Θ	VGSV	Θ	LS	Θ	LSSV1	Θ	LSSV2
$v0$	0.048	v_0^1	0.033	C	4.062	C	1.609	σ	1.625	α	1.587	α_1	1.812
	(0.005)		(0.012)		(1.016)		(1.748)		(0.232)		(0.321)		(0.353)
η	0.057	v_0^2	0.016	G	9.219	G	9.360	α	0.142	a	0.071	α_2	1.183
	(0.006)		(0.032)		(1.497)		(10.209)		(0.032)		(0.004)		(0.332)
κ	2.799	η_1	0.063	M	28.819	M	28.024			κ	2.042	a_1	0.124
	(1.269)		(0.032)		(4.619)		(5.560)				(0.632)		(0.053)
ρ	-0.727	η_2	0.044			κ	12.091			β	0.153	a_2	0.028
	(0.027)		(0.035)				(8.581)				(0.136)		(0.001)
λ	0.684	κ_1	2.532			η	2.836			v_0	0.0677	κ_1	4.745
	(0.252)		(0.843)				(2.916)				(0.083)		(0.801)
		κ_2	1.382			λ	3.938					κ_2	0.553
			(0.623)				(1.517)						(1.229)
		ρ_1	-0.683			v_0	0.467					β_1	0.263
			(0.036)				(1.769)						(0.620)
		ρ_2	-0.732									β_2	0.568
			(0.132)										(0.332)
		λ_1	0.865									v_0^1	0.045
			(0.132)										(0.035)
		λ_2	0.689									v_0^2	0.018
			(0.213)										(0.006)
mse	0.2721		0.6092		0.8839		0.4691		0.4023		0.3552		0.2599

Chapter 3

Dynamic optimal portfolio choice in a jump-diffusion model with investment constraints

3.1 Introduction

In this chapter, we solve the optimal dynamic portfolio choice problem in a jump-diffusion model with some realistic constraints on portfolio weights, such as the no-short-selling constraint and the no-borrowing constraint. The dynamic portfolio choice problem without portfolio constraints in pure-diffusion models is prompted by the seminal work of Merton (1969, 1971) and Samuelson (1969), and is further developed by Karatzas et al. (1987),

Kim and Omberg (1996), Wachter (2002), Detemple et al. (2003) and Liu (2007), among others. Wachter (2010) and Brandt (2009) are good references for portfolio choice problems. The constrained dynamic portfolio choice problem in pure-diffusion models is first studied by Karatzas et al. (1991), He and Pearson (1991) and Xu and Shreve (1992). In general, a market with portfolio constraints is incomplete. It is usually a daunting task to solve such a portfolio choice problem in an incomplete market, either through the HJB equation (due to limits on dimensionality) or the martingale-duality method (as there are infinitely many martingale measures). To overcome the market incompleteness caused by portfolio constraints, Cvitanic and Karatzas (1992) propose a general approach to solve dynamic portfolio choice in the presence of various constraints on portfolio weights, including no-short-selling constraints and no-borrowing constraints.

More precisely, by appropriately adjusting the risk-free rate and the drift terms of risky asset prices, Cvitanic and Karatzas (1992) convert the constrained portfolio choice problem in the original incomplete market into an unconstrained one in a set of fictitious complete markets. Hence, solving the optimal portfolio problem in the original incomplete market reduces to the one in a set of new complete markets to which the standard martingale method developed for complete pure-diffusion markets can be applied. Furthermore, it has been shown that the optimal consumption and portfolio rule in the original market is identical to those which are optimal in the worst of all the fictitious markets. However, it is generally hard to find the worst fictitious market and the corresponding optimal consumption and portfolio strategy in the presence of a large number of state variables.

For this reason, Bick et al. (2013) have recently developed some efficient simulation-based approximation algorithms to solve constrained consumption-investment problems in pure-diffusion markets via the martingale-duality approach.

In those models mentioned above, it is standard to assume that asset prices follow pure-diffusion processes, primarily due to their analytical tractability. However, much recent research in finance has documented empirical evidence of jumps in stock returns. See, for example, Bakshi et al. (1997b), Bates (2000) and Eraker et al. (2003). With jumps, an asset return model can explicitly allow for sudden but infrequent market movements of large magnitude, and thus capture the "skewed" and "fat-tailed" features of stock return distributions. Many empirical and theoretical studies find that the jump risk has a substantial impact on portfolio choice, risk management and option pricing. See Merton (1976), Liu et al. (2003) and Duffie et al. (2000), for example. More specifically, recent portfolio choice papers in jump-diffusion models demonstrate that optimal portfolios held by an investor facing jump risks differ markedly from those in the absence of jumps, and that the economic loss of ignoring jumps may be substantial. For more detailed analysis, see Liu et al. (2003) and Das and Uppal (2004).

Given the substantial impact of jumps on an investor's asset allocation decision, this chapter solves the optimal portfolio choice problem in realistic settings involving jumps in stock returns, portfolio constraints and potentially a large number of state variables. As demonstrated by Bardhan and Chao (1996), once unpredictable jumps are incorporated, a model with or without portfolio constraints is inherently incomplete, regardless of the

number of traded stocks. This is in striking contrast to pure-diffusion models which can be completed by including more stocks. Hence, unlike a pure-diffusion model with portfolio constraints, the incompleteness caused by jumps in a jump-diffusion model can not be removed through the "fictitious completion" techniques in Karatzas et al. (1991) and Cvitanic and Karatzas (1992) and thus, the martingale duality approaches they used do not directly apply to a jump-diffusion model. In this chapter, we solve the optimal portfolio choice problem in a multi-asset jump-diffusion model with portfolio constraints. To be more specific, we first establish equivalent optimality conditions similar to those in Cvitanic and Karatzas (1992), which convert the constrained portfolio choice problem in the original jump-diffusion model into an unconstrained one in a set of fictitious jump-diffusion models. Then, we apply a portfolio weight decomposition approach recently developed by Jin and Zhang (2012) to solve the portfolio choice problem in jump-diffusion models.

This chapter is related to several papers in the literature on portfolio choice problems in a jump-diffusion setting. Our model, however, differs from those in Liu et al. (2003) in that they consider single-stock jump-diffusion models with no portfolio constraints while we consider multi-asset jump-diffusion models with some realistic portfolio constraints. In Das and Uppal (2004) and Ait-Sahalia et al. (2009), meanwhile, they solve the portfolio selection problems in jump-diffusion models which can include a large number of assets. However, in their models, there is only one type of jump, all of the coefficients in stock return processes are constants and there are no portfolio constraints. In contrast,

we consider the optimal portfolio strategies in a multi-asset jump-diffusion model which includes a large number of assets, state variables and portfolio constraints.

This chapter is also related to Jin and Zhang (2012) on portfolio choice problems in a jump-diffusion setting, in which the authors develop decomposition methods for portfolio weights to obtain tractable solutions to optimal portfolio strategies in a jump-diffusion model, which includes a large number of assets and state variables. But only one portfolio constraint is considered. The constraint is that the number of traded risky assets is smaller than the sum of the number of diffusions and jumps, which is the case of an incomplete pure-diffusion market considered in Karatzas et al. (1991). In contract, we incorporate more general constraints in a jump-diffusion model.

In short, our work contributes to the dynamic portfolio choice literature by extending the pure-diffusion model in Cvitanic and Karatzas (1992) to a jump-diffusion model; incorporating more general portfolio constraints in Jin and Zhang (2012). To the best of our knowledge, our work is the first one to consider general and realistic constrained portfolio choice problems in jump-diffusion models with a large number of assets and state variables.

The remaining part of this chapter is organized as follows. In the next section, we lay out the framework of the constrained dynamic portfolio choice problem in a jump-diffusion model, construct an unconstrained dynamic portfolio choice problem in a set of fictitious markets and then present our results of equivalent optimality conditions. Section 3.3 applies the theoretical results developed in Section 3.2 to no-short-selling and no-borrowing

constraints respectively, and compares the method in the present chapter with the standard HJB equation method. Section 3.4 applies the theoretical results to several numerical examples. Section 3.5 concludes the chapter. All proofs are provided in the appendix.

3.2 The portfolio choice problem

This section describes the investment problem for an investor in allocating her wealth between a set of risky assets and one risk-less asset in a jump-diffusion model, with investment constraints. The investor is seeking to maximize the expected utility from intermediate consumption and terminal wealth.

3.2.1 The constrained portfolio choice problem

We fix a complete probability space $(\Omega, \mathcal{F}, \mathbb{P})$ and a filtration $\{\mathcal{F}_t\}$ satisfying the usual conditions. In the economy assumed, we use a l-dimensional state variable $X_t = (X_{1,t}, ..., X_{l,t})^\top$ to capture the stochastic variation in investment opportunities. Stochastic volatility and interest rates are typical examples of state variables. Here we use $\top$ to denote the transpose of a matrix or a vector. For analytical tractability, as illustrated in Jin and Zhang (2012) that flexible functions of state variables can be used, we assume that state variables X_t follow a pure diffusion process

$$dX_t = b^x(X_t)dt + \sigma^x(X_t)dB_t^X$$

where $B_t^X = (B_{1,t}^X, ..., B_{l,t}^X)^\top$ is an l-dimensional standard Brownian motion, $b^x(X_t)$ is an l-dimensional vector function and $\sigma^x(X_t)$ is an $l \times l$ matrix function of X_t.

An investor with a planning horizon $[0, T]$ seeks to allocate her wealth between one risk-less asset and n risky securities with portfolio constraints described below. The risk-less asset, called the bond, has a price $S_{0,t}$ which evolves according to the differential equation

$$dS_{0,t} = S_{0,t} r(X_t) dt$$

$$S_{0,0} = 1 \tag{3.1}$$

The prices of risky assets follow the dynamics

$$dS_{i,t} = S_{i,t-}[b_i(X_t)dt + \sigma_i^b(X_t)dB_t^S + \sigma_i^q(X_t)(Y \bullet dN_t)] \qquad \text{for } i = 1, ..., n \tag{3.2}$$

where $B_t^S = (B_{1,t}^S, ..., B_{d,t}^S)^\top$ is a d-dimensional standard Brownian motion correlated with B_t^X with a $d \times l$ correlation matrix ρ_t, and $N_t = (N_{1,t}, ..., N_{n-d,t})^\top$ is a $(n-d)$-dimensional multivariate Poisson process, with $N_{k,t}$ denoting the number of type k jumps up to time t. $\sigma_i^b(X_t)$ is the d-dimensional diffusion coefficient vector and $\sigma_i^q(X_t)$ is the $(n-d)$-dimensional jump coefficient vector. $Y = (Y_1, ..., Y_{n-d})^\top$ is a $(n-d)$-dimensional vector and $Y \bullet dN_t$ denotes the component-wise multiplication of Y and dN_t. More precisely, $Y \bullet dN_t = (Y_1 dN_{1,t}, ..., Y_{n-d} dN_{n-d,t})^\top$, where Y_k denotes the size of the type k jump. In particular, the Brownian motions represent frequent small movements in stock prices, while the jump processes represent infrequent large shocks to the market.

For illustrative purposes, we assume that N_k has finite activity with stochastic intensity λ_k, and the size Y_k of the type k jump has probability density $\Phi_k(t, dx)$.[1] For tractability,

[1]The results can be extended to a model with infinite activity by replacing $\lambda_k(t)\Phi_k(t, dx)$ with a Levy

we assume $\lambda_k = \lambda_k(X_t)$ is a non-negative function of state variables X_t, and represents the rate of the jump process at time t, and $\Phi_k(t, dx)$ is $\mathcal{F}_t$-predictable and denotes the probability of getting a jump size x if there is a jump at time t. We use A_k to denote the support of size of the k-th jump. In particular, we set $A_k = (0, \infty)$ for a positive jump, $A_k = (-1, 0)$ for a negative jump, and $A_k = (-1, \infty)$ for a mixed jump.

To set up the constrained portfolio choice problem, we follow the approach of Cvitanic and Karatzas (1992) to model portfolio constraints. More precisely, we fix throughout a non-empty, closed and convex set K in $\mathbb{R}^n$ to model the portfolio constraints. Let $\pi_t = (\pi_{1,t}, ..., \pi_{n,t}) \in K$ denote a trading strategy, where $\pi_{i,t}$ is the proportion of wealth invested in the i-th risky asset held at time t and $\mathcal{F}_t$-predictable. Consider, for example, a model where the short-selling of all stocks is prohibited. Then, the set K can be written as $K = \{\pi = (\pi_1, ..., \pi_n\} \in \mathbb{R}^n; \pi_i \geq 0, i = 1, ..., n\}$. In the case of prohibition of borrowing, the set K can be expressed as $K = \{\pi = (\pi_1, ..., \pi_n\} \in \mathbb{R}^n; \sum_{i=1}^n \pi_i \leq 1\}$.

We now consider an investor with utility function $U(x)$ for both consumption and terminal wealth and endowed with initial wealth W_0, which is invested in the above-mentioned $n + 1$ assets. For the given consumption rate c_t and the portfolio policy $\pi_t \in K$, the corresponding wealth process W_t evolves as

$$dW_t = rW_t dt - c_t dt + W_t \pi_t (b - r\mathbf{1}_n) dt + W_t \pi_t \Sigma_b dB_t^S + W_{t-} \pi_{t-} \Sigma_q (Y \bullet dN_t) \qquad (3.3)$$

where $b = (b_1(X_t), .., b_n(X_t))^\top$ and $\mathbf{1}_n$ is the n-dimensional vector of ones. Here Σ_b denotes the $n \times d$ matrix with $\sigma_i^b(X_t)$ being its i-th row and Σ_q is the $n \times (n - d)$ matrix with

measure.

$\sigma_i^q(X_t)$ being its i-th row.

A pair of consumption rate c and portfolio rule $\pi \in K$ is admissible if the corresponding wealth process satisfies $W_t \geq 0$ almost surely. We use $\mathcal{A}(w_0)$ to denote the set of all admissible pairs of consumption rate and trading strategies. As in Bick et al. (2013), the traditional Merton's problem is to maximize

$$J(0, W_0, X_0) = \max_{(c,\pi)\in\mathcal{A}(w_0)} \mathbb{E}\left[\int_0^T e^{-\beta t} U(c_t)dt + \alpha e^{-\beta T} U(W_T)\right],$$

where the constant $\beta > 0$ is the subjective time preference rate, and $\alpha > 0$ denotes the weight of bequests relative to consumption. Applying the standard optimal control method, we can derive the optimal portfolio weights, π, and the corresponding indirect value function, J, of the investor's problem following the HJB equation below (See Jin and Zhang (2012)):

$$\begin{aligned}\beta J = \max_{(c,\pi)\in\mathcal{A}(w_0)} \Bigg\{ & U(c) + J_t + \frac{1}{2}W^2\pi\Sigma_b\Sigma_b^\top\pi^\top J_{WW} + [W(\pi(b - r\mathbf{1}_n) + r) - c]J_W + b^x J_X \\ & + W\pi\Sigma_b\rho_t\sigma^{x\top} J_{WX} + \frac{1}{2}Tr\left(\sigma^x\sigma^{x\top} J_{XX^\top} + \sum_{k=1}^{n-d}\mathbb{E}\left[J(W + W\pi\mathbf{\Sigma}_{qk}Y_k) - J(W)\right]\right)\Bigg\}.\end{aligned} \tag{3.4}$$

3.2.2 The fictitious unconstrained portfolio choice problem

In this section, by following Cvitanic and Karatzas (1992), we embed the original constrained portfolio choice problem introduced in the previous section in an appropriate family of fictitious unconstrained ones.

Consider a market consisting of one riskless asset and m risky assets, the latter being

driven by an n-dimensional Brownian motion. In such a market, incompleteness arises when the risky assets cannot span the sources of uncertaintynamely, $m < n$. To overcome this problem, Karatzas et al. (1991) perform a "fictitious completion" of the incomplete market by introducing $n - m$ additional stocks into the market and then demonstrate that if the drift coefficients of the $n - m$ fictitious stocks are chosen in an appropriate manner, the optimal portfolio weight in the original market can be obtained by solving the portfolio choice problem in the fictitious market via the martingale method. In Cvitanic and Karatzas (1992), after the fictitious completion, the interest rate and the drift terms of n stock prices are adjusted, and then, by applying the martingale method developed for a complete market, the constrained portfolio choice problem is solved, with investment being restricted to only the first m stocks. Jin and Zhang (2012) extend the method of fictitious completion to a market with asset returns following jump-diffusion processes. As the new market remains incomplete after fictitious completion due to unpredictable jumps, the martingale method used in Cvitanic and Karatzas (1992) is not easily applicable.

First of all, we lay out some notation for an unconstrained portfolio choice problem. For a constraint on portfolio weights given by a set K, the support function of the set K is defined by

$$\delta(x) = \sup_{\pi \in K} \left(-\sum_{i=1}^{n} \pi_i x_i \right), \ \forall \ x = (x_1, ..., x_n) \in \mathbb{R}^n,$$

with its effective domain denoted by

$$\widetilde{K} = \{x = (x_1, ..., x_n) \in \mathbb{R}^n; \delta(x) < \infty\}$$

In particular, for the case of prohibition of short-selling, we can show that $\delta(x)$ can be represented as

$$\delta(x) = \begin{cases} 0, & x_1 \geq 0, ..., x_n \geq 0, \\ \infty, & \text{otherwise.} \end{cases}$$

Hence, $\widetilde{K} = \{x = (x_1, ..., x_n) \in \mathbb{R}^n; x_1 \geq 0, ..., x_n \geq 0\}$.

Given a $\nu = (\nu_1, ..., \nu_n) \in \widetilde{K}$, we now introduce a new fictitious financial market in which there are no portfolio constraints, but the asst prices are adjusted in the same way as that in Cvitanic and Karatzas (1992). More specifically, the bond price $S_{0,t}^{(\nu)}$ evolves according to the differential equation

$$\begin{aligned} dS_{0,t}^{(\nu)} =& S_{0,t}^{(\nu)}[r(X_t) + \delta(\nu)]dt, \\ S_{0,0}^{(\nu)} =& 1. \end{aligned}$$

The prices of risky assets follow the linear stochastic differential equation

$$dS_{i,t}^{(\nu)} = S_{i,t-}^{(\nu)} \left[(b_i(X_t) + \nu_i + \delta(\nu))dt + \sigma_i^b(X_t)dB_t^S + \sigma_i^q(X_t)(Y \bullet dN_t)\right]$$

with $S_{i,0}^{(\nu)} = S_{i,0}$, $i = 1, ..., n$.

In order to understand how the fictitious-market approach works, we consider the case of the no-short-selling constraint introduced above. Hence, the constrained consumption-investment problem in the original market is converted into an unconstrained one in a set of fictitious markets via the adjustment of interest rates and the drift terms of stock prices. As illustrated in Proposition 3.1 below, the optimal consumption and portfolio strategy in the original market with investment constraints can be obtained by optimally

adjusting the interest rate and the stock price drifts in the fictitious markets, such that the stocks are relatively attractive and hence the investor holds positive positions in all stocks in the worst fictitious market. As a result, the optimal consumption and portfolio strategy in the worst fictitious market is admissible in the original market, leading to an optimal solution to the original portfolio choice problem.

For expository purposes, we will denote by $\mathcal{M}$ and $\mathcal{M}_v$ the original market and the fictitious market, respectively, with $\nu \in \widetilde{K}$. Given a pair of consumption rate c and portfolio rule π in the market $\mathcal{M}_v$, the corresponding wealth process $W_t(\nu)$ satisfies

$$\begin{aligned} dW_t(\nu) &= (r + \delta(\nu))W_t(\nu)dt - c_t dt + W_t(\nu)\pi_t(b + \nu - r\mathbf{1}_n)ds \\ &\quad + W_t(\nu)\pi_t\Sigma_b dB_t^S + W_{t-}(\nu)\pi_{t-}\Sigma_q(Y \bullet dN_t) \\ &= rW_t(\nu)dt - c_t dt + W_t(\nu)\pi_t(b - r\mathbf{1}_n)dt + W_t(\nu)(\delta(\nu) + \pi_s\nu)dt \\ &\quad + W_t(\nu)\pi_t\Sigma_b dB_t^S + W_{t-}(\nu)\pi_{t-}\Sigma_q(Y \bullet dN_t), \end{aligned} \tag{3.5}$$

with $W_0(\nu) = W_0$. Analogously, we denote by $\mathcal{A}_\nu(w_0)$ the set of pair of consumption rate c and portfolio rule π for which $W_t(\nu) \geq 0, \forall t \in [0, T]$. Then, the unconstrained portfolio choice in the market $\mathcal{M}_v$ can be written as

$$J^{(\nu)}(0, W_0, X_0) = \max_{(c,\pi)\in\mathcal{A}_\nu(w_0)} \mathbb{E}\left[\int_0^T e^{-\beta t}U(c_t)dt + \alpha e^{-\beta T}U(W_T(\nu))\right].$$

In contrast to the original market $\mathcal{M}$, the investor solves an unconstrained optimal portfolio choice problem in the fictitious market $\mathcal{M}_v$ given $\nu \in \widetilde{K}$. In other words, we convert the constrained portfolio choice problem in the original market $\mathcal{M}$ into an unconstrained one in a set of fictitious markets $\mathcal{M}_v$ with $\nu \in \widetilde{K}$. The proposition below presents an

equivalent optimality condition in the two problems.

Proposition 3.1. *If there exists one* $\nu^* \in \widetilde{K}$ *and optimal consumption-portfolio strategy* (c^*, π^*) *in the market* $\mathcal{M}_{\nu^*}$ *such that* $\pi^* \in \widetilde{K}$ *and* $\delta(\nu^*) + \pi^*\nu^* = 0$*, then* (c^*, π^*) *is a pair of consumption and optimal portfolio strategy in the market* $\mathcal{M}$*. And furthermore, the variable* $\nu^* \in \widetilde{K}$ *above solves the minimization problem below*

$$\min_{\nu \in \widetilde{K}} J^{(\nu)}(0, W_0, X_0) = \mathbb{E}\left[\int_0^T e^{-\beta t} U(c_t) dt + \alpha e^{-\beta T} U(W_T(\nu))\right]. \tag{3.6}$$

Proof. See Appendix B.1. □

Proposition 3.1 enables us to derive the constrained optimal portfolio weights in $\mathcal{M}$ by solving the unconstrained optimal portfolio choice problem in the market $\mathcal{M}_{\nu^*}$ provided that we can find the vector $\nu^* \in \widetilde{K}$. To better understand Proposition 3.1, we consider an infinitesimal interval $[t, t + dt]$ and assume the consumption rate c and portfolio strategy π are same in this interval for both markets $\mathcal{M}$ and $\mathcal{M}_{\nu^*}$. Then, given the same wealth W_t at time t in both markets $\mathcal{M}$ and $\mathcal{M}_{\nu^*}$, the equations (3.3) and (3.5) suggest that the wealth increment $dW_t(\nu)$ in the fictitious markets is as least as high as the one dW_t in the original market since $\delta(\nu) + \pi\nu \geq 0$. This may lead to higher terminal wealth in the fictitious markets than in the original market, and thus higher expected utility in the fictitious markets. In particular, the two quantities $dW_t(\nu)$ and dW_t are identical when $\delta(\nu) + \pi\nu = 0$ and hence, the corresponding expected utilities are the same. Consequently, as indicated by Proposition 3.1, the optimal consumption, portfolio strategy and the corresponding indirect value function are identical to those which are

optimal in the worst of all fictitious markets.

In Section 3.4, we illustrate how to use Proposition 3.1 to solve the optimal portfolio choice problem in several examples. As mentioned earlier, the martingale approach developed by Cvitanic and Karatzas (1992) does not directly apply in a jump-diffusion model, since the fictitious markets remain incomplete. In the present chapter, we will not employ the martingale method to solve the optimal portfolio choice in the jump-diffusion model. The result in Proposition 3.1 presents a property of the optimal vector $\nu^* \in \widetilde{K}$ and provides an alternative method to solve the portfolio choice problem. In the examples given in the next section, applying this result in combination with some results in Jin and Zhang (2012), we will develop a procedure for evaluation of $\nu^* \in \widetilde{K}$ and the corresponding optimal portfolio strategy π^* in the market $\mathcal{M}_{\nu^*}$.

In the meantime, the existence of such a vector $\nu^* \in \widetilde{K}$ is guaranteed by Proposition 3.2 below if an optimal portfolio rule exists in the original market in which an investor maximizes her expected utility from the terminal wealth only.

Proposition 3.2. *If there exists an optimal portfolio strategy π^* in the market $\mathcal{M}$, then there exists one $\nu^* \in \widetilde{K}$ and an optimal portfolio strategy π^* in the market $\mathcal{M}_{\nu^*}$ such that $\pi^* \in \widetilde{K}$ and $\delta(\nu^*) + \pi^*\nu^* = 0$ and furthermore, π^* is an optimal portfolio strategy in the market $\mathcal{M}$.*

Proof. See Appendix B.2. □

3.3 Power utility function and deterministic price coefficients

In this section, we apply the methods developed in the previous section to the case of the power utility function and deterministic price coefficients. For illustrative purposes, we do not consider intermediate consumption. Considering two realistic portfolio constraints respectively, we illustrate how our methods simplify and facilitate solving the constrained optimal portfolio as opposed to the standard HJB equation method. More specifically, we now consider the case where the coefficients $r(\cdot)$, $b_i(\cdot)$, $\sigma_i^b(\cdot)$, $\sigma_i^q(\cdot)$ and λ_k are deterministic functions on $[0,T]$ for $i = 1, ..., n$, $k = 1, ..., n-k$, and the utility function is given by:

$$U(x) = \begin{cases} \frac{x^{1-\gamma}}{1-\gamma}, & \forall x > 0 \\ -\infty, & \forall x \leq 0 \end{cases} \tag{3.7}$$

We use Σ to denote the $n \times n$ matrix $[\Sigma_b, \Sigma_q]$ and assume Σ is invertible almost surely. In the remainder of this chapter, for a portfolio π, we use $\widetilde{\pi}_b = (\widetilde{\pi}_{b1}, ..., \widetilde{\pi}_{bd})$ and $\widetilde{\pi}_q = (\widetilde{\pi}_{q1}, ..., \widetilde{\pi}_{q(n-d)})$ to denote $\pi\Sigma_b$ and $\pi\Sigma_q$, respectively. As can be seen from (3.3), given a portfolio π, $\pi\Sigma_b$ and $\pi\Sigma_q$ are its jump and diffusion exposures, respectively. In particular, $\widetilde{\pi}_{qk}$ is the k-th jump exposure and $\widetilde{\pi}_{bi}$ is the i-th diffusion exposure. Given $\nu \in \widetilde{K}$, we define the relative risk premium as

$$\theta_t(\nu) = \begin{pmatrix} \theta_t^b(\nu) \\ \theta_t^q(\nu) \end{pmatrix} = \Sigma^{-1}[b + \nu - r\mathbf{1}_n + \mathbf{\Sigma}_q(\lambda \bullet \alpha)] \tag{3.8}$$

where $\theta_t^b(\nu) = (\theta_{1,t}^b(\nu), ..., \theta_{d,t}^b(\nu))^\top$, $\lambda = (\lambda_1, ..., \lambda_{n-d})^\top$, $\theta_t^q(\nu) = (\theta_{1,t}^q(\nu), ..., \theta_{n-d,t}^q(\nu))^\top$, $\alpha = (\alpha_1, ..., \alpha_{n-d})^\top$ and $\lambda \bullet \alpha = (\lambda_1\alpha_1, ..., \lambda_{n-d}\alpha_{n-d})^\top$ with $\alpha_k = \int_{E_k} z\Phi_k(dz)$, the expected

size of the k-th jump, for $k = 1, ..., n-d$. We now rewrite

$$\Sigma^{-1} = \begin{pmatrix} \Sigma_1^{-1} \\ \Sigma_2^{-1} \end{pmatrix},$$

where Σ_1^{-1} and Σ_2^{-1} are $d \times n$ and $(n-d) \times n$ matrices, respectively. Note that

$$\Sigma^{-1}\mathbf{\Sigma}_q = \begin{pmatrix} \mathbf{0}_{d\times(n-d)} \\ \mathbf{I}_{n-d} \end{pmatrix}$$

since $\Sigma^{-1}[\mathbf{\Sigma}_b, \mathbf{\Sigma}_q] = \mathbf{I}_n$, where $\mathbf{0}_{d\times(n-d)}$ is the $d \times (n-d)$ matrix of zeros and $\mathbf{I}_n$ is the $n \times n$ identity matrix. Hence, $\theta_t^b(\nu)$ and $\theta_t^q(\nu)$ can be rewritten as

$$\theta_t^b(\nu) = \Sigma_1^{-1}(b + \nu - r\mathbf{1}_n) = \theta_t^b + \Sigma_1^{-1}\nu, \tag{3.9}$$

$$\theta_t^q(\nu) = \Sigma_2^{-1}(b + \nu - r\mathbf{1}_n) + \lambda \bullet \alpha = \theta_t^q + \Sigma_2^{-1}\nu + \lambda \bullet \alpha, \tag{3.10}$$

with $\theta_t^q = (\theta_{1,t}^q, ..., \theta_{n-d,t}^q)^\top = \Sigma_2^{-1}(b - r\mathbf{1}_n)$ and $\theta_t^b = (\theta_{1,t}^b, ..., \theta_{d,t}^b)^\top = \Sigma_1^{-1}(b - r\mathbf{1}_n)$. First we present the main result of this section which will be used below for two portfolio constraints, respectively. For illustrative purposes, we assume $\gamma > 1$. Applying Proposition 3.2 to this model, we have

Proposition 3.3. *Under assumptions above, the optimal ν^* in Proposition 3.1 solves the following optimization problem:*

$$\inf_{\nu\in\widetilde{K}} \sup_{\widetilde{\pi}_{qk}\in F_k, k=1,...,n-d} f(\nu, \widetilde{\pi}_q) = \frac{1}{2\gamma}||\theta_t^b(\nu)||^2 + \delta(v) + \sum_{k=1}^{n-d} D_k(\widetilde{\pi}_{qk}),$$

where $D_k(\widetilde{\pi}_{qk})$ is defined in Appendix B.3 and F_k denotes the set of all $\widetilde{\pi}_{qk}$ which satisfy the no-bankruptcy condition: $\widetilde{\pi}_{qk} z > -1, \forall z \in A_k$.

Proof. See Appendix B.3. □

In the minimax problem stated above, the minimization problem is due to the minimization problem (3.6) in Proposition 3.1, while the maximization problem is obtained from the evaluation of optimal expected utility or indirect value function in each fictitious market in (3.6). As can be seen from Lemma B.3.1 in Appendix B.3, maximizing expected utility from the terminal wealth in each fictitious market is equivalent to maximizing the exposures $\widetilde{\pi}_{qk}$ to jumps. Moreover, the minimax problem can be converted to a combination of a minimization problem with an equivalent Nonlinear Linear Programming problem by embedding additional constraints of the objective function. Numerically, we can adopt a sequential quadratic programming method to solve this problem (See Brayton et al. (1979)).

3.3.1 Prohibition of borrowing

In this section, we assume the investor is prohibited from borrowing. As described in Section 3.2, the portfolio constraint set $K = \{\pi = (\pi_1, ..., \pi_n\} \in \mathbb{R}^n; \sum_{i=1}^n \pi_i \leq 1\}$, and the corresponding support function $\delta(x)$ can be represented as

$$\delta(x) = \begin{cases} -x_1, & x_1 = ... = x_n \leq 0, \\ \infty, & \text{otherwise}, \end{cases}$$

implying $\widetilde{K} = \{x = (x_1, ..., x_n) \in \mathbb{R}^n; x_1 = ... = x_n \leq 0\}$. Let $a^b(t) = (a_1^b(t), ..., a_d^b(t))^\top = \Sigma_1^{-1}\mathbf{1}_n$ and $a^q(t) = (a_1^q(t), ..., a_{n-d}^q(t))^\top = \Sigma_2^{-1}\mathbf{1}_n$. We then have the following result.

Proposition 3.4. *Suppose the investor is prohibited from borrowing. Then, the optimal vector* $\nu^* = (\nu_1^*, ..., \nu_1^*)$ *solves the following optimization problem:*

$$\inf_{\nu \in \widetilde{K}} \sup_{\widetilde{\pi}_{qk} \in F_k, k=1,...,n-d} f(\nu, \widetilde{\pi}_q) = \frac{1}{2\gamma} \sum_{i=1}^{d} (\theta_{i,t}^b + a_i^b(t)\nu_1)^2 - \nu_1 + \sum_{k=1}^{n-d} D_k(\widetilde{\pi}_{qk}), \tag{3.11}$$

Proof. See Appendix B.4. □

To compare our method with the standard HJB equation method, we consider a model similar to the one in Das and Uppal (2004) where all coefficients are constants. In this model, there are n risky assets driven by $n-1$ diffusions and one jump with the jump capturing the systemic risk. For illustrative purposes, we assume the jump size has support $A_1 = (-1, \infty)$, implying, by Appendix B.3, the feasible set for $\widetilde{\pi}_{q1}$ is $F_1 = [0, 1)$. As in Das and Uppal (2004), by conjecturing $J(t, W, X) = \frac{W^{1-\gamma}}{1-\gamma}(f(X,t))^\gamma$ and taking the first order condition with respect to π in HJB equation, we have

$$0 = b - r\mathbf{1}_n - \gamma \Sigma_b \Sigma_b^\top \pi^\top + \lambda_1 \int_{A_1} (1 + \pi \mathbf{\Sigma}_{q1} z)^{-\gamma} \mathbf{\Sigma}_{q1} z \Phi_1(dz) + y_1 \mathbf{\Sigma}_{q1} + y_2 \mathbf{1}_n,$$

where y_1 is called the Lagrange Multiplier for the jump exposure constraint, $\pi \mathbf{\Sigma}_{q1} \in F_1$, satisfying the standard complimentary slackness conditions

$$\pi \mathbf{\Sigma}_{q1} > 0,\ y_1 = 0 \quad \text{or} \quad \pi \mathbf{\Sigma}_{q1} = 0,\ y_1 \geq 0,$$

and similarly y_2 is the Lagrange Multiplier for the borrowing constraint. As a result, to use the HJB equation method to solve the portfolio choice problem in a market with n risky assets, one has to solve n nonlinear equations with $n+2$ variables, $\pi_1, ..., \pi_n$, y_1 and y_2, and with two constraints, which may be computationally intensive for a large n.

In contrast, by differentiating (3.11) in Proposition 3.4 with respect to $\widetilde{\pi}^*_{q1}$, we have the first-order conditions given by

$$\theta^q_{1,t} + a^q_1(t)\nu_1 + \lambda_1 \int_{A_1} z \left(\widetilde{\pi}^*_{q1} z + 1\right)^{-\gamma} \Phi_1(dz) + y_1 = 0,$$

where y_1 is the Lagrange Multiplier for jump exposure constraint, $\widetilde{\pi}^*_{q1} \in F_1$. And then, by taking derivative with respect to v_1, we have the first-order conditions given by

$$\frac{1}{\gamma} \sum_{i=1}^{n-1} a^b_i(t)(\theta^b_{i,t} + a^b_i(t)v_1) - 1 + \widetilde{\pi}^*_{q1} a^q_1(t) + y_2 = 0,$$

where y_2 is the Lagrange Multiplier for the constraint: $\nu_1 \leq 0$. Consequently, we only need to solve two nonlinear equations with four variables ν_1, $\widetilde{\pi}^*_{q1}$, y_1 and y_2 and with two constraints, regardless of the number n. This is a significant reduction in computational burden when the number n is large.

3.3.2 Prohibition of trading

In this section we consider the model where the investor is prohibited from trading m ($m < n$) risky assets out of the n risky assets. For simplicity, we assume that the investor is prohibited from trading assets $n - m + 1$ to n. In this case, as derived in Cvitanic and Karatzas (1992), the portfolio constraint set $K = \{\pi = (\pi_1, ..., \pi_n\} \in \mathbb{R}^n;$ $\pi_{n-m+1} = ... = \pi_n = 0\}$, and the corresponding support function $\delta(x)$ can be represented as

$$\delta(x) = \begin{cases} 0, & x_1 = ... = x_{n-m} = 0, \\ \infty, & \text{otherwise}, \end{cases}$$

implying $\widetilde{K} = \{x = (x_1, ..., x_n) \in \mathbb{R}^n; x_1 = ... = x_{n-m} = 0\}$. This model corresponds to the incompleteness in a pure-diffusion market, where the number of traded risky assets is less than the number of diffusions. Then, applying Proposition 3.3, we have the following result.

Proposition 3.5. *The optimal solution* $\nu^* = (0, ..., 0, \nu^*_{n-m+1}, .., \nu^*_n) \in \widetilde{K}$ *in Proposition 3.1 solves the following minimax problem:*

$$\inf_{\nu \in \widetilde{K}} \sup_{\widetilde{\pi}_{qk} \in F_k, k=1,...,n-d} f(\nu, \widetilde{\pi}_q) = \frac{1}{2\gamma} ||\theta^b_t(\nu)||^2 + \sum_{k=1}^{n-d} D_k(\widetilde{\pi}_{qk}),$$

with $\delta(\nu) = 0$.

Proof. The proof is similar to that of Proposition 3.4 and is omitted. □

To better understand the algorithm in Proposition 3.5, we consider the model in Das and Uppal (2004) where all coefficients are constants. In their model, there are n risky assets driven by n diffusions and one jump with the jump capturing the systemic risk. We assume the same jump size distribution as the one in the last section. As with the last section, in their approach, solving the optimal portfolio weights reduces to solving n nonlinear equations with $n + 1$ variables and with two constraints, which may be computationally intensive for a large n. To apply Proposition 3.5 to this model, we adopt the "fictitious completion" approach in Karatzas et al. (1991) by adding one fictitious stock with price following equation

$$dS_{n+1,t} = S_{n+1,t-}(b_{n+1}dt + Y_1 dN_{1,t}),$$

where the drift term b_{n+1} is determined below. We can then convert the original portfolio choice problem to the one in a model where there are $n+1$ risky assets and the investor is not allowed to trade the $(n+1)$-st risky asset. In particular, the portfolio constraint set $K = \{\pi = (\pi_1, ..., \pi_{n+1}\} \in \mathbb{R}^{n+1}; \pi_{n+1} = 0\}$ and $\widetilde{K} = \{x = (x_1, ..., x_{n+1}) \in \mathbb{R}^n; x_1 = ... = x_n = 0\}$ with the support function $\delta(x)$ given by $\delta(x) = 0$ if $x \in \widetilde{K}$; $\delta(x) = \infty$ otherwise. Given $\nu = (0, ..., 0.v_{n+1}) \in \widetilde{K}$, the price of the fictitious stock is modified as

$$dS^{(\nu)}_{n+1,t} = S^{(\nu)}_{n+1,t-}((b_{n+1} + v_{n+1})dt + Y_1 dN_{1,t}),$$

while the prices of the original bond and n stocks remain unchanged since $\nu_1 = ... = \nu_n = 0$ and $\delta(\nu) = 0$. And furthermore, $b_{n+1} + v_{n+1}$ can be solved by Proposition 3.5. In contrast, as with the previous section, by applying the method in this chapter, we only need to solve two nonlinear equations with four variables, and with two constraints, regardless of the number n. As a result, this method may lead to a significant reduction in computational burden for a large number n.

3.4 Numerical examples

In this section, we illustrate the applications of results obtained in the previous sections with several numerical examples. We investigate the effects of the no-short-selling and/or the no-borrowing constraints on the performance of the optimal portfolios in a four-stock model. We further quantify the portfolio improvements for including derivatives with the no-short-selling constraint.

3.4.1 Example I: constrained investment in a multi-stock model

In this section, we use a jump-diffusion model in Chacko and Viceira (2003), and Jin and Zhang (2012) to investigate the effects of no-short-selling and/or no-borrowing constraints on the performance of the optimal portfolios. More specifically, we model the stock price dynamics with asymmetric upward (positive) and downward (negative) jumps:

$$\begin{aligned}\frac{dS_i(t)}{S_i(t)} =&\mu_i dt + \sigma^z_{i1} dz_{1t} + \sigma^z_{i2} dz_{2t} + \sigma^z_{i3} dz_{3t} + \sigma^z_{i4} dz_{4t} \\ &+ \sigma^q_{i1} \left[\exp(Y_u) - 1\right] dN_{u,t} + \sigma^q_{i2} \left[\exp(-Y_d) - 1\right] dN_{d,t}\end{aligned}$$

where $i = 1, 2, 3, 4$. $\mu_i, \sigma^z_{i1}, \sigma^z_{i2}, \sigma^z_{i3}, \sigma^z_{i4}, \sigma^q_{i1}$ and σ^q_{i2} are all constants with $\sigma^q_{i1}, \sigma^q_{i2} \in [0, 1]$. Y_u and Y_d are both positive random variables. The quantities $\left[\exp(Y_u) - 1\right] dN_{u,t}$ and $\left[\exp(-Y_d) - 1\right] dN_{d,t}$ represent the common positive and negative jumps, respectively, with intensities λ_u and λ_d. Y_u has exponential distribution, with density

$$f(Y_u) = \begin{cases} \frac{1}{\eta_u} \exp\left(-\frac{Y_u}{\eta_u}\right), & \forall Y_u > 0 \\ 0, & \forall Y_u \leq 0 \end{cases}$$

where η_u is a positive constant. Y_d has an exponential distribution, with density

$$f(Y_d) = \begin{cases} \frac{1}{\eta_d} \exp\left(-\frac{Y_d}{\eta_d}\right), & \forall Y_d > 0 \\ 0, & \forall Y_d \leq 0 \end{cases}$$

where η_d is a positive constant.

This model has 32 parameters in total, of which the four parameters η_u, η_d, λ_u and λ_d describe the jump risk.

Data and estimation

To implement and evaluate the model specified, we simply use the parameters estimated by Jin and Zhang (2012) in which four equity indices are chosen from the global market including S&P 500 index (SPX), FESE 100 (UKX), HSI-Hang Seng (HSI) and Mexico IPC (MEX). The data of daily USD-valued index prices are collected from Bloomberg for the period of 1/1/2005 to 10/9/2008. The estimation of parameters is obtained by using the method of moments; details of the estimation procedure can be found in Jin and Zhang (2012). Table 3.1 reports the estimation results of the four indices used in the numerical experiment.

Effects of the no-short-selling constraint on portfolio performance

In this section, we measure the economic impact of the no-short-selling constraint on the portfolio selection problem by adopting the measurement developed in Liu and Pan (2003). We compute the certainty-equivalent wealth for the optimal portfolio allocations in two markets with and without no-short-selling constraint and then use the difference of return rates on the certainty-equivalent wealth as a measurement of the effect of the no-short-selling constraint on portfolio performance. More precisely, the certainty-equivalent wealth $\mathcal{W}^*$ satisfies

$$(\mathcal{W}^*)^{1-\gamma}/(1-\gamma) = J(0, W_0).$$

Table 3.1: *Parameter estimates for the jump-diffusion model*

This table reports the parameter estimates using the method of moments, based on the unconditional moments of the USD-valued historical returns of SPX, UKX, HSI and MEX from 1/1/2005 to 10/9/2008. Jump density parameters are common to all countries. Standard deviations, based on the Jacobian of the vector of moment conditions with respect to model parameters, are reported next to respective parameter estimates.

	SPX		UKX		HSI		MEX	
	para	stdev	para	stdev	para	stdev	para	stdev
μ	0.2683	0.0202	0.2956	0.0180	0.4661	0.0261	0.6317	0.0354
σ_1^z	0.0427	0.0361	0.0431	0.0336	0.1083	0.0258	0.0735	0.0318
σ_2^z	0.0626	0.0349	0.0380	0.0437	0.1249	0.0312	0.0850	0.0257
σ_3^z	0.1331	0.0463	0.0490	0.0412	0.1364	0.0276	0.0866	0.0435
σ_4^z	0.1304	0.0594	0.1317	0.0540	0.0571	0.0554	0.1084	0.0594
σ_1^q	0.5592	0.0471	0.9385	0.0970	0.5509	0.1333	0.6787	0.1773
σ_2^q	0.6893	0.0601	0.7668	0.0594	0.5677	0.1426	0.8168	0.2064

	Common	
	para	stdev
λ_u	0.5754	0.5435
λ_d	21.3366	1.5914
η_u	0.0516	0.0136
η_d	0.0302	0.0134

First we consider an optimal portfolio allocation in the market without constraint. The detailed procedure for solving the optimal portfolio and the corresponding indirect value function is given in Appendix F. We use $\nu = (0, 0, 0, 0, \nu_5, \nu_6) \in \widetilde{K}$ to denote the optimal solution in Proposition 3.5 and let $\widetilde{v} = (\nu_5, \nu_6)^\top$. In particular, the certainty-equivalent wealth can be obtained as

$$\mathcal{W}^* = W_0 \exp\left(\frac{T}{2\gamma}(\theta_1^b)^\top \theta_1^b + rT + TD_1(\widetilde{\pi}_q)\right)$$

where $W_0 = 1$ and

$$\begin{aligned}
\theta_1^b &= \left(\Sigma^z\right)^{-1}(\mu - r\mathbf{1}_4 - \Sigma_q(\widetilde{v} - r\mathbf{1}_2)) \\
D_1(\widetilde{\pi}_q) =& \widetilde{\pi}_{q1}(\nu_5 - r) + \frac{\lambda_u}{\eta_u(1-\gamma)} \int_0^\infty [(1 + \widetilde{\pi}_{q1} z)^{1-\gamma} - 1](1+z)^{-\frac{1}{\eta_u}-1} dz \\
&+ \widetilde{\pi}_{q2}(\nu_6 - r) + \frac{\lambda_d}{\eta_d(1-\gamma)} \int_{-1}^0 [(1 + \widetilde{\pi}_{q2} z)^{1-\gamma} - 1](1+z)^{\frac{1}{\eta_d}-1} dz
\end{aligned}$$

Similarly, with $\nu = (\nu_1, \nu_2, \nu_3, \nu_4, \nu_5, \nu_6) \in \widetilde{K}$ denoting the corresponding optimal solution, we can derive that the certainty-equivalent wealth with the short-selling constraint is

$$\mathcal{W}^*_{\text{no-short}} = W_0 \exp\left(\frac{T}{2\gamma}(\theta_2^b)^\top \theta_2^b + rT + TD_2(\widetilde{\pi}_q)\right)$$

where

$$\begin{aligned}
\theta_2^b &= \left(\Sigma^z\right)^{-1}(\mu + \widetilde{v}_1 - r\mathbf{1}_4 - \Sigma^q(\widetilde{v}_2 - r\mathbf{1}_2)) \\
D_2(\widetilde{\pi}_q) =& \widetilde{\pi}_{q1}(\nu_5 - r) + \frac{\lambda_u}{\eta_u(1-\gamma)} \int_0^\infty [(1 + \widetilde{\pi}_{q1} z)^{1-\gamma} - 1](1+z)^{-\frac{1}{\eta_u}-1} dz \\
&+ \widetilde{\pi}_{q2}(\nu_6 - r) + \frac{\lambda_d}{\eta_d(1-\gamma)} \int_{-1}^0 [(1 + \widetilde{\pi}_{q2} z)^{1-\gamma} - 1](1+z)^{\frac{1}{\eta_d}-1} dz,
\end{aligned}$$

where $\widetilde{v}_1 = (\nu_1, \nu_2, \nu_3, \nu_4)^\top$ and $\widetilde{v}_2 = (\nu_5, \nu_6)^\top$.

Finally, the measurement of the performance improvement is defined by

$$R^W = \frac{\log \mathcal{W}^* - \log \mathcal{W}^*_{\text{no-short}}}{T} \tag{3.12}$$

Generally speaking, R^W can be considered as an annual return rate, which indicates how much better-off it can be by dropping off the no-short-selling constraint, which also gauges the impact of the no-short-selling constraint on portfolio performance. It is evident that the performance of an optimal portfolio allocation without the no-short-selling constraint cannot be worse than that with the no-short-selling constraint.

Table 3.2 provides a quantitative analysis of the performance improvements based on a variety of risk aversion levels, and we assume that the investment horizon is 1 year. Intuitively, the more risk averse the investor is, the less leveraged the optimal allocation will be. According to Table 3.2, the performance improvement decreases dramatically while the magnitude of risk aversion increases from a small value to a extremely large level. For example, given $\gamma = 14$ the improvement rate is 2.69 and it decreases to 0.19 when γ increases to 200. $R^W = 0.19$ means that the return rate of an optimal portfolio allocation without constraint is approximately 19% higher than that of an optimal portfolio allocation with the no-short-selling constraint.

For low levels of risk aversion, the performance improvement is abnormally high. We can also observe that the corresponding unconstrained portfolio weights are extremely large. This is because an investor who has little fear of the potential risk is willing to have large exposure to some risky assets with high expected returns. With a highly leveraged portfolio allocation, abnormal return rates are attainable. As in Egloff et al. (2010), we

choose a particular high level of risk aversion ($\gamma = 200$) to prevent the allocation from being overly leveraged. We use the same value of γ as a common risk aversion level of investors, and conclude that the no-short-selling constraint has a significant impact on the portfolio performance.

When short-selling is prohibited, a very different situation occurs. No matter how less risk-averse the investor is, a conservative allocation is always observed, which is no surprise. Roughly speaking, an investor cannot increase the leverage too much without taking short positions on risky assets. Hence, the expected returns are also very limited, compared to those without constraint. In conclusion, the no-short-selling constraint can lower the portfolio performance due to the prohibition of leverage. The more risk averse the investor is, the less leveraged the optimal portfolio allocation will be and thus, the smaller impact the no-short-selling constraint will behave.

A cautionary note is that the significant impact of the no-short-selling constraints on the portfolio performance may be caused by imprecise estimates of moments of stock returns. Financial econometricians seem to agree that it is feasible to obtain good estimates of variance parameters, but notoriously difficult to estimate expected returns (see Merton (1980) for detailed discussions). In the present model, the optimal portfolio strategy is a myopic mean-variance portfolio, due to the constant investment opportunity set, and hence the expected returns matter for the investor. As is well understood, the mean-variance efficient portfolio constructed using sample moments often involves extreme weights in a number of assets due to imprecise estimates of the true mean, variance and covariance

matrix. Given the relatively short data set in this example, the estimates of model parameters reported in Table 3.1 are likely to be biased. In particular, asset 1 may be underpriced while assets 2 and 4 may be overpriced. This leads to a huge excess demand for asset 1 and huge supply of assets 2 and 4. This situation can not be an equilibrium. Moreover, when a large data set becomes available, the estimates of parameters will be improved and hence the significant improvement in portfolio performance may not be observed.

Table 3.2: *Performance comparison between no-short-selling constrained and unconstrained portfolios*

This table reports the performance comparison between the optimal portfolios with and without the no-short-selling constraint given different magnitudes of risk aversion. R^W is the difference of portfolio performances in terms of annualised, continuously compounded return rates. For $i = 1, 2, 3, 4$, $\omega_i = \pi_i / \sum_{i=1}^{4} \pi_i$ is the relative portfolio weight of i-th asset on risky assets. There are six different levels of risk aversion including $\gamma = \{12, 14, 16, 18, 20, 200\}$. The risk-free rate is 1% and the investment horizon T is 1. The numbers R^W and ω_i are in percentages.

		Without Constraint				With Constraint			
γ	R^W	ω_1	ω_2	ω_3	ω_4	ω_1	ω_2	ω_3	ω_4
12	3.13	11.81	-6.84	1.85	-5.81	0	0	40.28%	59.72%
14	2.69	11.71	-6.73	1.80	-5.79	0	0	39.83%	60.17%
16	2.35	11.62	-6.61	1.76	-5.76	0	0	39.65%	60.35%
18	2.09	11.53	-6.51	1.72	-5.74	0	0	39.55%	60.45%
20	1.88	11.45	-6.41	1.68	-5.72	0	0	39.48%	60.52%
200	0.19	9.35	-3.89	0.70	-5.16	0	0	39.26%	60.74%

Table 3.3: *Performance comparison between no-short-selling constrained and unconstrained portfolios (unnormalized weights).*

This table reports the performance comparison between the optimal portfolios with and without the no-short-selling constraint given different magnitudes of risk aversion. R^W is the difference of portfolio performances in terms of annualised, continuously compounded return rates. For $i = 1, 2, 3, 4$, $\omega_i = \pi_i / \sum_{i=1}^{4} \pi_i$ is the relative portfolio weight of i-th asset on risky assets. There are six different levels of risk aversion including $\gamma = \{12, 14, 16, 18, 20, 200\}$. The risk-free rate is 1% and the investment horizon T is 1. The numbers R^W and ω_i are in percentages.

		Without Constraint				With Constraint			
γ	R^W	ω_1	ω_2	ω_3	ω_4	ω_1	ω_2	ω_3	ω_4
12	7.25	16.53	-9.58	2.59	-8.13	0	0	0.48	0.72
14	6.99	18.15	-10.43	2.79	-8.97	0	0	0.52	0.78
16	6.83	16.85	-9.59	2.55	-8.35	0	0	0.50	0.75
18	6.72	16.49	-9.31	2.46	-8.21	0	0	0.44	0.66
20	6.61	17.29	-9.68	2.54	-8.64	0	0	0.41	0.64
200	0.56	1.87	-0.78	0.14	-1.03	0	0	0.09	0.14

Effects of the no-borrowing constraint on portfolio performance

The no-short-selling constraint has a significant impact on portfolio performance, which has been analyzed above. It is also interesting to quantify the economic effects if the no-borrowing constraint is imposed. With the framework developed in this chapter, it is easy to implement a constrained allocation problem which can be solved precisely and quickly.

In Table 3.4, we give a quantitative analysis of the economic effects for a variety of relative risk aversion coefficients. Since we allow short-selling here, the constrained optimal allocations short the second and the fourth assets in all the cases. Surprisingly, the economic loss of prohibiting borrowing is larger than that of the no-short-selling constraint. For example, given a risk-aversion level of $\gamma = 12$, the economic loss of prohibiting short-selling is 3.13 while the loss of no-borrowing is 7.25. This might be mainly due to the inability to enhance the level of leverage, although an investor can achieve better benefit by short-selling some risky assets.

The performance improvements are very significant, and decrease with the increasing of the risk aversion level. Even with an extremely high level of $\gamma = 200$, the economic gain of borrowing is 0.56. The intuitive explanation is similar to that in the no-short-selling case as both constraints limit the ability of leveraging. Hence, the less risk averse the investor is, the less impact the constraint has. It is intuitive to observe that economic difference is small providing high risk averse level. This is because that an extreme conservative investor will not consider too much about lifting the leverage level by extreme borrowing

or undertaking high short positions.

The choice of the risk averse level follows the common choice of existing relevant literature. Usually, the normal level is assumed to be 3 or 5. The medium level falls between 7 and 9. Here, we also test the extreme case of $\gamma = 200$. It is hard to backout the risk averse level from the market in a way of calibration or estimation. Especially, our purpose is to explain the market in a qualitative sense. For example, we would want to investigate the impact of risk averse level on the portfolio choice problem rather than determine the exact portfolio weights.

Table 3.4: *Performance comparison between no-borrowing constrained and unconstrained portfolios*

This table reports the performance comparison between the optimal portfolios with and without the no-borrowing constraint given different magnitudes of risk aversion. R^W is the difference of portfolio performances in terms of annualised, continuously compounded return rates. For $i = 1, 2, 3, 4$, $\omega_i = \pi_i / \sum_{i=1}^{4} \pi_i$ is the relative portfolio weight of i-th asset on risky assets. There are six different levels of risk aversion including $\gamma = \{12, 14, 16, 18, 20, 200\}$. The risk-free rate is 1% and the investment horizon T is 1. The numbers R^W and ω_i are in percentages.

		Without Constraint				With Constraint			
γ	R^W	ω_1	ω_2	ω_3	ω_4	ω_1	ω_2	ω_3	ω_4
12	7.25	11.81	-6.84	1.85	-5.81	4.71	-2.29	0.35	-1.77
14	6.99	11.71	-6.73	1.80	-5.79	4.55	-2.19	0.31	-1.67
16	6.83	11.62	-6.61	1.76	-5.76	4.43	-2.08	0.27	-1.62
18	6.72	11.53	-6.51	1.72	-5.74	4.36	-1.99	0.23	-1.60
20	6.61	11.45	-6.41	1.68	-5.72	4.27	-1.91	0.20	-1.59
200	0.56	9.35	-3.89	0.70	-5.16	1.56	-0.98	0.09	-0.67

Table 3.5: *Performance comparison between no-borrowing constrained and unconstrained portfolios (unnormalized weights).*

This table reports the performance comparison between the optimal portfolios with and without the no-borrowing constraint given different magnitudes of risk aversion. R^W is the difference of portfolio performances in terms of annualised, continuously compounded return rates. For $i = 1, 2, 3, 4$, $\omega_i = \pi_i / \sum_{i=1}^{4} \pi_i$ is the relative portfolio weight of i-th asset on risky assets. There are six different levels of risk aversion including $\gamma = \{12, 14, 16, 18, 20, 200\}$. The risk-free rate is 1% and the investment horizon T is 1. The numbers R^W and ω_i are in percentages.

		Without Constraint				With Constraint			
γ	R^W	ω_1	ω_2	ω_3	ω_4	ω_1	ω_2	ω_3	ω_4
12	7.25	16.53	-9.58	2.59	-8.13	4.38	-2.13	0.33	-1.65
14	6.99	18.15	-10.43	2.79	-8.97	4.14	-2.00	0.28	-1.52
16	6.83	16.85	-9.59	2.55	-8.35	3.90	-1.83	0.24	-1.43
18	6.72	16.49	-9.31	2.46	-8.21	4.10	-1.87	0.22	-1.50
20	6.61	17.29	-9.68	2.54	-8.64	3.89	-1.74	0.18	-1.45
200	0.56	1.87	-0.78	0.14	-1.03	0.23	-0.15	0.01	-0.10

3.4.2 Example II: constrained investment with derivatives

In this subsection, we solve the asset allocation problem given a jump-diffusion market in which an investor can trade not only risky stocks but also derivatives. The market actually takes into account three different risk factors, including the diffusive shock, the jump risk and the volatility risk.

For tractability and comparison, we adopt the dynamics defined in Liu and Pan (2003) to evaluate how valuable derivatives are in a setting that multiple risk factors play together. The dynamics of the underlying asset is defined as:

$$dS_t = (r + \eta\sigma^2 + \mu(\lambda - \lambda^Q)\sigma^2)S_t dt + \sigma S_t dB_t + \mu S_{t-}(dN_t - \lambda\sigma^2 dt) \tag{3.13}$$

where r is the risk-free rate, σ is the constant volatility, and B is a standard Brownian motion and N is a pure-jump process with stochastic arrival intensity $\lambda\sigma^2$ for a constant $\lambda > 0$. The constant η captures the equity premium of the diffusion component and λ^Q captures the equity premium of the jump. Denote O_t as the derivative price at time t and $f(\cdot)$ as the payoff function. Let τ denote the time to maturity, and we can have $O_t = \frac{1}{\pi_t} E_t[\pi_\tau f(S_\tau)]$, for any $t \leq \tau$. Suppose $\{\pi_t, 0 \leq t \leq T\}$ is the pricing kernel which is defined as

$$d\pi_t = -\pi_t \left(r dt + \eta\sigma dB_t\right) + \left(\frac{\lambda^Q}{\lambda} - 1\right) \pi_{t-}(dN_t - \lambda\sigma^2 dt) \tag{3.14}$$

where $\pi_0 = 0$. Apparently, the ratio λ^Q/λ controls the risk premium from the jump N. Consistent with the pricing kernel π_t, we can obtain the dynamics of the derivative price:

$$dO_t = rO_t dt + g_s S_t(\eta\sigma^2 dt + \sigma dB_t) + \Delta g \left[(\lambda - \lambda^Q)\sigma^2 dt + dN_t - \lambda\sigma^2 dt\right] \tag{3.15}$$

where g_s measures the sensitivity of the price of the derivative used to infinitesimal changes in the stock price, and Δg measures the change in the price of the derivative for each jump in the stock price. v_0 is the constant variance. Details of the setting can be found in Liu and Pan (2003). In this example, the investor can invest not only in risky stock but also in European puts. We let ϕ and ψ denote the portfolio weights on the stock and the derivative respectively. The corresponding wealth process then satisfies the following self-financing condition

$$\begin{aligned} dW_t =& rW_t dt + \left[\phi_t(\eta\sigma^2 - \mu\lambda^Q\sigma^2) + \frac{\psi_t(g_s S_t \eta\sigma^2 - \Delta g \lambda^Q \sigma^2)}{O_t}\right] W_t dt \\ &+ \left[\phi_t\sigma + \frac{\psi_t g_s S_t \sigma^2}{O_t}\right] W_t dB_t + \left[\phi_t\mu + \frac{\psi_t \Delta g}{O_t}\right] W_{t-} dN_t. \end{aligned}$$

The objective of the investor is to maximize the expected utility of his terminal wealth W_T,

$$\max_{\phi_t \geq 0, \psi_t, 0 \leq t \leq T} \mathbb{E}\left[\frac{W_T^{1-\gamma}}{1-\gamma}\right],$$

where $\gamma > 1$. As with the example in Section 3.4.1, this problem can be solved by using Proposition 3.3 but we omit the procedure to save the space.

We choose $r = 5\%$ as the constant risk-free rate, $\eta = 8\%$ as the diffusion premium and $\sigma = 15\%$ as the constant volatility. We consider three different jump sizes: small jump $\mu = -10\%$ in every 10 years, medium jump $\mu = -25\%$ in every 50 years and large jump $\mu = -50\%$ in every 200 years. We also let the jump-risk premium λ^Q/λ vary from 1 to 5, while $\lambda^Q/\lambda = 1$ indicates that there is no jump risk. In Table 3.6, we present the optimal asset allocations with and without options, which are actually based on the

same parameters in Liu and Pan (2003). However, the model in this chapter differs from theirs in that the investor is not allowed to short-sell the stock but she is allowed to either write or buy puts. As observed in Liu and Pan (2003), when the compensation ratio λ^Q/λ increases to a high level, a risk averse investor might want to write puts and short-sell the risky stock to earn the high premium associated with jump risk; however, if the constraint prevents her from short-selling, the allocation of the stock is close to zero. Hence, it would be interesting to see how the no-short-selling constraint affects the performance of the optimal portfolio with put options available for investment.

We can find several negative positions of puts in the optimal allocations. Sometimes the short positions are relatively large. The portfolio allocations are very sensitive to the jump risk premium λ^Q/λ. If the ratio is large, the investor is willing to take large short positions in puts. With the no-short-selling constraint, the holding of stocks can not be negative. Therefore, if the jump risk premium increases to a high level, say 5, the holding of the stock will be close to zero. It is because the investor wants to earn premium associated with jump risk by short-selling stocks and writing puts; however, she can only write puts because of the no-short-selling constraint on the stock. This also leads to much smaller positions in puts. We can still observe the "switch" observed in Liu and Pan (2003), which is a break-even point that the relative attractiveness of jump risks and diffusive risks. In other words, the investor prefers writing puts to purchasing puts.

We quantify the portfolio improvements for including puts in portfolio allocations. The difference R^W between certainty-equivalent wealth which has been defined in (3.12) is used

to measure the improvements. The portfolio improvements for including puts are reported in terms of annualized, continuously compounding returns in Table 3.7. It can be easily understood with the help of the related allocations reported in Table 3.6. In principle, the portfolio improvement decreases with the increasing of the jump-risk premium because, as argued by Liu and Pan (2003), the presence of jump risk suppresses the level of leveraged positions. In Table 3.6, we find that the all the positions of stocks and puts decrease with the increasing of jump risk premium, which explains why we also observe the improvement decreases when the ratio λ^Q/λ increases. However, we do observe several cases of "switch". For instance, given $\gamma = 0.5$ the improvement is increased from 0.113% a year to 11.280% a year while theλ^Q/λ increase from 2 to 5. As analyzed in Liu and Pan (2003), this is because that the investor can use puts as a way to have positive exposure to jump risk. When the risk-premium is large, she can write more puts to get higher returns. As documented by Liu and Pan (2003) in their Table 2, when the relative risk aversion coefficient γ and jump risk premium λ^Q/λ are high, including puts in the optimal portfolio may lead to significant improvement of portfolio performance since the investor can write puts and short sell stocks at the same time. In contrast, the improvements achieved in this chapter are much smaller, primarily due to the no-short-selling constraint. For example, with $\gamma = 5$ and $\lambda^Q/\lambda = 5$, the corresponding improvement is 5.12% a year in Liu and Pan (2003) as opposed to 1.98% a year in our results. Moreover, the improvement is also sensitive to jump risk. In Table 3.7, we can compare the third and fifth columns as they represent the improvements given $\mu = -10\%$ once every 10 years and $\mu = -50\%$ once every 200 years respectively. It is clear that the rarer and larger the jumps are, the more

improvements can be obtained. If the jump risk premium is also large, an investor can get even more by writing more puts, despite the jumps being frequent and small. The benefits of leveraging positions are reduced by the no-short-selling constraint.

Table 3.6: *Performance comparison between portfolios without and with options*

This table reports the performance comparison between the optimal portfolios with and without derivatives given different magnitudes of risk aversion. The options used are one-month 5% out-of-the-money European puts. The volatility parameter is 15% per year. The ratios of $\lambda^{\mathcal{Q}}/\lambda$ is the jump-risk premium.

Jump	cases	$\mu = -10\%$ every 10 years			$\mu = -25\%$ every 50 years			$\mu = -50\%$ every 200 years		
		stock only	stock and put		stock only	stock and put		stock only	stock and put	
γ	$\lambda^{\mathcal{Q}}/\lambda$	ϕ	ϕ^*	ψ^*	ϕ	ϕ^*	ψ^*	ϕ	ϕ^*	ψ^*
0.5	1	5.68	8.13	4.01%	4.05	8.25	2.12%	1.99	8.18	1.79%
	2	5.68	6.87	-0.65%	4.05	7.47	1.37%	1.99	7.93	1.52%
	5	5.68	2.20	-5.60%	4.05	5.44	0.95%	1.99	7.02	1.51%
3	1	1.08	1.59	0.72%	0.95	1.33	0.44%	0.97	1.57	0.31%
	2	1.08	0.91	-0.62%	0.95	1.01	0.18%	0.97	1.41	0.23%
	5	1.08	0.09	-1.40%	0.95	0.02	-0.22%	0.97	1.21	0.11%
5	1	0.81	0.97	0.41%	0.69	0.87	0.23%	0.67	0.88	0.18%
	2	0.81	0.43	-0.51%	0.69	0.75	0.05%	0.67	0.79	0.11%
	5	0.81	0.01	-0.98%	0.69	0.48	-0.27%	0.67	0.71	0.03%
10	1	0.33	0.45	0.21%	0.37	0.44	0.12%	0.35	0.43	0.09%
	2	0.33	0.25	-0.20%	0.37	0.37	0.02%	0.35	0.37	0.07%
	5	0.33	0.03	-0.43%	0.37	0.27	-0.17%	0.35	0.35	0.01%

Table 3.7: *Portfolio improvements for including options*

This table reports the performance improvements of the optimal portfolios for including derivatives given different magnitudes of risk aversion. The parameter setting is given in Table 3.6.

Jump Cases		$\mu = -10\%$ every 10 years	$\mu = -25\%$ every 50 years	$\mu = -50\%$ every 200 years
γ	λ^Q/λ	$R^w(\%)$	$R^w(\%)$	$R^w(\%)$
0.5	1	1.986	8.593	15.972
	2	0.113	5.955	15.102
	5	11.280	2.018	13.891
3	1	0.257	0.456	0.805
	2	0.218	0.059	0.481
	5	3.014	0.510	0.110
5	1	0.140	0.218	0.381
	2	0.096	0.025	0.213
	5	1.981	0.383	0.031
10	1	0.080	0.131	0.159
	2	0.093	0.009	0.095
	5	0.391	0.219	0.003

3.5 Conclusion

In this chapter, we solved the constrained optimal portfolio choice problem in a jump-diffusion model with a large number of assets and state variables. Specifically, by suitably embedding the constrained problem in an appropriate family of unconstrained ones, we established some equivalent optimality conditions for optimal portfolio weights and thus convert the constrained portfolio choice problem into a set of unconstrained ones. These results simplify and help to solve the constrained optimal portfolio choice problem in the jump-diffusion model. We then applied our methods to several numerical examples to show that the prohibition of short-selling and prohibition of borrowing have sizable effects on portfolio performance.

Chapter 4

Rare events, asymmetric correlation and under-diversification

4.1 Introduction

The problem of optimal asset allocation is a core subject in asset pricing theory, while rare events bring a new challenge for researchers as pure diffusion models are not able to capture such a stylized feature. Market participants started observing large movements of financial returns that could be either positive or negative, from the history of the credit crunch. The existence of jumps is one of the main reasons that gaussian distribution should be abandoned while modelling return series.

Asymmetry is not a brand new concept for financial modelling. Many non-Gaussian dis-

tributions have been proposed to introduce asymmetry, as non-zero skewness is observed and confirmed in practice. In this chapter, we focus on the asymmetric dependence structure between returns of financial assets. It is well known that asset returns are correlated with one another, but it is not clear how to model the dependence. Existing literature has documented that the dependence structure between asset returns is not symmetric. Usually, stronger dependence can be observed in bearish markets than in bullish markets. Conditional correlations might vary significantly away from the unconditional correlation. This suggests that dependence should not be modelled by a simple constant correlation coefficient. It needs great care when constructing a portfolio or pricing some financial derivatives that are sensitive to the dependence structure across financial assets.

The reason why people should pay attention to asymmetric correlation is twofold. First, investors have an intuitive understanding that prices of financial assets tend to go down together in bad times. In general, asymmetric correlations can be understood as assets returns become more correlated in a bear market or a market with high volatility. Investors who believe in diversification might suffer heavily in such two circumstances. According to Ang and Chen (2002), a selected US equity portfolio and the US domestic market are, on average, 11.6% more correlated than that implied by a bivariate normal distribution. This partially reveals that the diversification value might be overrated if not considering the possibility that correlations between asset returns are not constant and that asset prices might jump downward together, despite the unconditional correlations.

Second, the hedging performance will be very sensitive to the dependence structure across

asset returns. For example, suppose that an investor uses a hedging instrument that is negatively correlated with her current holding position. When the investor is experiencing a hard time, her hedging instrument might become positively correlated with her exposure. Asymmetric correlation simply describes the phenomena that correlations between returns might have very different scenarios during different market times. Apparently, failure to take into account asymmetric correlations will cause severe problems to the hedging performance.

Asymmetric correlations started drawing the attention of academia in the works of Ang and Bekaert (2000) and Longin and Solnik (2001). Asymmetries in correlations, covariances, volatilities and betas of returns have been widely documented. However, identifying asymmetry requires extraordinary care. People might wrongly claim the existence of asymmetry, due to the exceedance bias. Boyer et al. (1997) and Forbes and Rigobon (2002) firstly indicate the conditioning bias of high or low returns. Not taking into account this bias will lead to incorrectly reporting the finding of asymmetry. Ang and Chen (2002) continue to use the exceedance correlation and firstly propose an H-statistic to quantify the asymmetry. The H-statistic can be understood as a weighted differences of correlations computed based on the model and the data, separately. Apparently, a model needs to be proposed before using the H-statistic. This statistic is not suitable to test whether a sample of data is of asymmetry. Hong et al. (2007) extend the H-statistic and propose a J-statistic, which enables a new model-free test. The J-statistic computes the weighted difference of positive and negative exceedance correlations based on the same exceedance

levels. In practice, the J-statistic is a little too strong as many sample data that obviously exhibit asymmetry cannot be rejected. Besides statistical tests, some graphic tools are also useful in identifying and displaying the asymmetry, such as exceedance correlation plot and frequency table.

Asymmetry exists across both domestic and international markets. Longin and Solnik (2001) use extreme value theory to model multivariate distribution tails, and demonstrate why great care is needed to claim the existence of asymmetries. They introduce the exceedance correlation which has been widely used as a naive measurement of testing asymmetric correlation. Ang and Chen (2002) are the first that provides a comprehensive analysis of asymmetric correlations observed in US market, based on the Fama-French dataset. They reject all existing standard models and claim that the regime-switching GARCH model outperforms other candidates.

Modelling asymmetry takes even more effort than measuring it. Existing standard models cannot provide sufficiently good performance on capturing asymmetries exhibited in real data. Continuous-time diffusion models and compound Poisson jump-diffusion models show poor performance on fitting asymmetric correlations. Regime-switching models have been specially developed for modelling the asymmetry. Good examples include the regime-switching GARCH model in Ang and Chen (2002) and the regime-switching jump-diffusion model that has been recently developed. Although regime-switching models can generate better results for fitting asymmetry, it is far from perfection. Regime-switching models might be reasonable while trying to explain asymmetry, as the existence of multiple

regimes and the transitions of regimes can be an intuitive reason. It is not so reasonable to solve the portfolio allocation problem based on regime-switching models, since it is not clear how to deal with the unpredictable transition of regimes.

The under-diversification problem describes a fact that investors tend to focus on few individual stocks. This contradicts to the benefit of diversification. Portfolio theory suggests that risk-averse investors should prefer a strategy with low volatility. A perfectly diversified allocation should provide an expected return rate with the smallest risk; however, empirical studies have documented that many investors only hold a small amount of individual stocks. Under-diversified portfolios cannot eliminate the idiosyncratic risk. It is a puzzle why a rational investor does not want to diversify her exposure as much as possible. A similar question can be raised that why a risk averse investor prefers a under-diversified strategy to a perfectly diversified one. Recently, Goetzmann and Kumar (2008) study the case that US individual investors hold under-diversified portfolios and show that under-diversified allocation is costly to most investors except for someone who has superior information. Anderson (2013) relates the under-diversification with trading preference based the data of detailed trading records from the Swedish market.

For investors who have the access to international investment, the under-diversification problem will appear in a different representation, which is the home bias puzzle. The home bias puzzle reveals an empirical finding that investors tend to spend a large amount of money on domestic assets without taking the benefits of international diversification. Many literature has documented this puzzle. Home bias can be observed in both developed

and emerging countries. (See French and Poterba (1991) and Tesar and Werner (1994)). Ahearne et al. (2004) test whether information barriers cause the home bias and suggest that information asymmetry plays an important role. Nieuwerburgh and Veldkamp (2005) also try to explain the bias by asymmetric information. Guidolin and Timmermann (2008) suggest that high-moment preference mainly causes the under-diversification by using international market data. It is believed that the home bias is a result of combined impacts from many aspects.

The first contribution of this chapter is to develop a multi-variate jump-diffusion model equipped with stochastic volatility, in order to capture asymmetric correlation. With parsimoniousity, the special pattern of asymmetry can be modelled correctly. We also have stochastic correlation and volatility automatically for granted. Since no regime-switching is assumed, there is no need to test the 'artificial regimes'. Our framework can be extended to support a large number of state variables, so the asymmetries can be driven by different sources. Using statistical tests along with graphic tools, we demonstrate how well our model can capture asymmetric correlations across both domestic markets and international markets. Comparisons with benchmark models are presented, which suggests that our model outperforms all benchmark models.

The second contribution is that the portfolio allocation problem is solved under the jump-diffusion model. With numerical experiments, we investigate the impact of asymmetric correlation on the portfolio allocation problem. The economic loss of ignoring asymmetry is quantified via measuring the economics losses. We also conclude that asymmetry

correlations might be driven by the asymmetric jump structure.

Aside from the modelling and estimation results, we also investigate the market impact of asymmetry. Asymmetric correlations are directly related to the under-diversification problem. In particular, we focus on solving the home bias puzzle that is a special case of under-diversification. The proposed model can predict the under-diversified weights which coincide with empirical research work.

The remaining part of this chapter is organized as follows. In the next section, we present the framework of the multivariate jump-diffusion model as well as the solution to an optimal portfolio allocation. Section 4.3 provides the estimation results of capturing the asymmetry. Several statistical tests along with graphic tools are adopted to show that our model can outperform existing benchmark models. Section 4.4 applies the theoretical results to the US domestic market and discusses the impact of asymmetric correlations on portfolio allocation. The economic value of ignoring the asymmetry is quantified. Section 4.5 solves the international portfolio allocation problem and provides a reasonable intuition of the home bias puzzle. Section 4.6 concludes the chapter and discusses potential future research.

4.2 Modelling and the optimal portfolio problem

This section describes the jump-diffusion model proposed and how to solve the portfolio choice problem between a set of risky assets and a risk-less asset.

4.2.1 Model

Fix a complete probability space $(\Omega, \mathcal{F}, \mathbb{P})$ with a filtration $\{\mathcal{F}_t\}$ satisfying the usual conditions. Suppose there are n risky assets $\{S_{i,t}\}_{i=1,\ldots,n}$ and a riskless asset $S_{0,t}$. The price of the riskless asset follows the following stochastic differential equation:

$$\begin{aligned} dS_{0,t} &= S_{0,t} r dt \\ S_{0,0} &= 1, \end{aligned} \tag{4.1}$$

where r is the constant interest rate. Let $\mathbf{S}_t = (S_{1,t}, \ldots, S_{n,t})^\top$ and assume that it follows the differential equations:

$$\begin{aligned} dS_{i,t} = S_{i,t-} \Big[& (r + \mu_i \sqrt{V_{i,t}}) dt + \sqrt{V_{i,t}} \sum\nolimits_{j=1}^{N} \sigma_{i,j} dz_{j,t} \\ & + \sqrt{V_{i,t}} \left(\sigma_{i,1}^q \left(\exp(Y_u) - 1 \right) dN_t^u + \sigma_{i,2}^q \left(\exp(-Y_d) - 1 \right) \right) dN_t^d \Big] \\ dV_{i,t} = \kappa_i (1 - V_{i,t}) dt & + \sigma_{v,i} \sqrt{V_{i,t}} \left(\rho_i dz_{i,t} + \sqrt{1 - \rho_i^2} dw_t \right), \qquad i = 1, \ldots, n \end{aligned} \tag{4.2}$$

where $\mu = (\mu_1, \ldots, \mu_n)^\top$ is the excess risk premium vector, $\mathbf{z}_t = (z_{1,t}, \ldots, z_{n,t})^\top$ is a n-dimensional independent standard Brownian motion, and N_t^u and N_t^d are two independent Poison processes with jump intensity of λ_u and λ_d, respectively. Y_u and Y_d are two independent random variables which control the jump sizes. w_t is a standard Brownian motions being independent of $\mathbf{z}_t$. For each asset $S_{i,t}$, the spot price and the variance has a correlation parameter ρ_i which enables the leverage effect. The stochastic variance $V_{i,t}$ has an impact not only on the diffusion component but also on the common jumps N_t^u and N_t^d. V_t can also be seen as the activity rate of variance, and is assumed to have a unit long-run mean. This assumption does not restrict the performance of the proposed

model as the vocality parameters $\sigma_{i,j}$ can control the variance of diffusion components. Similarly, the parameters $\sigma^q_{i,1}$ and $\sigma^q_{i,2}$ can control the jump sizes with the unit variance.

Since the model is equipped with common positive and negative jumps, asset prices $\mathbf{S}_t = S_{1,t}, \ldots, S_{n,t}$ will jump simultaneously. However, the jumps sizes of each asset are different and random as $\exp(Y_u) - 1$ and $\exp(-Y_d) - 1$ are independent of each other. This is fairly intuitive, because jumps represent large and rare movements of returns. The risk exposure on the common jumps can be understood as the systemic risk. The systemic risk describes the potential risk caused by a single event that can trigger a collapse in a certain economy. Different assets will react to sudden information at the same time, but the effects of reactions are very different. To return to the model, this is why assets share the same jumps while keeping the freedom of jump sizes. Particularly, we define Σ^0_b and Σ^0_q as

$$\Sigma^0_b = \begin{pmatrix} \sigma_{1,1} & \sigma_{1,2} & \ldots & \sigma_{1,n} \\ \sigma_{2,1} & \sigma_{2,2} & \ldots & \sigma_{2,n} \\ \ldots & \ldots & \ldots & \ldots \\ \sigma_{n,1} & \sigma_{n,2} & \ldots & \sigma_{n,n} \end{pmatrix} \quad \text{and} \quad \Sigma^0_q = \begin{pmatrix} \sigma^q_{1,1} & \sigma^q_{1,2} \\ \sigma^q_{2,1} & \sigma^q_{2,2} \\ \ldots & \ldots \\ \sigma^q_{n,1} & \sigma^q_{n,2} \end{pmatrix} \tag{4.3}$$

Σ^0_b is the $n \times n$ diffusion coefficient matrix and Σ^0_q is the $n \times 2$ jump coefficient matrix, respectively. The jump sizes can be modelled by a variety of distributions. In this section,

Y_u and Y_d are both assumed to be exponentially distributed, with the density

$$f(Y_u) = \begin{cases} \frac{1}{\eta_u} \exp\left(-\frac{Y_u}{\eta_u}\right), & \forall Y_u > 0 \\ 0, & \forall \quad Y_u \leq 0 \end{cases}$$

and

$$f(Y_d) = \begin{cases} \frac{1}{\eta_d} \exp\left(-\frac{Y_d}{\eta_d}\right), & \forall Y_d > 0 \\ 0, & \forall \quad Y_d \leq 0 \end{cases}$$

given constant scale parameters: η_u and η_d.

Basically, the present model is a multi-variate Heston model if the jumps are ignored. The idea of the model comes from the Variance Gamma (VG) process proposed by Madan et al. (1998). The VG process has several representations. For example, we can decompose the process as the difference of two independent gamma processes. Suppose X_t is a VG process, and we can have

$$X_t = \Gamma_t^+ - \Gamma_t^-$$

where Γ_t^+ and Γ_t^- are two independent gamma processes. Since gamma processes are strictly positive processes, the VG process actually models the jump structure separately. Intuitively, good news brings positive incentives to the market while bad news provides a negative impact on the market. It is not a bad idea to assume that information comes independently. The variance gamma distribution is an asymmetric distribution that produces non-zero skewness. We just borrow this idea and model the jump component separately by decomposing the jump into two jumps: positive jump and negative jump. In the model presented in (4.2), there are two common jumps representing the macro

or common information. The price of each asset $S_{i,t}$ has different risk exposure to the common information, which are controlled by σ_q.

The assumption of using common jump processes does not restrict the ability of the proposed model as there are random variables that control the dependence structure. This assumption has even more intuition related to systemic risk. The use of stochastic volatility is to allow more flexility rather than generating asymmetric correlation. In fact, a model without stochastic volatility has the potential to capture asymmetric correlations well. The purpose of this chapter is to provide a good exhale of jump-diffusion model that can fit asymmetric correlations and demonstrate the impact of asymmetry on portfolio weights. This can be seen as a preliminary result of exploring this field and a more sophisticated model can be proposed by employing stochastic volatility in future research.

4.2.2 The optimal portfolio problem

Consider an investor with the CRRA utility endowed with initial wealth $W_0 = \omega_0$, and there are $n+1$ available assets mentioned above. To construct the constrained portfolio choice problem, we follow the approach in Cvitanic and Karatzas (1992) to model portfolio constraints. The unconstrained portfolio weights can easily be solved by setting a trivial constraint. Fix a non-empty, closed and convex set $K \in \mathbb{R}^n$ to denote the constraints. Let $\pi(t) = (\pi_1(t), \ldots, \pi_n(t)) \in K$ denote a trading strategy, where $\pi_i(t)$ is the normalized portfolio weights of the i-th risky asset held at time t and $\mathcal{F}_t$-predictable. The proportion invested in the riskless asset is simply $1 - \sum_{i=1}^{n} \pi_i$. For an arbitral portfolio strategy $\pi(t)$,

we have the associated wealth process W_t as

$$W_t = W_0 + \int_0^t rW_s ds + \int_0^t W_s \pi(s)(\mu\sqrt{V}ds + \int_0^t W_s \pi(s)\Sigma_b dz_t + \int_0^t W_{s-}\pi(s-)\Sigma_q \mathbf{Y} d\mathbf{N}(s) \tag{4.4}$$

where

$$\Sigma_b = \begin{pmatrix} \sqrt{V_{1,t}}\sigma_{1,1} & \sqrt{V_1,t}\sigma_{1,2} & \dots & \sqrt{V_1,t}\sigma_{1,n} \\ \sqrt{V_{2,t}}\sigma_{2,1} & \sqrt{V_{2,t}}\sigma_{2,2} & \dots & \sqrt{V_{2,t}}\sigma_{2,n} \\ \dots & \dots & \dots & \dots \\ \sqrt{V_{n,t}}\sigma_{n,1} & \sqrt{V_{n,t}}\sigma_{n,2} & \dots & \sqrt{V_{n,t}}\sigma_{n,n} \end{pmatrix} \quad \text{and} \quad \Sigma_q = \begin{pmatrix} \sqrt{V_{1,t}}\sigma^q_{1,1} & \sqrt{V_{1,t}}\sigma^q_{1,2} \\ \sqrt{V_{2,t}}\sigma^q_{2,1} & \sqrt{V_{2,t}}\sigma^q_{2,2} \\ \dots & \dots \\ \sqrt{V_{n,t}}\sigma^q_{n,1} & \sqrt{V_{n,t}}\sigma^q_{n,2} \end{pmatrix}$$

As shown, $\pi\Sigma_b$ and $\pi\Sigma_q$ are the diffusion and jump exposures, respectively. A portfolio strategy $\pi(t)$ is said to be admissible if the associated wealth process W_t is non-negative almost surely. Let $\mathcal{A}(\omega_0)$ denote the set of all admissible portfolio strategies, and the traditional Merton's problem is to maximize:

$$u(W_0) = \max_{\pi_i \in \mathcal{A}(\omega_0)} J(W_0, \pi) = E[U(W_T)] \tag{4.5}$$

where

$$U(x) = \begin{cases} \frac{x^{1-\gamma}}{1-\gamma} \\ -\infty \end{cases} \tag{4.6}$$

Following Merton (1971), the optimal portfolio problem can be solved by solving HJB equation. The optimal portfolio weights π can be derived by solving

$$0 = \max \left\{ J_t + \frac{1}{2}W^2 \pi\Sigma_b\Sigma^\top\pi^\top J_{WW} + W\left(\sum_{i=1}^n \mu_i\sqrt{V_{i,s}}\right) J_W \right.$$
$$\left. + \mathbb{E}\left[J(W + W\pi\Sigma_{q1}Y_1) - J(W)\right] + \mathbb{E}\left[J(W + W\pi\Sigma_{q2}Y_2) - J(W)\right]\right\} \tag{4.7}$$

Following Proposition 1 in Jin and Zhang (2012), the optimal portfolio weights $\pi(t)^* = (\pi_1(t)^*, \ldots, \pi_n(t)^*)$ is given by

$$\pi(t)^* = (\pi_{b,1}, \ldots, \pi_{b,n})^\top = \frac{(\Sigma_b^0)^{-1}(\mu' - \Sigma_q^0 \nu')}{\gamma}$$

with

$$\begin{pmatrix} \\ \pi_{q,1} \\ \\ \pi_{q,2} \end{pmatrix} = \pi_b (\Sigma_b^0)^{-1} \Sigma_q^0$$

where $(\pi_{q,1}, \pi_{q,2})$ solves the following equations:

$$\max \pi_{q,1}\nu_1 + \frac{\lambda_u}{1-\gamma} \int_0^\infty \left[(1+\pi_{q,1}z)^{1-\gamma} - 1\right] \Phi_u(dz)$$
$$\max \pi_{q,2}\nu_2 + \frac{\lambda_d}{1-\gamma} \int_{-1}^0 \left[(1+\pi_{q,2}z)^{1-\gamma} - 1\right] \Phi_d(dz)$$

and

$$\Phi_u(dz) = \frac{(1+z)^{-\frac{1}{\eta_u}-1}}{\eta_u} dz$$
$$\Phi_d(dz) = \frac{(1+z)^{\frac{1}{\eta_d}-1}}{\eta_d} dz$$

The constrained problem can be solved similarly. Details can be found in Jin and Zhang (2012).

4.3 Capturing asymmetric correlation

In this section, much detailed analysis is provided to show how well the proposed model can capture asymmetric correlations across both the US domestic market and the international market.

4.3.1 Exceedance correlation and H-statistic

To measure the existence of asymmetric correlations, many measurements and proxies have been proposed. A simple but popular measurement is known as exceedance correlation. Suppose there are two return series: x and y. First, we standardize return series and have $\tilde{x}$ and $\tilde{y}$. Then, the exceedance correlation is defined as

$$\rho(\theta) = \begin{cases} corr(\tilde{x}, \tilde{y} | \tilde{x} > \theta, \tilde{y} > \theta), & \text{if} \quad \theta \geq 0 \\ \\ corr(\tilde{x}, \tilde{y} | \tilde{x} < \theta, \tilde{y} < \theta), & \text{if} \quad \theta \leq 0 \end{cases}$$

where θ is the exceedance level. Usually, $\rho(0)$ has two different values, namely ρ^+ and ρ^-. If the market is of asymmetry, it is unlikely to observe $\rho^+ = \rho^-$. Exceedance correlation can be understood as a type of conditional correlation. For example, if setting $\theta = 1$, $\rho(1)$ represents the correlation where $\tilde{x}$ and $\tilde{y}$ are both less than one unit of standard deviation or x and y are both less than one standard deviation. $\rho(1)$ and $\rho(-1)$ measure the correlation of large positive and negative returns, respectively.

If we set up a series of exceedance levels, we will have a series of corresponding exceedance correlations. Plotting exceedance correlations will provide an intuitive understanding on asymmetric correlations. If the dependence structure of the market is symmetric, the exceedance correlation plot will also be symmetric. Apparently, we need more sophisticated tools to identify and assess asymmetric correlation. Ang and Chen (2002) propose a statistic test named as the H-statistic. Suppose we have a sample of data collected from the market. First, we choose N exceedance levels $\theta = (\theta_1, ..., \theta_N)$, and $\rho(\theta) = (\rho(\theta_1), ...\rho(\theta_N)$ is the corresponding exceedance correlations of the data. Then, we propose a model ϕ

and estimate the model based on the sample data. We denote the exceedance correlations implied by the model ϕ as $\rho(\theta, \phi)$. If model ϕ is able to perfectly explain the degree of asymmetric correlations in the data, we will have $\rho(\theta) = \rho(\theta, \phi)$. The H-statistic is defined as the weighted sum of quadratic differences of exceedance correlations. More precisely,

$$H = \left[\sum_{i=1}^{N} \omega(\theta_i) \cdot (\rho(\theta_i) - \rho(\theta_i, \phi))^2 \right]^{1/2}$$

where $\sum_{i=1}^{N} \omega(\theta_i) = 1$ and $\omega(\theta_i) \geq 0$. The choice of weights is flexible. Ang and Chen (2002) suggest that results are robust to different choices of weights. In this paper, we use two different types of weights: weighted by the number of observations and equal weights.

4.3.2 Data

Most of the research work on asymmetric correlations focuses on the US market. For example, Ang and Chen (2002) and Hong et al. (2007) adopt similar portfolios based on the Fama-French dataset. In this section, we select portfolios grouped by size, book-to-market ratio and momentum, respectively, following the same construction rules in Ang and Chen (2002). The sample period is from July 1963 to December 2012. We only adopt weekly returns that are calculated in excess of risk-free rate. This enables us to compare the results with related literature. The risk-free rate is the one-month US Treasury bill rate. In addition, international portfolios are chosen so as to test the ability to capture asymmetry across global financial markets. Indices from both developed and emerging countries are used, including the United States, the United Kingdom, the Europe ex UK,

Japan and the Asia ex Japan. In all, we have used four data sets including both domestic portfolios and international portfolios.

A summary of statistical description of all data used in this experiment is provided in Table 4.1. The first three panels depict the statistical result of the US domestic portfolios, while panel D describes that of the international portfolios. Exceedance correlations of all portfolios are also reported in Table 4.1. ρ^+ and ρ^- represent both positive and negative exceedance correlations with the exceedance level of 0, respectively. It turns out that all the values of ρ^- are larger than the corresponding values of ρ^- except for the High Tech portfolio. The differences of ρ^+ and ρ^- vary significantly. For example, the smallest size portfolio has $\rho^- = 0.8198$ which is 0.2 bigger than its counterpart ρ^+. As the size of portfolios is getting bigger, ρ^+ and ρ^- are becoming closer to each other. Every domestic portfolio is actually a part of the market portfolio. Hence, it is not surprising to note that the largest size portfolio has a correlation of 0.9895 with the market portfolio, as it plays as a huge proportion of the market portfolio. The international portfolios are different from the domestic portfolios. We investigate the relationships between the US portfolio and other international portfolios. Hence, it is not likely that extremely large correlations will be observed between the US market and other international markets. Among all indices, the Japan index exhibits the least correlation with the US index; it also provides the largest asymmetry as its ρ^- is about 32% larger than its ρ^+. The Japan index seems to be the 'outlier' as all other three indices exhibit similar behaviours.

The plots of exceedance correlations based on Table 4.1 are given in Figure 4.1. Accord-

Table 4.1: *A statistical description for domestic portfolios and international portfolios*

For the market portfolio and all other domestic portfolios, the number observations is 2583. For the international portfolios, the number of observations is 608. All returns are annualized log-returns in excess of the annualized 1-month T-bill rate. The sample period of the domestic portfolios is from July 1963 to December 2012. The international portfolios are sampled from May 2001 to December 2012.

	Mean	Standard deviation	Correlation	ρ^+	ρ^-
Market portfolio	0.0504	0.1598			
Panel A. Size portfolios (value-weighted)					
1 Smallest	0.0641	0.1750	0.8317	0.6404	0.8198
2	0.0708	0.1812	0.8966	0.7597	0.8677
3	0.0701	0.1732	0.9349	0.8476	0.9079
4	0.0656	0.1696	0.9632	0.9147	0.9505
5 Largest	0.0445	0.1570	0.9895	0.9786	0.9805
Panel B. Book-to-market portfolios (value-weighted)					
1 Growth	0.0436	0.1734	0.9658	0.9256	0.9375
2	0.0522	0.1572	0.9657	0.9353	0.9422
3	0.0559	0.1569	0.9379	0.8862	0.8996
4	0.0716	0.1530	0.9122	0.8409	0.8704
5 Value	0.0871	0.1694	0.8856	0.7525	0.8392
Panel C. Industry portfolios (value-weighted)					
Consumer	0.0690	0.1600	0.8667	0.8392	0.8781
Manufacturing	0.0585	0.1576	0.9157	0.8529	0.8778
High Technology	0.0519	0.1920	0.8910	0.8190	0.7892
Health	0.0717	0.1786	0.7935	0.6793	0.6991
Other	0.0694	0.1926	0.8599	0.8606	0.8740
Panel D. International portfolios (MSCI)					
US	0.0114	0.1918			
Japan	-0.0166	0.1982	0.4838	0.1744	0.4979
Europe	0.0308	0.2475	0.8275	0.7061	0.7773
UK	0.0291	0.2283	0.8129	0.7222	0.7570
Asia	0.0984	0.2368	0.7230	0.6270	0.7568

ing to Ang and Chen (2002), there are two typical patterns of asymmetry. First, the exceedance correlations for negative exceedance levels are always greater than those for the counter-parties. Second, the left tail of the exceedance correlation plot is either flat or slightly increasing. Our results match with existing research findings. However, there are two 'outliers' that contradict the two typical patterns. One is the B/M 4 portfolio and the other one is the High Tech portfolio. The B/M 4 portfolio still has a larger ρ^- than ρ^+, but its left tail decreases with the increase of the exceedance level. The High Tech portfolio has a larger ρ^+, which indicates that it is more correlated with the market portfolio during a bullish time. Indeed, these two portfolios are not outliers. The patterns found in Ang and Chen (2002) are not always observable in practice. In some period, the dependence structure does show some symmetry. The patterns documented in Ang and Chen (2002) are very common in the market, but sometimes $\rho^+ > \rho^-$ can be observed. We need to develop a model that captures asymmetric correlations exhibited in the market, but not a model that only captures some documented patterns.

4.3.3 Empirical performance of fitting asymmetry

The estimation is implemented by using the method of moments. To simplify the framework, we have assumed that the volatility process has a long-run mean of unit. This assumption does not restrict the flexility of the framework, since there is volatility parameter σ_{ij} that can control the variance of innovation. Hence, the estimation procedure can be split into two. First we estimate the multi-variate jump-diffusion model with-

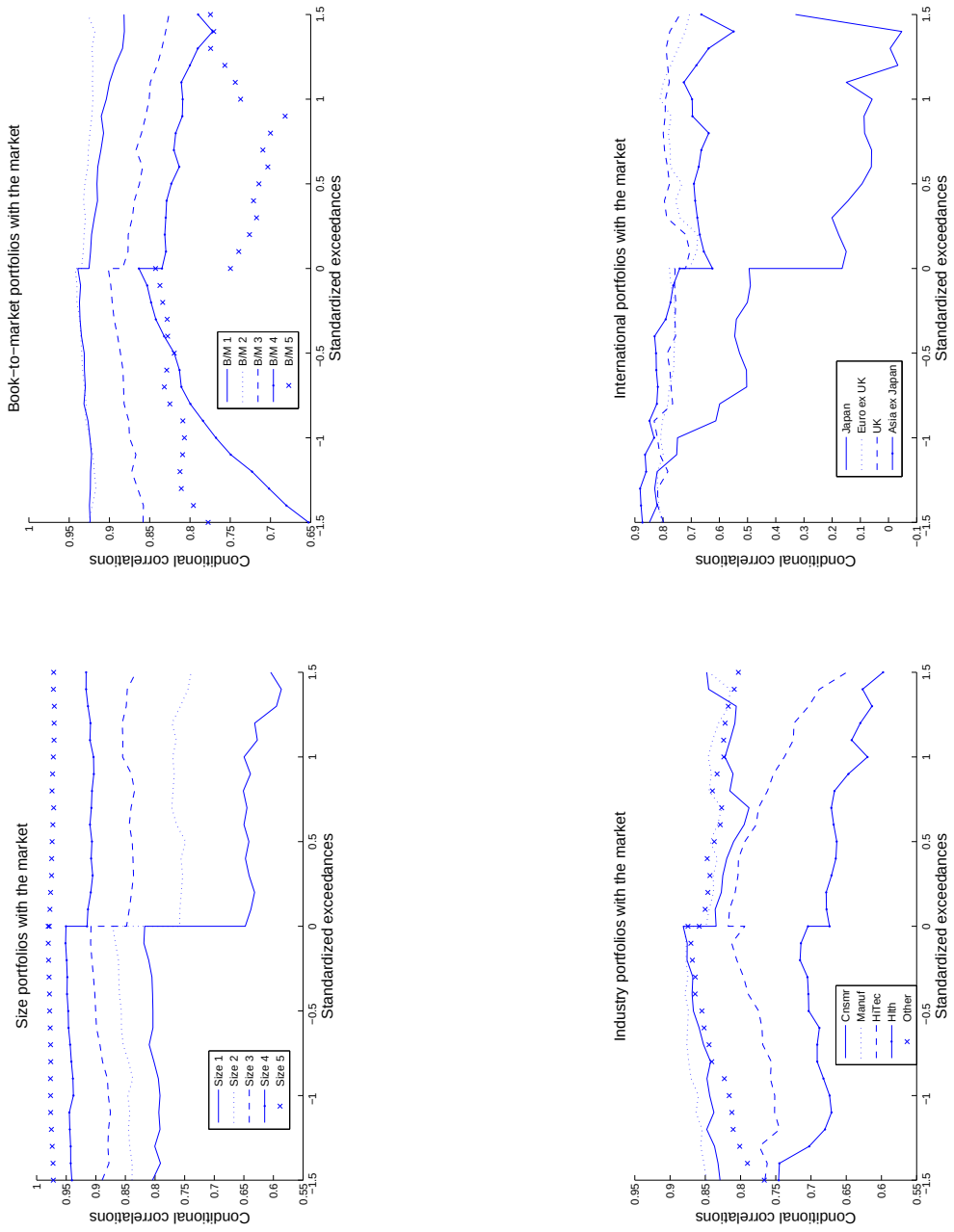

Figure 4.1: *Exceedance correlations of size, book-to-market, industry and international portfolios*

out stochastic volatility. Then, we estimate the stochastic volatility process individually. The estimation results of optimal parameters are given in Appendix C.1. We use the two-sample Kolmogorov-Smirnov test to compare the real data and the simulation data obtained based on estimates, in order to show the goodness of fit. Table 4.2 presents the statistical results. No portfolio is rejected with the level of 5%. We also provide comparisons of moments in Appendix C.1 as an addition to the goodness of fitting. In all, the estimation results show that our model is capable of fitting the market data well.

Table 4.2: *Kolmogorov-Smirnov test of estimation results*

	P-value	KS-stat
Size 1	0.1034	0.5064
Size 2	0.0897	0.5184
Size 3	0.2501	0.4241
Size 4	0.1598	0.4677
Size 5	0.4030	0.3714
Book-to-market 1	0.1494	0.4739
Book-to-market 2	0.4136	0.3683
Book-to-market 3	0.2504	0.4239
Book-to-market 4	0.0508	0.5638
Book-to-market 5	0.1225	0.4917
Industry 1	0.2259	0.4344
Industry 2	0.8529	0.2532
Industry 3	0.5668	0.3271
Industry 4	0.5104	0.3416
Industry 5	0.0642	0.5456
US	0.8108	0.2661
Japan	0.3209	0.3987
Europe	0.2328	0.4326
UK	0.0722	0.5378
Asia	0.2367	0.4309

Empirical cdf plot is another useful tool to access the goodness of fit. Figure 4.2, 4.3, 4.4 and 4.5 provide the corresponding empirical cdf plots for Size portfolios, Book-to-market portfolios, Industry portfolios and international portfolios. Apparently, our model fits both the domestic portfolios and the international portfolios well. Especially, the international portfolios demonstrate very good fitting results.

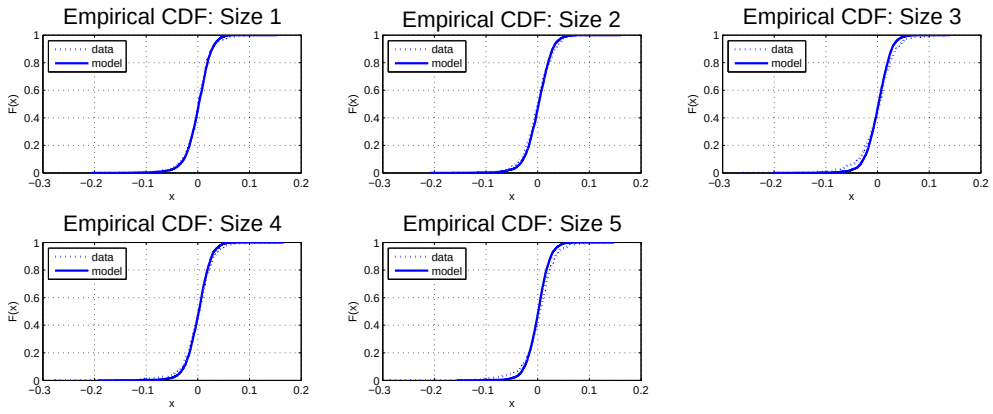

Figure 4.2: *CDF plots of empirical distribution against model distribution (Size portfolios)*

Apart from some general statistic tests, we also want to investigate if our model does capture asymmetric correlations. The best choice is the H-statistic proposed by Ang and Chen (2002).

We choose two weighting methods including the average weight and the weight based on the number of observations. Table 4.3 depicts the statistic results for both domestic portfolios and international portfolios. Under $H2$, namely the weights that are proportional to the number of observations, none portfolio is rejected. Under the average weight $H1$, we only have 4 portfolios rejected. The reason why we do not use the J-statistic developed

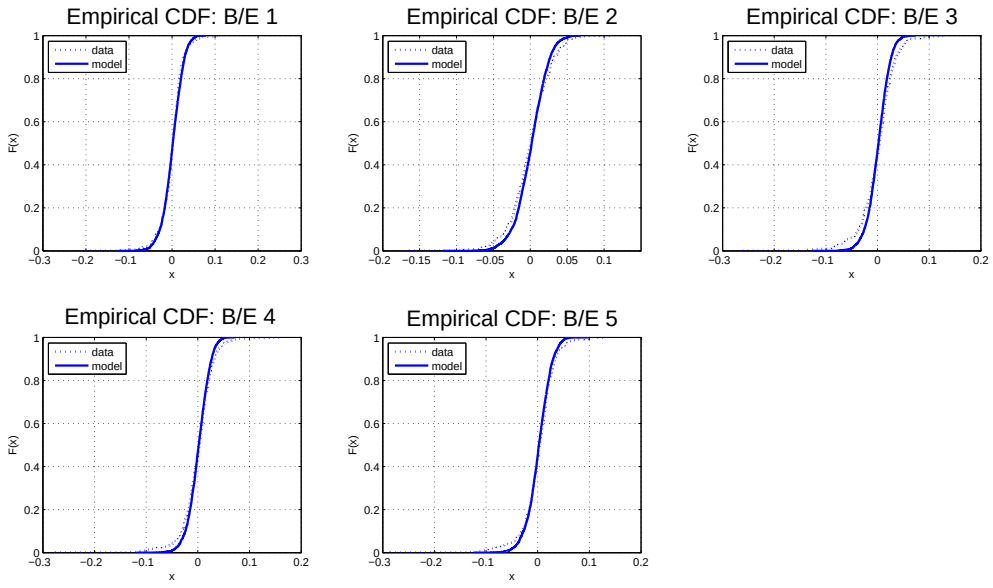

Figure 4.3: *CDF plots of empirical distribution against model distribution (Book-to–market portfolios)*

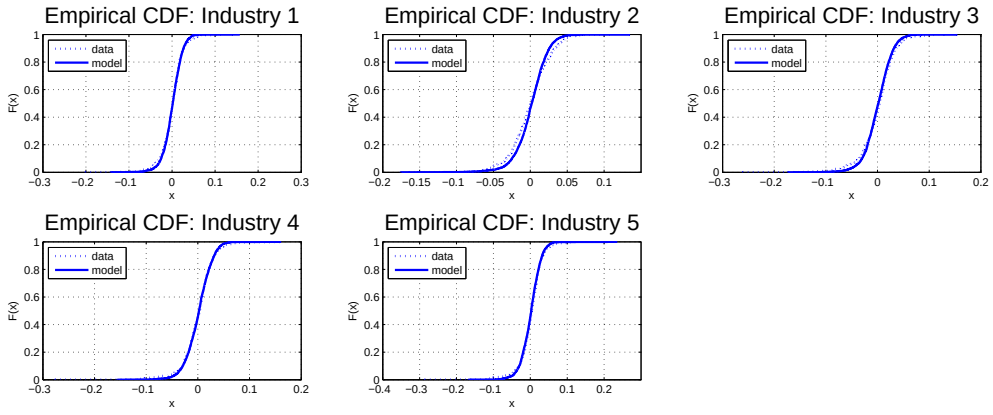

Figure 4.4: *CDF plots of empirical distribution against model distribution (Industry portfolios)*

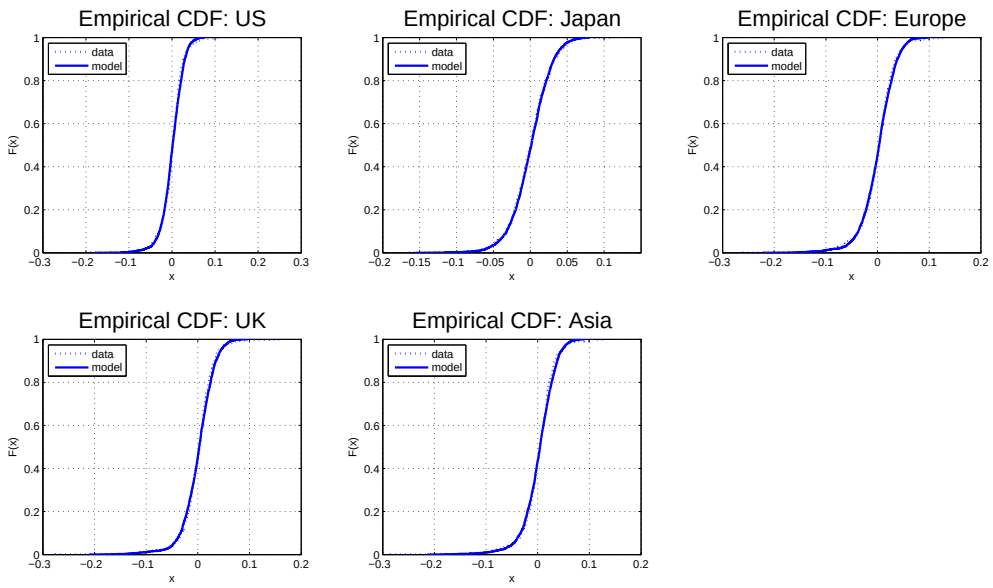

Figure 4.5: *CDF plots of empirical distribution against model distribution (International portfolios)*

in Hong et al. (2007) is because it is too strong to be used to identify the existence of asymmetry. For example, Hong et al. (2007) suggest that strong evidence of asymmetries only exists for some size portfolios. In another word, 4 out of 30 portfolios are not rejected for the null hypothesis of no asymmetry. The aim of the J-statistic is to test if the data is of asymmetry. The meaning of the J-statistic is that a sample data that is of asymmetry cannot be modelled by a symmetric distribution. In principle, the J-statistic computes the difference of positive and negative exceedance correlations and uses a Chi-square test to finish the hypothesis test. Indeed, it is similar to the procedure of the H-statistic.

The plots of exceedance correlation contain a large amount of information. We present the exceedance plots of simulation data in Figure 4.6. Based on estimation results, we

Table 4.3: *A summary of H-statistic for domestic portfolios and international portfolios*

This table reports the H-statistics for domestic and international portfolios under the null hypothesis. $H1$ and $H2$ represent the values of the H-statistic computed with the average weights and the weights based on the number of observations. Frequency of return data is weekly. * indicates that the test was rejected at the level of 5%.

	Size 1	Size 2	Size 3	Size 4	Size 5
H1	0.0763	0.0658	0.0112	0.0057	0.0513
H2	0.0409	0.0341	0.006	0.0028	0.0266
	BE/ME 1	BE/ME 2	BE/ME 3	BE/ME 4	BE/ME 5
H1	0.0362	0.0164	0.0169	0.0466	0.0067
H2	0.0173	0.0084	0.0081	0.0221	0.0032
	Consumer	Manufacturing	High Tech	Health	Other
H1	0.1377*	0.0285	0.0554	0.0501	0.1651*
H2	0.0664	0.0141	0.0271	0.0239	0.0786
	Japan	Europe ex UK	UK	Pacific ex Japan	
H1	0.0551	0.1529*	0.0712	0.1874*	
H2	0.0280	0.0723	0.0369	0.0873	

simulate 3000 samples which are similar to the real data set. With each group of portfolios, we apply the exceedance plots and compare them with those presented in Figure 4.1. Generally speaking, the exceedance plots based on simulation data are quite similar to the corresponding plot based on real data except for the two "outliers". For example, our model does not recover the decreasing left tail of the B/E4 portfolio. For most of portfolios, the simulation data exhibits dependence patterns that are quite close to those of real data.

We do find situations where the estimation error is extremely small while the H-statistic is significantly large. It is suggested that the H-statistic should be taken into account while estimating the data. If an incorrect model is used, it might be the case that the estimation error is not huge and acceptable. However, the dependence structure is very wrong as indicated by the H-statistic. It is not easy to incorporate the H-statistic into the estimation procedure as calculating H relies on the simulation technique for most of the cases.

Apart from the H-statistic, we also use some graphic tools such as the contour plot to investigate the difference of dependence structure between real data and the model. The contour plot is a graphic tool that can show both linear dependence and non-linear dependence. Hong et al. (2007) use this tool to show the goodness of fit for their copula model. Figure 4.7 and Figure 4.8 present the contour plots for the real data and the simulation data, respectively. The simulation data used is the same as used in the exceedance plots. According to the contour plot, the model fits the empirical distribution very well. Al-

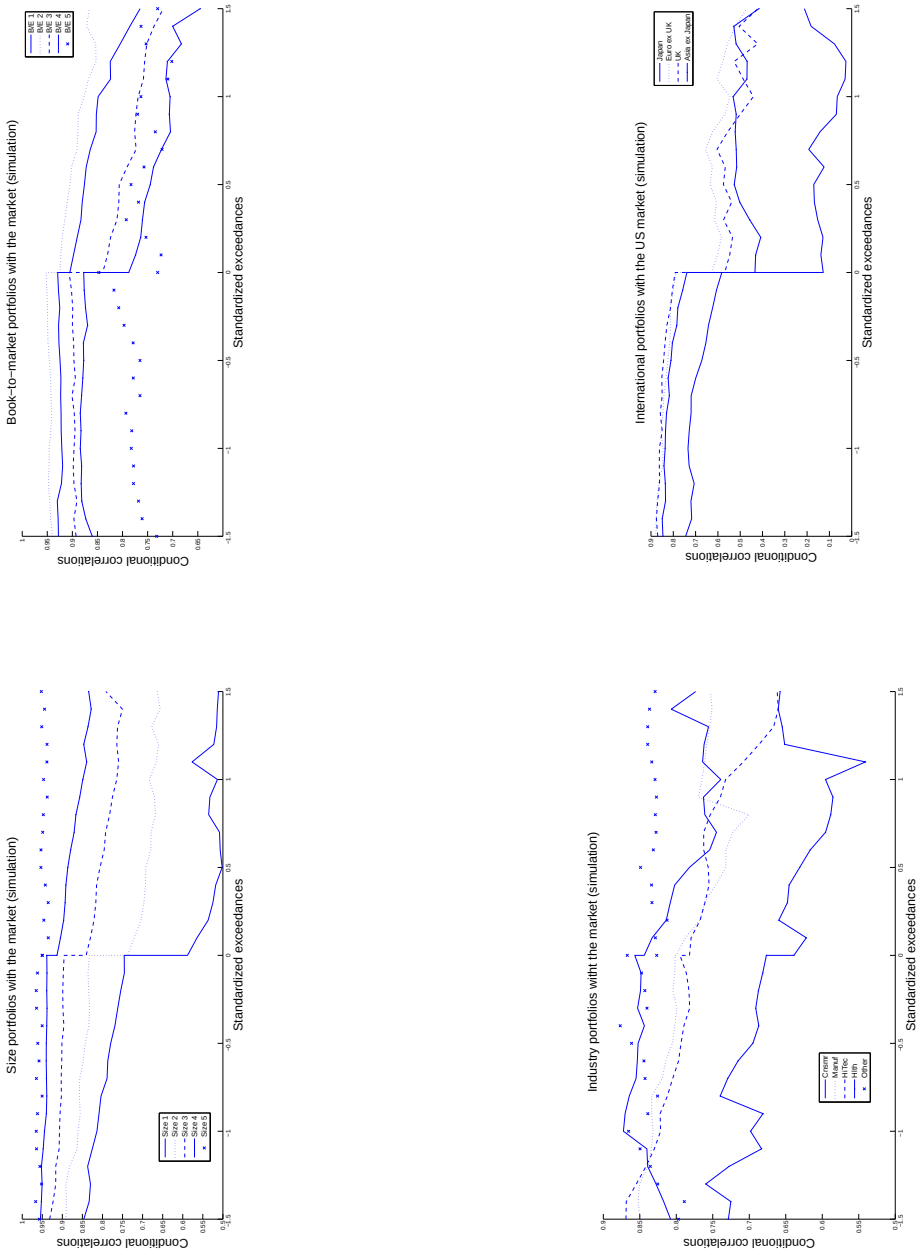

Figure 4.6: *Exceedance correlations of size, book-to-market, industry and international portfolios (simulation data)*

though contour plot cannot provide a direct view on asymmetric dependence, it shows a complete image on the bivariate distribution. Hence, no matter the dependence is asymmetric or not, similar contour plots can confirm that two distributions are close to one another. In our case, the contour plots of the simulation data are very close to those of the real data. This can imply that the model can fully describe the empirical distribution as well as the bivariate dependence structure.

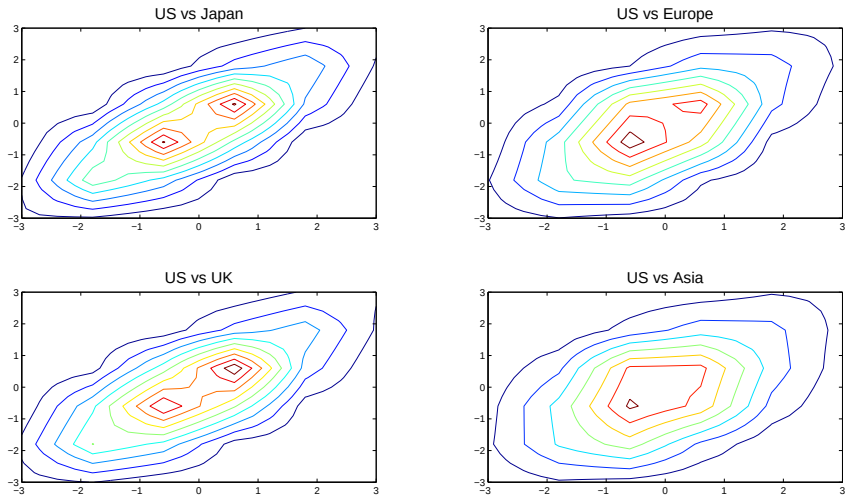

Figure 4.7: *Contour plots of the international portfolios (real data)*

4.4 Impacts of asymmetry on portfolio allocation

After demonstrating the ability to capture asymmetry, we provide examples of how asymmetric correlations affect the portfolio allocation problem in this section. To compare the difference between an optimal allocation and a suboptimal allocation, a benchmark model

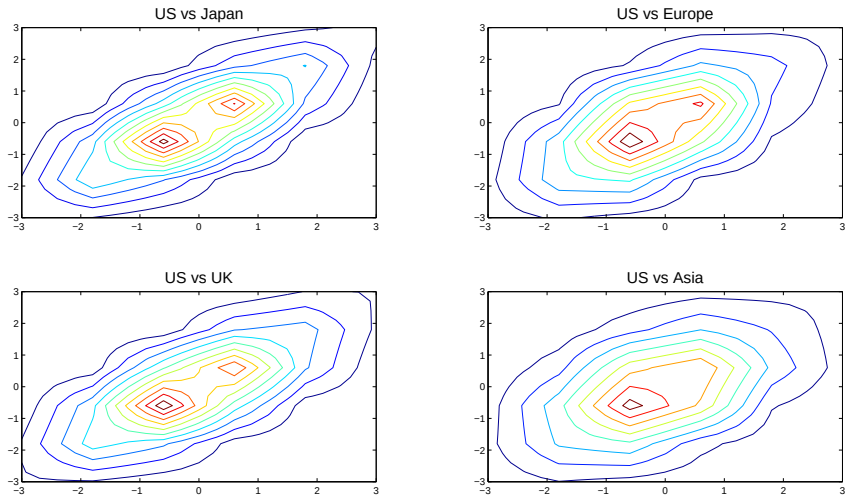

Figure 4.8: *Contour plots of the international portfolios (simulation data)*

that does not admit asymmetry is adopted.

4.4.1 Benchmark Model

To investigate the effect of taking into account asymmetric correlation, a benchmark model that ignores this stylized feature has to be provided. Since we want to figure out to what extent asymmetric correlations affect the portfolio allocation, the benchmark model has to be a solid one that has been widely used. A single jump-diffusion mode is assumed, which has the representation:

$$\frac{dS_t^i}{S_t^i} = \mu_i dt + \sigma_i dz_t + (J_i - 1)dN_t, \qquad i = 1, ..., N \tag{4.8}$$

where S_t^i models the spot price of the ith asset. μ is a N-dimensional drift vector, and σ_i is volatility parameter. N_t is a Poisson process with intensity λ. $J_i - 1$ controls the random

jump amplitude for the ith asset. Assume that $\log(J_i)$ follows a normal distribution with mean μ_i and variance v_i. This model has been recommend by Das and Uppal (2004) and used as a benchmark model in Ang and Chen (2002). (4.8) allows negative jumps so that the correlations of downward moves could be very large. However, Ang and Chen (2002) suggest that model (4.8) cannot generate enough asymmetry compared with real market data.

This benchmark model can be easily estimated with the method of moments. The optimal portfolio weights under the CRRA utility can be obtained by solving the following equation:

$$0 = \mu - \gamma \Sigma w + \lambda \mathbb{E}\left[J_t (1 + w' J_t)^{-\gamma}\right] \tag{4.9}$$

where $\mu = [\mu_1, ..., \mu_n]'$, γ is the risk aversion, and $J_t = [J_1, ..., J_n]'$. The optimal weights $w = [w_1, ..., w_n]$ can only be solved by numerical method. Details can be found in Das and Uppal (2004).

To avoid the impact of the home bias puzzle, only domestic assets are chosen in this experiment. Following Ang and Chen (2002), a similar data set is used, that is the Size portfolios with the sample period from July 1963 to December 2012 selected. This has been used in section 4.3 to show the fit of asymmetries. Only the Size portfolios are used. This is because the Size portfolios exhibit the greatest number of asymmetries compared with other Fama-French portfolios, as suggested by Hong et al. (2007).

4.4.2 Effects of asymmetric correlation and under-diversification

In the first example, we solve the unconstrained portfolio allocation with different levels of risk aversion. The unconstrained portfolio weights are reported in Table 4.4 with γ varying from 5 to 50. The left panel of Table 4.4 provides the actual weights of Size portfolios, while the corresponding right panel presents the normalized weights.

To measure economic value of ignoring asymmetry, the certainty equivalent loss is reported in annualized return rate, known as R^W, as well. The certainty equivalent loss can provide a direct view of how much compensation the investor needs to switch to a suboptimal strategy. For a portfolio weight $\pi = (\pi_1, ..., \pi_n)$, the expected utility $J(\pi)$ of the terminal wealth W_T^π can be calculated as

$$J(\pi) = \frac{W_0^{1-\gamma}}{1-\gamma} E\left\{\exp\left((1-\gamma)\widetilde{W}_T^\pi\right)\right\}$$

where

$$\begin{aligned}\widetilde{W}_T^\pi = &\int_0^T \left[r + \pi_s(b - r\mathbf{1}_N) - \frac{1}{2}\pi_s\Sigma_b\Sigma_b^\top\pi_s^\top\right] ds + \int_0^T \pi_s\Sigma_b dB_s^S \\ &+ \sum_{k=1}^{2}\int_0^T \log(1+\pi_s\Sigma_{qk}Y_k) dN_{k,s}\end{aligned}$$

In our experiment, $J(\pi) = \frac{W_0^{1-\gamma}}{1-\gamma}\exp\left(\kappa(\pi)T\right)$, where

$$\begin{aligned}\kappa(\pi) = &(1-\gamma)[\pi(b - r\mathbf{1}_N) + r] - \frac{1}{2}(1-\gamma)\gamma\pi\Sigma_b\Sigma_b^\top\pi^\top \\ &+ \lambda_u\int_0^\infty [(1+\widetilde{\pi}_{q1}z)^{1-\gamma} - 1]\frac{1}{\eta_u}\frac{1}{(1+z)^{1+\frac{1}{\eta_u}}}dz \\ &+ \lambda_d\int_{-1}^0 [(1+\widetilde{\pi}_{q2}z)^{1-\gamma} - 1]\frac{1}{\eta_d}\frac{1}{(1+z)^{\frac{1}{\eta_d}-1}}dz\end{aligned}$$

The certain equivalent simple return R^{π}_{cer} for the portfolio π is defined as

$$\frac{[W_0(1+R^{\pi}_{cer})^T]^{1-\gamma}}{1-\gamma} = J(\pi),$$

then equivalently,

$$R^{\pi}_{cer} = \left(E\left\{\exp((1-\gamma)\widetilde{W}^{\pi}_T)\right\}\right)^{\frac{1}{T(1-\gamma)}} - 1$$

If we want to compare the performance of two portfolios, we can use the certainty equivalent loss rate $R^W = R^{\pi^*}_{cer} - R^{\pi}_{cer}$ where π^* is the optimal portfolio and π is the suboptimal portfolio.

As shown in Table 4.4, the holdings of all assets shrink with the increase of risk aversion. This is quite intuitive since risk averse investors become more conservative when they are becoming more risk averse. For example, with a low risk aversion level, $\gamma = 5$, the optimal strategy is quite aggressive. The absolute holdings of Size 4 and Size 5 are both bigger than 10. Even the smallest holding is about 1, for Size 3. The holding of the optimal strategy is mainly located on Size 4 and Size 5 but with different directions. Size 4 and Size 5 represent the largest two size portfolios, which means that these two have the smallest average return and the largest variances. The optimal strategy also admits a large negative position on Size 1 portfolio that can be seen as the most risky one. In general, the investor tends to long Size 4 and short Size 5, in order to earn the less risky premium for the purpose of hedging. She also tries to take a notable risk exposure by short-selling Size 1. The exceedance correlation of Size portfolios is depicted in Figure 4.9. Apparently, asymmetries of Size 5 against the other four portfolios are very sizeable

and follow the typical pattern. Size 4 and Size 5 exhibit the least asymmetry, which might be the reason why this pair is chosen to hedge with each other. Size 1 and Size 5 show the largest asymmetry, which implies the intuition that Size 1 portfolio is adopted for speculation.

Table 4.4: *Unconstrained optimal portfolio allocation with risk aversion*

γ	Size 1	Size 2	Size 3	Size 4	Size 5	Size 1	Size 2	Size 3	Size 4	Size 5
5	-6.29	5.25	1.09	10.10	-10.97	7.68	-6.41	-1.33	-12.33	13.40
7	-5.75	4.80	1.00	9.23	-10.03	7.68	-6.42	-1.33	-12.33	13.40
9	-5.06	4.23	0.88	8.12	-8.83	7.70	-6.43	-1.33	-12.36	13.42
11	-4.47	3.74	0.78	7.18	-7.80	7.69	-6.42	-1.33	-12.34	13.41
50	-1.66	1.39	0.29	2.65	-2.88	7.63	-6.39	-1.33	-12.20	13.28

To see what the optimal strategy will be under an extreme case, the optimal weights are reported as well with a very high level of risk aversion, $\gamma = 50$. The holding of Size 3 decreases to 0.29, while other exposures come to a similar level. It turns out that the optimal allocation goes to a pure diversified strategy when the investor is extremely risk averse. The risk of asymmetries does not play an important role in this case. Our finding implies that investors with low risk aversion should pay more attention to asymmetric correlation.

With the right panel of Table 4.4, we also compare the actual weights with the normalized weights. An interesting finding is that the optimal weights do not become more diversified as the investor becomes more risk averse. This might be explained by the concern of asymmetries, as a more risk averse investor should still consider the asymmetry

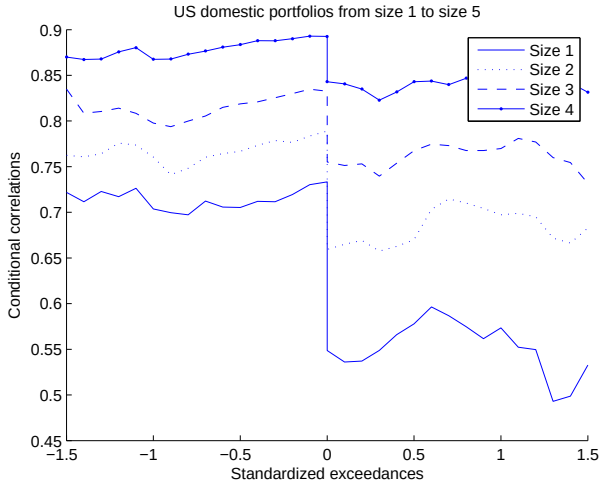

Figure 4.9: *The exceedance correlation plot of size portfolios*

risk. Hence, the actual weights are very sensitive to the level of risk aversion, while the normalized weights are stable with respect to γ.

Now, to derive the suboptimal portfolio, we solve the benchmark model and present the portfolio weights in Table 4.5. To measure economic value of ignoring asymmetry, the certainty equivalent loss is reported in Table 4.5 in annualized return rate, known as R^W, as well. The certainty equivalent loss can provide a direct view of how much compensation the investor needs to switch to a suboptimal strategy. Compared with Table 4.4, it is suggested that the suboptimal weights exhibit more diversification. For example, the exposure on Size 3 portfolio is 3.53 while ignoring asymmetry with $\gamma = 5$, which is about times larger than that 1.09 suggested by the optimal strategy. The economic loss of ignoring asymmetry is not very huge, according to the values of R^W. The largest loss is reported as 0.05 while $\gamma = 5$. This indicates that 5% more is required to compensate the investor if the risk of asymmetric correlation is neglected. The loss increases as the investor

becomes more risk averse. When the investor is extremely risk averse, the economic loss is only 0.002 as the difference between the weights of the optimal allocation and the suboptimal allocation is very small. Ang and Chen (2002) show that the jump-diffusion model presented in (4.8) cannot capture asymmetric correlations. For instance, there are 28 portfolios used in the hypothesis tests and 11 portfolios are rejected. Based on our example, it is suggested that the benchmark model can capture asymmetric correlations to some extent, even it cannot exhibits enough asymmetries. The certain equivalent cost can provide a direct view of how much compensation the investor needs to switch to a suboptimal strategy.

Table 4.5: *Unconstrained optimal portfolio allocation with risk aversion (benchmark model)*

γ	R^W	Size 1	Size 2	Size 3	Size 4	Size 5
5	0.05	-8.32	6.15	3.53	9.32	-5.97
7	0.04	-7.84	5.92	3.10	8.53	-5.03
9	0.04	-6.45	5.63	2.89	7.62	-4.56
11	0.03	-5.32	5.26	2.22	6.92	-3.74
50	0.002	-1.57	1.39	0.49	3.12	-1.82

The extent of asymmetric correlation can be understood by measuring the risk exposure to the negative jump. Hence, it is reasonable and informative to observe the variation of optimal weights given different negative risk exposure. Let the value of λ_d, that is that the intensity of the negative jump. The true estimate of λ_d is 13.3205, and we let it vary from 12.2094 to 14.4316. Intuitively, larger λ_d generates higher asymmetry risk.

Table 4.6 reports the unconstrained portfolio weights, given different additivity rates of negative jumps. With the actual weights shown in the left panel, the optimal strategy does not vary too much with the variation of λ_d. This is a simple case of the under-diversification problem. If the market does not change too much, the investor tend not to change her portfolio weights. In another word, the asymmetry has dominated the strategy in some sense. The normalized weights in the right panel provides a different view as the normalized weights are much more sensitive to the change of λ_d. Generally speaking, it is not surprising to observe that all weights shrink as negative returns become more frequent; however, the normalized weights reflect the change of the investor's investment preference.

Table 4.6: *Unconstrained optimal portfolio allocation with risk exposure to negative jump ($\gamma = 5$)*

λ_d	Size 1	Size 2	Size 3	Size 4	Size 5	Size 1	Size 2	Size 3	Size 4	Size 5
12.2094	-5.97	4.88	0.99	9.56	-10.00	11.20	-9.16	-1.86	-17.92	18.74
12.7650	-5.80	4.83	1.00	9.40	-10.02	9.84	-8.19	-1.69	-15.95	17.00
13.3205	-5.75	4.80	1.00	9.23	-10.03	7.68	-6.42	-1.33	-12.33	13.40
13.8760	-5.46	4.72	0.99	9.07	-10.76	3.80	-3.29	-0.69	-6.31	7.49
14.4316	-5.29	4.69	0.99	8.83	-10.42	4.39	-3.89	-0.82	-7.33	8.65

It is also interesting to investigate the effect of investment constrains with respect to asymmetric correlations. In this example, we prevent from short-selling assets and solve the optimal portfolio weights. Table 4.7 presents the constrained portfolio allocation with different levels of risk aversion. The left and right panel of Table 4.7 provide the actual

and normalized weights, respectively. As short-selling has been prohibited, the investor allocates about 97% of her wealth to Size 4 with the rest on Size 3. More than half of her wealth is invested on the riskless bond. This optimal allocation is provided based on a low level of risk aversion, $\gamma = 5$. It can be easily concluded that the short-selling constraint significantly reduces the leverage and limits the portfolio performance, even for an aggressive investor. When $\gamma = 50$, the investor nearly invests nothing on the risky assets, as only 4% of her wealth is spent on Size 4. A similar image is depicted in Table 4.8 to show the constrained portfolio weights given different jump risk. The market becomes less volatile as λ_d decreases. In this case, the investor is likely to take a higher position on risky assets. The actual portfolio weights drop quickly when the market becomes more volatile. The portfolio weights exhibit severe under-diversification with the ban of short-selling.

Table 4.7: *Constrained optimal portfolio allocation with risk aversion*

γ	Size 1	Size 2	Size 3	Size 4	Size 5	Size 1	Size 2	Size 3	Size 4	Size 5
5	0.00	0.00	0.01	0.45	0.00	0.00	0.00	0.03	0.97	0.00
7	0.00	0.00	0.01	0.32	0.00	0.00	0.00	0.03	0.97	0.00
9	0.00	0.01	0.01	0.25	0.00	0.00	0.04	0.03	0.93	0.00
11	0.00	0.03	0.01	0.20	0.00	0.00	0.13	0.03	0.85	0.00
50	0.00	0.00	0.00	0.04	0.00	0.00	0.00	0.03	0.97	0.00

Table 4.8: *Constrained optimal portfolio allocation with risk exposure to negative jump ($\gamma = 5$)*

γ	Size 1	Size 2	Size 3	Size 4	Size 5	Size 1	Size 2	Size 3	Size 4	Size 5
12.2094	0.00	0.00	0.13	0.50	0.00	0.00	0.00	0.21	0.79	0.00
12.7650	0.00	0.00	0.07	0.47	0.00	0.00	0.00	0.13	0.87	0.00
13.3205	0.00	0.00	0.01	0.45	0.00	0.00	0.00	0.03	0.97	0.00
13.8760	0.00	0.00	0.00	0.38	0.00	0.00	0.00	0.00	1.00	0.00
14.4316	0.00	0.00	0.00	0.30	0.00	0.00	0.00	0.00	1.00	0.00

4.5 Home bias with asymmetry

Home bias is a well-known puzzle that investors tend to spend a large amount of money on domestic assets, which contradicts the diversification effect of international investment. French and Poterba (1991) and Tesar and Werner (1994) are the first literature that documented this economic puzzle. For example, Thomas et al. (2004) show that US investors only held 14% of portfolio allocation in foreign assets by the end of 2003. Home bias can also be observed in other countries like the UK and Japan (See French and Poterba (1991) and Tesar and Werner (1994)). Many possible explanations have been proposed to solve this puzzle, including the investment barrier, truncation costs and information asymmetry; however, there is no convincing solution that can be commonly accepted and verified. In this section, we try to relate the home bias puzzle with asymmetric correlation and explain the intuition of why asymmetry can affect investors' preference.

Besides the potential explanations discussed above, Guidolin and Timmermann (2008)

try to explain the puzzle with using a four-moment International CAPM model. They suggest that high-moment preference with the presence of regimes leads to the home bias. In this section we adopt the same market data used in Guidolin and Timmermann (2008), which includes five international indices: the United States, Japan, the United Kingdom, the Pacific region ex Japan, Europe ex UK. All index prices are denominated in US dollars, and we calculate monthly excess log returns on Morgan Stanley Capital International (MSCI) indices from January 1975 to December 2005. Returns are continuously compounded, and dividends have been adjusted along with other non-cash payments.

A summary of statistics is presented in Table 4.9. All five international portfolio indices are downloaded from Bloomberg. The risk-free rate is approximated by the 1-month US T-Bill rate that can be found from French's homepage[1]. In addition to the statistical summary, a view of unconditional correlations of all indices is depicted in Table 4.10.

All average returns in Table 4.9 are positive, but the higher moments of returns are different from each other. For example, UK and Japan exhibit positive skewness while other indices are of negative skewness. The levels of kurtosis also vary. The Pacific ex Japan index has the highest kurtosis. The summary of statistic we provide is a little different to Table 1 in Guidolin and Timmermann (2008). This might be due to the different sources of obtaining the MSCI index data. One index name sometimes represents several price series as it might be differently adjusted or denominated. The US return

[1]We are grateful to Ken French for offering the data at www.mba.tuck.dartmouth.edu/faculty/ken.french

Table 4.9: *Statistic summary of excess returns of MSCI indices*

This table provides the statistic summary of returns on five portfolio indices and US 1-month T-bills rate. Returns are reported in monthly excess log returns, denominated in US dollars. Bloomberg ticker names for five indices are 'GDDUUS' (US), 'GDDUJN' (Japan), 'GDDUPXJ' (Pacific ex Japan), 'GDDUE15X' (Europe ex UK) and 'GDDUUK' (UK). Data are collected from Jan. 1975 to Dec. 2005. Normality of return data is verified by Jarque-Bera test. Ljung-Box test is used to test the autocorrelation of returns and square returns.

* Denotes significance at 5% level.

** Denotes significance at 1% level.

Index	Mean	Standard Deviation	Skewness	Kurtosis	Jarque-Bera	Ljung-Box	Ljung-Box (squares)
MSCI US	0.5415	4.3548	-0.7083	5.9135	162.67**	1.81	2.52
MSCI Japan	0.3733	6.3965	0.0700	3.5044	4.25	7.09	11.75
MSCI Pacific ex JP	0.5413	6.6506	-1.9670	19.0911	4253.20**	3.59	0.29
MSCI Europe ex UK	0.5264	4.9138	-0.6361	4.7794	74.17**	3.59	9.11
MSCI UK	0.7503	6.1898	0.7586	10.3158	865.25**	4.23	19.96
1-month US T-bills	0.4906	0.2517	0.8319	3.9943	58.23**	1259.80	1092.50

Table 4.10: *Unconditional correlations of international MSCI indices (from Jan. 1975 to Dec. 2005)*

	US	JP	Pacific ex JP	Europe ex UK	UK
US	1.0000	0.3139	0.5599	0.6111	0.5434
JP	0.3139	1.0000	0.3760	0.4858	0.3842
Pacific ex JP	0.5599	0.3760	1.0000	0.5550	0.5733
Europe ex UK	0.6111	0.4858	0.5550	1.0000	0.6479
UK	0.5434	0.3842	0.5733	0.6479	1.0000

series admits the smallest volatility among the five indices, and the Japan return series has the smallest mean and highest volatility. Ticker names are provided in Table 4.9 for comparison.

A plot of exceedance correlations in Figure 4.10 provides an insight into the dependence structure across indices. Exceedance correlations are computed based on monthly returns, so the precision might be not good enough; however, it still depicts the trends. The largest exceedance level is set to be 0.8 due to the lack of return data. It provides a typical view of stylised pattern of asymmetric correlation except for the Japan index. Figure 4.10 exactly shows the concerns we have when considering the diversification effect. For instance, an investor holds positions on both the US index and the UK index. When the market worsens, the correlation approaches to 0.75. When the market is good, the correlation decreases to 0.3. The unconditional correlation between the US index and the UK index is about 0.54. Apparently, diversification performs very differently given the complicated dependence structure. We also find negative exceedance correlations for the pair of US and Japan when $\theta > 0.6$. The left tail of the Japan index decreases and is very close to zero. In general, it is suggested that the Japan index does not have too much in common with the US index. This means that an investor looking forward to using the Japan index to hedge her position on the US index will be very disappointed in a bearish market. More precisely, according to Figure 4.10, when the US index has a large positive jump, the Japan index tends to decrease. When the US index has a large negative drop, Japan index is unlikely to decrease. The data set is very typical as all main international markets

are included. The Japan index even brings something special to the allocation problem. It is a good example to show that the conditional correlations varies in different market conditions.

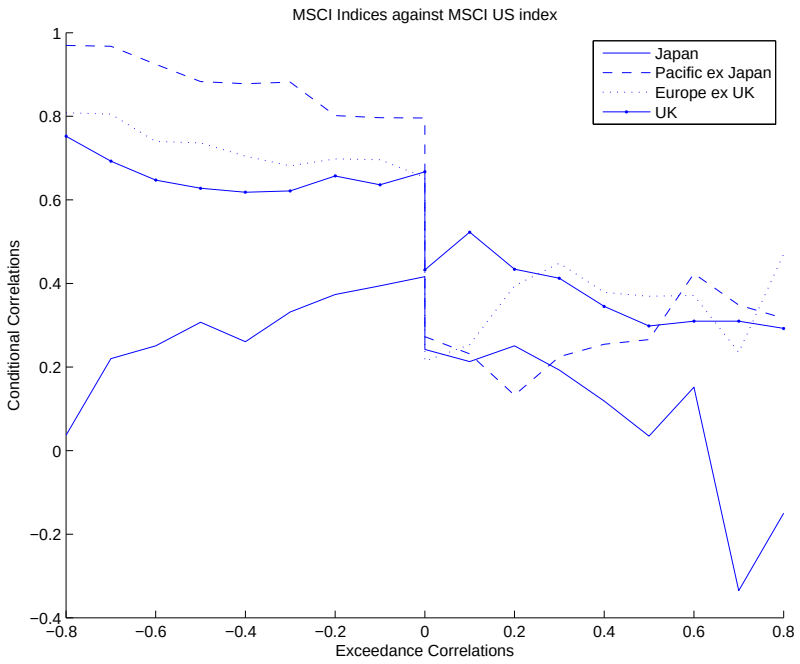

Figure 4.10: *Exceedance correlations of MSCI indices*

Now, suppose an investor can spend her total wealth freely on all five international indices including US, Japan, Europe ex UK, Pacific ex Japan and UK, without any barrier or transaction cost. She can either borrow money from banks or invest in 1 month US T-bills. With the framework we developed in this chapter, optimal portfolio weights are computed. Firstly, we set a range of values centred at the true estimate of λ_d, namely the jump intensity rate of negative jumps. The investor is not allowed to short any index. With different values of λ_d, we solve optimal portfolio weights with the risk aversion level

$\gamma = 4$, and report the result in Table 4.11. In the left panel of Table 4.11, portfolio weights are reported in actual value, while normalised weights are reported in the right panel. Since we aim to investigate the home bias problem, we are more interested in the right panel. Given all cases of artificial values of λ_d, the holding of the US index is more than 70%. The line in bold represents the case of the true λ_d. The intensity rate of λ_d describes the risk exposure on negative jumps. Across all the values of λ_d, the holding position of the US index is very robust. According to Figure 4.11, it is suggested that both the percentages and the actually holdings of the US index decrease with the increase of λ_d. Intuitively, this is due to the fact that an investor is more keen to hedge her portfolio when the jump risk is getting bigger. When the jump risk is relatively low ($\lambda_d = 18.4694$), the investor is satisfied to hold more than 0.82% on the US index; when the jump risk is relatively high ($\lambda_d = 27.3583$), the investor needs to hold more on the UK index for the purpose of hedging or diversification. The home bias problem indeed is a case of under-diversification problem exhibited in the international market. It is not surprising to see that the diversification effect can be observed in international investment problem, although the effect is very week.

Besides holding the US index, the investor prefers to take some positions on the UK and the Pacific indices. The fact that the UK index has the highest average return and the volatility is only medium explains the preference of the investor. The Pacific ex Japan index has high volatility and the unconditional correlation between the Pacific and the US indices is the smallest, so the investor might aim to benefit from holding some

Pacific assets as diversification. The reason why we observe zero weights on Japan and Europe indices is because our model does not admit hedging demand. If short-selling is prohibited, negative positions will be turned to zero. A comparison can be found in Jin and Zhang (2013). An interesting finding is that the investor does not like the Japan index, while it is very similar to the Pacific ex Japan index. These two indices have a similar average mean and standard deviation. Given Table 4.10 and Figure 4.10, the exceedance correlations between the US and Japan indices vary in a very volatile way and sometimes these two indices are even negatively correlated. It is not straightforward to estimate the diversification effect with such a 'volatile' financial instrument. This might explain why the Pacific ex Japan index wins from a risk averse investor's point of view.

Table 4.11: *Optimal portfolio weights of international portfolio given* $\gamma = 4$

	Actual Weights					Normalised Weights				
λ_d	Japan	UK	US	Euro	Pacific	Japan	UK	US	Euro	Pacific
18.4694	0.0000	0.1472	1.4351	0.0000	0.1623	0.0000	0.0844	0.8226	0.0000	0.0930
19.5805	0.0000	0.1874	1.3733	0.0000	0.1265	0.0000	0.1111	0.8140	0.0000	0.0750
20.6916	0.0000	0.2271	1.3124	0.0000	0.0911	0.0000	0.1393	0.8049	0.0000	0.0559
21.8028	0.0000	0.2661	1.2523	0.0000	0.0562	0.0000	0.1690	0.7953	0.0000	0.0357
22.9139	0.0000	0.3047	1.1930	0.0000	0.0218	0.0000	0.2005	0.7851	0.0000	0.0143
23.4694	**0.0000**	**0.3238**	**1.1636**	**0.0000**	**0.0048**	**0.0000**	**0.2170**	**0.7798**	**0.0000**	**0.0032**
24.0250	0.0000	0.3366	1.1338	0.0000	0.0000	0.0000	0.2289	0.7711	0.0000	0.0000
25.1361	0.0000	0.3573	1.0740	0.0000	0.0000	0.0000	0.2496	0.7504	0.0000	0.0000
26.2472	0.0000	0.3777	1.0147	0.0000	0.0000	0.0000	0.2713	0.7287	0.0000	0.0000
27.3583	0.0000	0.3980	0.9560	0.0000	0.0000	0.0000	0.2940	0.7060	0.0000	0.0000

It is also interesting to observe the variation of portfolio weights given different levels of risk-aversion. Let γ vary from 4 to 24. We solve the optimal portfolio weights and report them in Table 4.12. The normalised holding of the US index does not change too much and is around 78%; the actual holding of the US index drop dramatically as the

amplitude of risk aversion increases. This finding is a perfect complement to our results. Compared with the left panel and the right panel in Table 4.12, it is suggested that the actual weights shrink with the increasing of the levels of risk aversion. This is intuitive. A more aggressive investor should have larger exposures, so it cannot be expected that similar portfolio weights can be derived for different investors. Table 4.12 display exactly the same situations. As different investor will have a similar percentage of holding on the domestic index. Although risk-averse investors have different levels of risk-aversion, the percentage holdings of domestic assets are approximately at the same level. Our

Table 4.12: *Optimal weights of international portfolios under different risk aversion levels*

	Actual weights					normalised weights				
γ	Japan	UK	US	Euro(UK)	Pacific(Japan)	Japan	UK	US	Euro(UK)	Pacific(Japan)
4	0.0000	0.2426	0.8731	0.0000	0.0038	0.0000	0.2167	0.7799	0.0000	0.0034
6	0.0000	0.1939	0.6987	0.0000	0.0031	0.0000	0.2165	0.7800	0.0000	0.0035
8	0.0000	0.1615	0.5823	0.0000	0.0027	0.0000	0.2164	0.7800	0.0000	0.0036
10	0.0000	0.1384	0.4992	0.0000	0.0023	0.0000	0.2163	0.7801	0.0000	0.0036
12	0.0000	0.1211	0.4368	0.0000	0.0021	0.0000	0.2162	0.7801	0.0000	0.0037
14	0.0000	0.1076	0.3883	0.0000	0.0019	0.0000	0.2162	0.7801	0.0000	0.0037
16	0.0000	0.0968	0.3495	0.0000	0.0017	0.0000	0.2161	0.7801	0.0000	0.0037
18	0.0000	0.0880	0.3177	0.0000	0.0015	0.0000	0.2161	0.7801	0.0000	0.0038
20	0.0000	0.0807	0.2913	0.0000	0.0014	0.0000	0.2161	0.7801	0.0000	0.0038
24	0.0000	0.0745	0.2689	0.0000	0.0013	0.0000	0.2161	0.7802	0.0000	0.0038

results demonstrate how asymmetry risk can be used to explain the home bias puzzle; however, this does not imply that asymmetry risk can fully explain and drive the home bias. Asymmetry of information and investment barriers can be expected to play crucial roles in generating the bias. Nevertheless, our results related the home bias puzzle with the under-diversification problem by embedding asymmetric correlations. It is suggested

that the home bias puzzle observed in the global market can be seen as a special case of the under-diversification problem. The reason why the extent of the home bias puzzle is much higher might be due to the combined action of other driven forces, such as the asymmetry of information and other constraints.

4.6 Conclusion

In this chapter, we adopt a multi-variate jump-diffusion model equipped with stochastic volatility to capture asymmetric correlations. Plenty of statistical measures are used to show the goodness of fit. It is believed that our model is capable of fitting asymmetries across domestic markets and international markets. With numerical experiments, we also demonstrate the huge impact of asymmetry on portfolio allocation. Asymmetric correlation also brings a new idea to economic puzzles. In section 4.5, the home-bias puzzle is analyzed and efforts have been made to solve this puzzle. It is believed that asymmetry risk plays an important role in the allocation problem.

More empirical tests should be done in future, in order to test the robustness of our results. For example, a large sample period can be selected, which might cover several main credit crisis. The main purpose of investigating asymmetry is to evaluate the diversification benefit under severe economic environment. It is a necessary work to test our model with different market conditions. We plan to enhance the proposed model by incorporating stochastic volatility and evaluate the model performance based on market data collected

from not only domestic markets but also the international market.

Chapter 5

General conclusions, contributions and further research

In this thesis, three separate topics are presented and discussed. These topics are three applications that how Lévy processes can used to solve problems in asset pricing.

The numerical pricing framework proposed in the first topic can be applied to any time-changed Lévy model. Although a multi-scale Lévy model is proposed and solved with the pricing framework, an obvious contribution is that the framework enable people to discover the potential of time-changed Lévy models. It is a numerical application of the Leverage-measure introduced in the brilliant work of Carr and Wu (2004). The new model also suggests that multi-scale volatility can enhance the performance of calibration. According to the calibration results, a long-run component with a short-run one can be observed.

There are many aspects that can be improved to complete the related research. For example, attentions should be drawn to developing more reliable lévy processes. Modelling the dependence is a challenging work. The framework enable people to develop more flexible models.

The second and third topics are two successive research work. In the chapter 3, we solve a constrained portfolio and investigate the effects of imposing investment constraints. In chapter 4, we revisit the optimal portfolio problem by taking into account asymmetry. This phenomenon can be observed everywhere in the market. Failure to model it correctly will lead to severe economic losses. Our findings concentrates on providing suggestions on how to correctly measure the risk exposure.

Future research can be concluded in different fields. The most important one would be how to hedge a portfolio that consists of asymmetric risk. Apparently, our research focuses on how to find and measure the risk caused by the asymmetric dependence. It has not been discussed how to deal with such a risk. Perhaps, purchasing options will be a brilliant idea.

Bibliography

Ahearne, A., Griever, W. L., and E.Warnock, F. (2004). Information costs and home bias: an analysis of us holdings of foreign equities. *Journal of International Economics*, 62:313–336.

Ait-Sahalia, Y., Cacho-Diaz, J., and Hurd, T. (2009). Portfolio choice with jumps: a closed-form solution. *Annals of Applied Probability*, 19:556–584.

Anderson, A. (2013). Trading and under-diversification. *Review of Finance*.

Ang, A. and Bekaert, G. (2000). International asset allocation with time-varying correlations. *Review of Financial Studies*, 15:1137–1187.

Ang, A. and Chen, J. (2002). Asymmetric correlations of equity portfolios. *Journal of Financial Economics*, 63:443–494.

Attari, M. (2004). Option pricing using fourier transforms: A numerically efficient simplification. *Charles River Associates working paper*.

Bakshi, G., Cao, C., and Chen, Z. (1997a). Empirical performance of alternative option pricing models. *The Journal of Finance*, 52(5):2003–2049.

Bakshi, G., Cao, Z., and Chen, Z. (1997b). Empirical performance of alternative option pricing model. *Journal of Finance*, 52:2003–2049.

Bardhan, I. and Chao, X. (1996). On martingale measures when asset returns have unpredictable jumps. *Stochastic Processes and their Applications*, 63:35–54.

Bates, D. (2000). Post-'87 crash fears in S&P 500 futures options. *Journal of Econometrics*, 94:181–238.

Bick, B., Kraft, H., and Munk, C. (2013). Solving constrained consumption-investment problems by simulation of artificial market strategies. *Management Science*, 59(2):485–503.

Black, F. and Scholes, M. (1973). The pricing of options and corporate liabilities. *Journal of Political Economy*, 81(3):637–654.

Boyer, B. H., Gibson, M. S., and Loretan, M. (1997). Pitfalls in tests for changes in correlations. Technical report.

Brandt, M. (2009). *Portfolio choice problems, in Y. Ait-Sahalia and L.P. Hansen (eds.). Handbook of Financial Econometrics, Volume 1: Tools and Techniques*. North Holland.

Brayton, R., Director, S., Hachtel, G., and Vidigal, L. (1979). A new algorithm for statistical circuit design based on quasi-newton methods and function splitting. *IEEE Trans. Circuits and Systems*, CAS-29:784–794.

Carr, P., Geman, H., Madan, D. B., and Yor, M. (2002). The fine structure of asset returns: An empirical investigation. *Journal of Business*, 75(2):305–332.

Carr, P., Geman, H., Madan, D. B., and Yor, M. (2003). Stochastic volatility for lévy processes. *Mathematical Finance*, 13(3):345–382.

Carr, P. and Madan, D. (1999). Option valuation using the fast fourier transform. *Journal of Computational Finance*, 2(4):61–73.

Carr, P. and Wu, L. (2003). The finite moment log stable process and option pricing. *Journal of Finance*, 58(2):753–777.

Carr, P. and Wu, L. (2004). Time-changed lévy processes and option pricing. *Journal of Financial Economics*, 71(1):113–141.

Chacko, G. and Viceira, L. (2003). Spectral GMM estimation of continuous-time processes. *Journal of Econometrics*, 116:259–292.

Chourdakis, K. (2004). Option pricing using the fractional fft. *Journal of Computational Finance*, 8(2):1–18.

Christoffersen, P., Heston, S. L., and Jacobs, K. (2009). The shape and term structure of the index option smirk: Why multifactor stochastic volatility models work so well. *Management Science*, 55:1914–1932.

Cvitanic, J. and Karatzas, I. (1992). Convex duality in constrained portfolio optimization. *Annals of Applied Probability*, 2:767–818.

Das, S. and Uppal, R. (2004). Systemic risk and international portfolio choice. *Journal of Finance*, 59:2809–2834.

Detemple, J. B., Garcia, R., and Rindisbacher, M. (2003). A Monte Carlo method for optimal portfolios. *The Journal of Finance*, 58(1):401–446.

Duffie, D., Pan, J., and Singleton, K. (2000). Transform analysis and asset pricing for affine jump-diffusions. *Econometrica*, 68:1343–1376.

Egloff, D., Leippold, M., and Wu, L. (2010). The term structure of variance swap rates and optimal variance swap investments. *Journal of Financial and Quantitative Analysis*, 45:1279–1310.

Engle, R. and Lee, G. (1999). A permanent and transitory component model of stock return volatility. *Working Paper*.

Eraker, B., Johannes, M., and Polson, N. (2003). The impact of jumps in equity index volatility and returns. *Journal of Finance*, 58:1269–1300.

Fama, E. (1970). Efficient capital markets: A review of theory and empirical work. *Journal of Finance*, 25(2):383–417.

Fang, F. and Oosterlee, C. (2008). A novel pricing method for european options based on fourier-cosine series expansions. *SIAM Journal on Scientific Computing*, 12:265–292.

Filipović, D. (2001). A general characterization of one factor affine term structure models. *Finance and Stochastics*, 5(3):389–412.

Forbes, K. J. and Rigobon, R. (2002). No contagion, only interdependence: Measuring stock market comovements. *The Journal of Finance*, 57(5):2223–2261.

Fouque, J.-P., Papanicolaou, G., Sircar, R., and Sølna, K. (2011). *Multiscale Stochastic Volatility for Equity, Interest Rate, and Credit Derivatives*. Cambridge University Press.

French, K. and Poterba, J. (1991). Investor diversification and international equity markets. *American Economic Review*, 81:222–226.

Gatheral, J. (2006). *The Volatility Surface: A Practitioner's Guide*. Wiley Finance, 1 edition.

Goetzmann, W. N. and Kumar, A. (2008). Equity portfolio diversification. *Review of Finance*, 12:433.

Guidolin, M. and Timmermann, A. (2008). International asset allocation under regime switching, skew, and kurtosis preferences. *Review of Financial Studies*, 21(2):889–935.

Haslip, G. G. and Kaishev, V. K. (2013). A novel fourier transform b-spline method for option pricing. *Working Paper*.

He, H. and Pearson, N. (1991). Comsumption and portfolio policies with incomplete markets and short-sale constraints: infinite dimensional case. *Journal of Economic Theory*, 54:259–304.

Heston, S. and Nandi, S. (2000). A closed-form garch option pricing model. *Review of Financial Studies*, 13:585–626.

Heston, S. L. (1993). A closed-form solution for options with stochastic volatility with applications to bond and currency options. *Review of Financial Studies*, 6:327–343.

Hong, Y., Tu, J., and Zhou, G. (2007). Asymmetries in stock returns: Statistical tests and economic evaluation. *Review of Financial Studies*, 20:1547–1581.

Huang, J. and Wu, L. (2004). Specification analysis of option pricing models based on time-changed lévy processes. *Journal of Finance*, 59(3):1405–1440.

Ikeda, N. and Watanabe, S. (1981). *Stochastic differential equations and diffusion processes*. North-Holland.

Jin, X. and Zhang, A. X. (2012). Decomposition of optimal portfolio weight in a jump-diffusion model and its applications. *Review of Financial Studies*, 25(9):2877–2919.

Jin, X. and Zhang, K. (2013). Dynamic optimal portfolio choice in a jump-diffusion model with investment constraints. *Journal of Banking and Finance*, 37(5).

Karatzas, I., Lehoczky, J., and Shreve, S. (1987). Optimal portfolio and consumption decisions for a small investor on a finite horizon. *SIAM Journal of Control and Optimization*, 25:1557–1586.

Karatzas, I., Lehoczky, J., Shreve, S., and Xu, G. (1991). Martingale and duality methods for utility maximization in an incomplete market. *SIAM Journal of Control and Optimization*, 29:702–730.

Kilin, F. (2011). Accelerating the calibration of stochastic volatility models. *Journal of Derivatives*, 18(3):7–16.

Kim, T. and Omberg, E. (1996). Dynamic nonmyopic portfolio behavior. *Review of Financial Studies*, 9:141–161.

Liu, J. (2007). Portfolio selection in stochastic environments. *Review of Financial Studies*, 20:1–39.

Liu, J., Longstaff, F., and Pan, J. (2003). Dynamics asset allocation with event risk. *Journal of Finance*, 58:231–259.

Liu, J. and Pan, J. (2003). Dynamic derivative strategies. *Journal of Financial Economics*, 69:401–430.

Longin, F. and Solnik, B. (2001). Extreme correlation of international equity markets. *Journal of Finance*, 56:649–676.

Lord, R., Fang, F., Bervoets, F., and Oosterlee, C. (2008). A fast and accurate fft-based method for pricing early-exercise options under levy processes. *SIAM J. Sci. Comput.*, 30:1678–1705.

Madan, D., Carr, P., and Chang, E. (1998). The variance gamma process and option pricing. *European Finance Review*, 2:79–105.

Merton, R. (1969). Lifetime portfolio choice: the continuous-time case. *Review of Economics and Statistics*, 51:247–257.

Merton, R. (1971). Optimum consumption and portfolio rules in a continuous-time model. *Journal of Economic Theory*, 3:373–413.

Merton, R. (1976). Option pricing when underlying stock returns are discontinuous. *Journal of Financial Economics*, 3:125–144.

Merton, R. (1980). On estimating the expected return on the market: an exploratory investigation. *Journal of Financial Economics*, 8:323–362.

Monroe, I. (1978). Processes that can be embedded in brownian motion. *Annals of Probability*, 6(1):42–56.

Nieuwerburgh, S. V. and Veldkamp, L. (2005). Information immobility and the home bias puzzle. *NYU Working Paper*.

Nocedal, J. and Wright, S. (2006). *Numerical Optimization*. Springer Series in Operations Research. Springer Verlag, 2nd edition.

Samuelson, P. (1969). Lifetime portfolio selection by dynamic stochastic programming. *Review of Economics ans Statistics*, 51:239–246.

Tesar, L. and Werner, I. (1994). International equity transactions and u.s. portfolio choice. *NBER Working Paper No. 4611*.

Thomas, C. P., Warnock, F. E., and Wongswan, J. (2004). The performance of international portfolios. *Working Paper*.

Wachter, J. (2002). Portfolio and consumption decisions under mean-reverting returns: an exact solution for complete markets. *Journal of Financial an Quantitative Analysis*, 37:63–91.

Wachter, J. (2010). Asset allocation. *Annual Reviews of Financial Economics*, 2:175–206.

Xu, G. and Shreve, S. (1992). A duality method for optimal consumption and investment under short-selling prohibition. i. general market coefficients. *Annals of Applied Probability*, 2:87–112.

Appendix A

A.1 Derivation of corresponding characteristic function

We have five benchmark models that have explicit solutions. The characteristic functions of log returns are:

- Heston model: the model representation is

$$\frac{dS_t}{S_t} = (r-q)dt + \sqrt{v_t}dW_t$$
$$dv_t = \kappa(\eta - v_t)dt + \lambda\sqrt{v_t}dZ_t, \qquad v_0 = \sigma_0^2 > 0$$
$$cov[dW_t dZ_t] = \rho dt$$

and the characteristic function of log return is

$$\Phi(u) = \exp(iu(r-q)t)\exp\left(\eta\kappa\lambda^{-2}\left((\kappa - iu\rho\lambda - d)t - 2\log\left(\frac{1-ge^{-dt}}{1-g}\right)\right)\right)$$
$$\exp\left(\sigma_0^2\lambda^{-2}(\kappa - iu\rho\lambda - d)\frac{1-e^{-dt}}{1-ge^{-dt}}\right)$$

where $d = \sqrt{(iu\rho\lambda - \kappa)^2 - \lambda^2(-iu - u^2)}$ and $g = (\kappa - iu\rho\lambda - d)/(\kappa - iu\rho\lambda + d)$.

- Double Heston model: the model representation is

$$\begin{aligned}
&\frac{dS_t}{S_t} = (r-q)dt + \sqrt{v_t^1}dW_t^1 + \sqrt{v_t^2}dW_t^2 \\
&dv_t^1 = \kappa_1(\eta_1 - v_t^1)dt + \lambda_1\sqrt{v_t^1}dZ_t^1, \qquad v_0^1 = \sigma_{1,0}^2 > 0 \\
&dv_t^2 = \kappa_2(\eta_2 - v_t^2)dt + \lambda_2\sqrt{v_t^2}dZ_t^2, \qquad v_0^2 = \sigma_{2,0}^2 > 0 \\
&cov[dW_t^i dZ_t^i] = \rho_i dt, \qquad i = 1, 2;
\end{aligned}$$

  and the characteristic function of log return is

$$\Phi(u) = 1;$$

- VG model: the model representation is

$$S_t = S_0 \exp\left((r - q - \xi)t + X_t\right)$$

  where $\xi = -C\log(GM/(GM + (M-G) - 1))$ and X_t is a VG process governed by the parameter triplet (C, G, M). The characteristic function of log return is

$$\Phi(u) = \exp(iu(r-q)t)\left(\frac{GM}{GM + (M-G)iu + u^2}\right)^{Ct}$$

- VGSV model: the model representation is

$$\begin{aligned}
&S_t = S_0 \exp\left((r-q)t + X_{T_t} - \xi T_t\right) \\
&T_t = \int_0^t v_s ds \\
&dv_t = \kappa(\eta - v_t)dt + \lambda\sqrt{v_t}dW_t, \qquad v_0 = \sigma_0^2
\end{aligned}$$

where $\xi = -C\log(GM/(GM + (M - G) - 1))$ and X_t is a VG process governed by the parameter triplet (C, G, M). The activity rate v_t is governed by $(\kappa, \eta, \lambda, \sigma_0^2)$. The characteristic function of log return is

$$\Phi(u) = \exp(iu(r-q)t)\frac{\phi_{CIR}(-i\Psi(u))}{\phi_{CIR}(-i\Psi(-i))}$$

where $\Psi(u)$ is the characteristic exponent of X_t, $\phi_{CIR}(u)$ is the characteristic function of CIR process and has the representation:

$$\begin{aligned}\phi_{CIR}(u) &= E\left[\exp\left(iu\int_0^t v_s ds\right)\right] \\ &= A(t,u)\exp\left(B(t,u)v_0\right)\end{aligned}$$

where

$$\begin{aligned}A(t,u) &= \frac{\exp\left(\frac{\kappa^2\eta t}{\lambda^2}\right)}{\left(\cosh\left(\frac{\gamma t}{2}\right) + \frac{\kappa}{\gamma}\sinh\left(\frac{\gamma t}{2}\right)\right)^{2\kappa\eta/\lambda^2}} \\ B(t,u) &= \frac{2iu}{\kappa + \gamma\coth(\frac{\gamma t}{2})} \\ \gamma &= \sqrt{\kappa^2 - 2iu\lambda^2}\end{aligned}$$

- LS models: the model representation is

$$S_t = S_0\exp\left((r-q-\xi)t + \sigma L_{T_t}\right)$$

where $\xi = -\sigma^\alpha\sec(\pi\alpha/2)$. The characteristic function of log return is

$$\phi(u) = \exp(iu(r-q-\xi)t - t(iu\sigma)^\alpha\sec(\pi\alpha/2))$$

The LSSV1 model does not have an explicit solution, so it relies on the numerical framework. It can be done simply by elimianing the activity rate process v_t^2.

A.2 Solving Heston model numerically

Given the time-changed representation of the Heston model, we can derive the correspond ODEs as

$$\begin{aligned} b'(t) &= \frac{u^2 + iu}{2} - \kappa^Q b(t) - \frac{\eta^2 b^2(t)}{2} \\ c'(t) &= ab(t) \end{aligned} \tag{A.2.1}$$

where

$$\kappa^Q = \kappa - iu\eta\rho.$$

Fortunately, $b(t)$ has an explicit solution with the initial condition $b(0) = 0$. $c(t)$ can be directly obtained by taking integral of $b(t)$. Finally, we can have the solutions as:

$$\begin{aligned} b(t) &= \frac{u^2(1 - e^{-\delta t})}{(\delta + \kappa^Q) + (\delta - \kappa^Q)e^{-\delta t}} \\ c(t) &= \frac{a}{\eta^2}\left[2\log\frac{(2\delta - (\delta - \kappa^Q)(1 - e^{-\delta t}))}{2\delta} + (\delta - \kappa^Q)t\right] \end{aligned} \tag{A.2.2}$$

where

$$\delta = (\kappa^Q)^2 + u^2\eta^2.$$

The solution (A.2.2) is the same to the well-known solution to the Heston model. It is slightly different from that given in Heston (1993). This is because the original solution

has a problem with the principal branch. The solution (A.2.2) is the correct and stable one.

A.2.1 Derive characteristic function of LS

The Lévy triplet of FMLS process is $(a, 0, \pi)$, where $\pi(dx) = cx^{-\alpha-1}$.

A.2.2 Derive $b(t)$ and $c(t)$

$$\begin{aligned} b'(t) &= \Psi_x(u) - \kappa b(t) + \beta \int_{\mathbb{R}_0^+} (1 - e^{-b(t)x}) \mu^u(dx) \\ &= \Psi_x(u) - \kappa b(t) + \sec \frac{\pi\alpha}{2} \beta \left[(b(t) + iu)^\alpha - (iu)^\alpha \right] \end{aligned}$$

due to

$$\begin{aligned} \int_{\mathbb{R}_0^+} (1 - e^{-b(t)x}) \mu^u(dx) &= \int_{\mathbb{R}_0^+} (1 - e^{-b(t)x}) e^{-iux} c x^{-\alpha-1} dx \\ &= c \left(\int_{\mathbb{R}_0^+} e^{-iux} x^{-\alpha-1} dx - \int_{\mathbb{R}_0^+} e^{-(iu+b(t))x} x^{-\alpha-1} dx \right) \\ &= c \left(-(iu)^\alpha \Gamma(-\alpha, iux) |_0^\infty + (iu + b(t))^\alpha \Gamma\left(-\alpha, (iu + b(t))x\right) |_0^\infty \right) \end{aligned}$$

And

$$\Gamma(a, \infty) = 0, \quad \Gamma(a, 0) = \Gamma(a)$$

hence

$$\int_{\mathbb{R}_0^+} (1 - e^{-b(t)x}) \mu^u(dx) = c\Gamma(-\alpha) \left[(iu)^\alpha - (iu + b(t))^\alpha \right]$$

A.3 Sampling FMLS distribution

Let Θ and W be two independent random variables. $\Theta \sim U(-\frac{\pi}{2}, \frac{\pi}{2})$ and $W \sim \exp(1)$.

Define $\theta_0 = arctan(\beta \tan(\pi\alpha/2))/\alpha$, then

$$Z = \begin{cases} \frac{\sin \alpha(\theta_0+\Theta)}{(\cos \alpha\theta_0 \cos \Theta)^{1/\alpha}} \left[\frac{\cos(\alpha\theta_0+(\alpha-1)\Theta)}{W}\right]^{(1-\alpha)/\alpha} \\ \frac{2}{\pi}\left[\left(\frac{\pi}{2}+\beta\Theta\right)\tan\Theta - \beta\log\left(\frac{\frac{\pi}{2}W\cos\Theta}{\frac{\pi}{2}+\beta\Theta}\right)\right] \end{cases} \tag{A.3.1}$$

Appendix B

B.1 Proof of Proposition 3.1

First we prove the first result in Proposition 3.1. Let $W_t^{c,\pi}$ and $W_t^{c,\pi}(\nu)$ be the wealth processes corresponding to a portfolio rule π in the market $\mathcal{M}$ and $\mathcal{M}_\nu$, respectively. Like $\mathcal{A}(w_0)$ in the market $\mathcal{M}$, we denote by $\mathcal{A}_\upsilon(w_0)$ the class of consumption rate process c and portfolio strategies π in the market $\mathcal{M}_\nu$ for which $W_t^\pi(\nu) \geq 0$, $0 \leq t \leq T$. For a fixed pair of c and π, we now prove $W_t^{c,\pi}(\nu) \geq W_t^{c,\pi}$. To this end, we let $\widetilde{W}_t = W_t^{c,\pi}(\nu) - W_t^{c,\pi}$. Then from (3.3) and (3.5), $\widetilde{W}_t$ satisfies

$$\begin{aligned}\widetilde{W}_t = &\int_0^t \widetilde{W}_s[\pi_s(b - r\mathbf{1}_n) + r]ds + \int_0^t W_s(\nu)(\delta(\nu) + \pi_s\nu)ds + \int_0^t \widetilde{W}_s\pi_s\Sigma_b dB_s^S \\ &+ \int_0^t \widetilde{W}_{s-}\pi_{s-}\Sigma_q(Y \bullet dN_s). \qquad \text{(B.1.1)}\end{aligned}$$

We set

$$\xi_t = \int_0^t \pi_s \Sigma_b dB_s^S - \frac{1}{2}\int_0^t \pi_s \Sigma_b \Sigma_b^\top \pi_s^\top ds + \sum\nolimits_{k=1}^{n-d} \int_0^t \ln(1+\pi_s \Sigma_{qk} Y_k) dN_{k,s},$$
$$\eta_t = \exp\left\{\int_0^t [r + \pi_s(b - r\mathbf{1}_n)]ds + \xi_t\right\},$$
$$V_t = \eta_t \left[\int_0^t \frac{W_s(\nu)(\delta(\nu)+\pi_s\nu)}{\eta_s} ds\right].$$

Note that by a Itō's lemma,

$$d\eta_t = \eta_t\{[\delta(\nu) + \pi_t\nu + r + \pi_t(b - r\mathbf{1}_n)]dt + \pi_t \Sigma_b dB_t^S\} + \eta_{t-} \sum\nolimits_{k=1}^{n-d} \int_0^t \pi_t \Sigma_{qk} Y_k dN_{k,t}.$$

Then, applying Itō's lemma, we can verify that V_t solves the equation (B.1.1) and hence that $V_t = \widetilde{W}_t$ since (B.1.1) has an unique solution by Theorem 9.1 of Ikeda and Watanabe (1981). As a result, $\widetilde{W}_t = V_t \geq 0$ since $\delta(\nu) + \pi_s\nu \geq 0$ for $\pi \in K$ and $\eta_t \geq 0$, implying $\mathbb{E}\left[U(W_T^{c,\pi}(\nu))\right] \geq \mathbb{E}\left[U(W_T^{c,\pi})\right]$. Consequently,

$$\begin{aligned} J(0, W_0, X_0) =& \max_{(c,\pi)\in\mathcal{A}(w_0)} \mathbb{E}\left[\int_0^t e^{-\beta t} U(c_t)dt + \alpha e^{-\beta T} U(W_T)\right] \\ \leq& \max_{(c,\pi)\in\mathcal{A}_\nu(w_0)} \mathbb{E}\left[\int_0^t e^{-\beta t} U(c_t)dt + \alpha e^{-\beta T} U(W_T^\pi(\nu))\right] \\ =& J^{(\nu)}(0, W_0, X_0). \end{aligned} \tag{B.1.2}$$

On the other hand, by assumption, we know $\pi^* \in K$ and $\delta(\nu^*) + \pi^*\nu^* = 0$, and therefore, $J^{(\nu^*)}(0, W_0, X_0) \leq J(0, W_0, X_0)$, indicating $J^{(\nu^*)}(0, W_0, X_0) = J(0, W_0, X_0)$ by (B.1.2). Thus, π^* is an optimal portfolio strategy for the original market $\mathcal{M}$, completing the proof of the first result.

We now turn to the proof of the second conclusion. Let $\widetilde{\nu^*}$ be an optimal solution to the optimization problem in Proposition 3.1. If we can show $\delta(\widetilde{\nu^*}) + \pi^*\widetilde{\nu^*} = 0$, then $\widetilde{\nu^*}$ is a

desired vector in Proposition 3.1 by the proof of the result above. From the definition of $\delta(\widetilde{\nu^*})$, we have $\delta(\widetilde{\nu^*}) + \pi^*\widetilde{\nu^*} \geq 0$ since $\pi^* \in K$. We use ν^* to denote the optimal vector obtained in Proposition 3.1. From the proof of the sufficient condition of Proposition 3.1, we have

$$\begin{aligned} J(0, W_0, X_0) &= \max_{(c,\pi)\mathcal{A}(w_0)} \mathbb{E}\left[\int_0^T e^{-\beta t} U(c_t)dt + \alpha e^{-\beta T} U(W_T)\right] \\ &= J^{(\nu^*)}(0, W_0, X_0) \\ &\leq J^{(\nu)}(0, W_0, X_0) \\ &= \max_{(c,\pi)\in\mathcal{A}_\nu(w_0)} \mathbb{E}\left[\int_0^T e^{-\beta t} U(c_t)dt + \alpha e^{-\beta T} U(W_T^\pi(v))\right], \end{aligned}$$

for $\nu \in \widetilde{K}$. More specifically,

$$\begin{aligned} &J(0, W_0, X_0) \\ &\quad = \max_{(c,\pi)\in\mathcal{A}(w_0)} E\left[\int_0^T e^{-\beta t} U(c_t)dt + \alpha e^{-\beta T} U(W_T)\right] \\ &\quad = J^{(\nu^*)}(0, W_0, X_0) \\ &\quad = J^{(\nu)}(0, W_0, X_0) \qquad \text{, if } \delta(v) + \pi^*\nu = 0; \end{aligned}$$

and

$$\begin{aligned} &J(0, W_0, X_0) \\ &\quad = \max_{(c,\pi)\in\mathcal{A}(w_0)} E\left[\int_0^T e^{-\beta t} U(c_t)dt + \alpha e^{-\beta T} U(W_T)\right] \\ &\quad = J^{(\nu^*)}(0, W_0, X_0) \\ &\quad < J^{(\nu)}(0, W_0, X_0) \qquad \text{, if } \delta(v) + \pi^*\nu > 0. \end{aligned}$$

As a result, ν^* is an optimal solution to the optimization problem and $\delta(\widetilde{\nu^*}) + \pi^*\widetilde{\nu^*} = 0$ since, by assumption, $\widetilde{\nu^*}$ solves the optimization problem, completing the proof.

B.2 Proof of Proposition 3.2

We prove Proposition 3.2 by adapting the method in Appendix A of Cvitanic and Karatzas (1992) to the jump-diffusion model. Unlike their proof, we do not use the exponential martingale defined by (2.8) in Cvitanic and Karatzas (1992) as there are infinitely many exponential martingales in the jump-diffusion model. For illustrative convenience, we consider the case $A_k = (-1, 0)$. Given the optimal portfolio π^* in $\mathcal{M}$, we consider the martingale

$$M_t = \mathbb{E}\left[W_T^{\pi^*} U'(W_T^{\pi^*})|\mathcal{F}_t\right] \tag{B.2.1}$$

In particular, $M_T = W_T^{\pi^*} U'(W_T^{\pi^*})$. Applying the martingale representation theorem, we have

$$M_t = y_0 + \int_0^t \varphi(s) dB_s^S + \int_0^t \int \psi(s, z) dq(s, dz) \tag{B.2.2}$$

for some predictable φ and ψ, where $y_0 = \mathbb{E}[M_T]$, where

$$q(s, dz) = (q_1(dt, dz), ..., q_{n-d}(dt, dz))$$

and $q_k(dt, dz) = dN_{k,t} - \lambda_k \Phi_k(t, dz)dt$ is the compensated Poisson process. Taking an arbitrary portfolio strategy $\pi \in \mathcal{A}(w_0)$ and a number $0 < \varepsilon < 1$, we define a perturbed

strategy $\pi_t^{(\varepsilon)}$ of π^* as

$$\pi_t^{(\varepsilon)} = \begin{cases} (1-\varepsilon)\pi_t^* + \varepsilon\pi_t \triangleq \widetilde{\pi}_t^{(\varepsilon)}, & 0 \le t \le \tau_n \\ \\ \pi_t^*, & \tau_n < t \le T \end{cases}$$

for every $n \in \mathbb{N}$. Here τ_n is a stopping time to be defined below. The corresponding wealth process $W_t^{\pi^{(\varepsilon)}}$ satisfies the equation (3.3) in Section 3.2. Then, applying Itō's Lemma to the equation (3.3) and function $\ln[W_t^{\pi^{(\varepsilon)}}]$, the wealth process $W_t^{\pi^{(\varepsilon)}}$ can be rewritten as

$$\begin{aligned} W_t^{\pi^{(\varepsilon)}} =& W_0 \exp\left\{ \int_0^t \left[r + \pi_s^{(\varepsilon)}(b - r\mathbf{1}_n) - \frac{1}{2}\pi_s^{(\varepsilon)}\Sigma_b\Sigma_b^\top(\pi_s^{(\varepsilon)})^\top \right] ds + \int_0^t \pi_s^{(\varepsilon)}\Sigma_b dB_s^S \right. \\ & \left. + \sum\nolimits_{k=1}^{n-d} \int_0^t \ln(1 + \pi_s^{(\varepsilon)}\Sigma_{qk}Y_k) dN_{k,s} \right\} \\ =& W_t^{\pi^*} \exp\left\{ \varepsilon \int_0^{t\wedge\tau_n} \left[(\pi_s - \pi_s^*)(b - r\mathbf{1}_n - \Sigma_b\Sigma_b^\top \pi_s^{*\top}) \right] ds + \varepsilon \int_0^{t\wedge\tau_n} (\pi_s - \pi_s^*)\Sigma_b dB_s^S \right. \\ & + \sum\nolimits_{k=1}^{n-d} \int_0^{t\wedge\tau_n} \ln\left(\frac{1 + \widetilde{\pi}_s^{(\varepsilon)}\Sigma_{qk}Y_k}{1 + \pi_s^*\Sigma_{qk}Y_k} \right) dN_{k,s} \\ & \left. - \frac{1}{2}\varepsilon^2 \int_0^{t\wedge\tau_n} (\pi_s - \pi_s^*)\Sigma_b\Sigma_b^\top(\pi_s - \pi_s^*)^\top ds \right\} \end{aligned}$$

The stopping time τ_n above is defined as

$$\begin{aligned} \tau_n \triangleq T \wedge \inf\{ t \in [0,T]; & \left| \int_0^t \left[(\pi_s - \pi_s^*)(b - r\mathbf{1}_n - \Sigma_b\Sigma_b^\top \pi_s^{*\top}) \right] ds \right| \ge n \\ & \text{or } \left| \int_0^t (\pi_s - \pi_s^*)\Sigma_b dB_s^S \right| \ge n, \text{ or } N_{1,t} \ge n, \\ & \text{or } \widetilde{\pi}_t^{(\varepsilon)}\Sigma_{q1} \ge 1 - \frac{1}{n}, \text{or } \pi_t^*\Sigma_{q1} \ge 1 - \frac{1}{n}, ..., \\ & \text{or } N_{n-d,t} \ge n, \text{ or } \widetilde{\pi}_t^{(\varepsilon)}\Sigma_{q(n-d)} \ge 1 - \frac{1}{n}, \\ & \text{or } \pi_t^*\Sigma_{q(n-d)} \ge 1 - \frac{1}{n}. \Big\} \end{aligned}$$

Hence, by the same token as in (A.25), (A.26) and (A.27) of Cvitanic and Karatzas (1992), we apply the Dominated Convergence Theorem to obtain

$$\begin{aligned}\lim_{\varepsilon\downarrow 0}\frac{1}{\varepsilon}\mathbb{E}\left[U(W_T^{\pi^{(\varepsilon)}})-U(W_T^{\pi^*})\right] =&\mathbb{E}\left\{\lim_{\varepsilon\downarrow 0}\frac{1}{\varepsilon}\left[U(W_T^{\pi^{(\varepsilon)}})-U(W_T^{\pi^*})\right]\right\}\\ =&\mathbb{E}\left[U'(W_T)W_T L_{\tau_n}\right]\\ =&\mathbb{E}\left[M_T L_{\tau_n}\right], \end{aligned} \tag{B.2.3}$$

where

$$\begin{aligned}L_t=&\int_0^t\left[(\pi_s-\pi_s^*)(b-r\mathbf{1}_n-\Sigma_b\Sigma_b^\top\pi_s^{*\top})\right]ds+\int_0^t(\pi_s-\pi_s^*)\Sigma_b dB_s^S\\ &+\sum\nolimits_{k=1}^{n-d}\int_0^t\frac{(\pi_s-\pi_s^*)\Sigma_{qk}Y_k}{1+\pi_s^*\Sigma_{qk}Y_k}dN_{k,s}.\end{aligned} \tag{B.2.4}$$

Note that $E\left[M_T L_{\tau_n}\right]=E\left[M_{\tau_n}L_{\tau_n}\right]$ since M_t is a martingale and τ_n is a stopping time. Hence, applying Itō's Lemma to M_tL_t using (B.2.2) and (B.2.4), we have

$$\begin{aligned}E\left[M_{\tau_n}L_{\tau_n}\right]=&\mathbb{E}\left[\int_0^{\tau_n}M_t\left[(\pi_t-\pi_t^*)(b-r\mathbf{1}_n-\Sigma_b\Sigma_b^\top\pi_t^{*\top})\right]dt\right.\\ &+\sum\nolimits_{k=1}^{n-d}\int_0^{\tau_n}\int_{A_k}\frac{M_t(\pi_t-\pi_t^*)\Sigma_{qk}z}{1+\pi_t^*\Sigma_{qk}z}\lambda_k\Phi_k(t,dz)dt+\int_0^{\tau_n}(\pi_t-\pi_t^*)\Sigma_b\varphi^\top(t)dt\\ &\left.+\sum\nolimits_{k=1}^{n-d}\int_0^{\tau_n}\int_{A_k}\frac{\psi_k(t,z)(\pi_t-\pi_t^*)\Sigma_{qk}z}{1+\pi_t^*\Sigma_{qk}z}\lambda_k\Phi_k(t,dz)dt\right]\\ =&\mathbb{E}\int_0^{\tau_n}(\pi_t-\pi_t^*)M_t\Lambda_t dt\end{aligned} \tag{B.2.5}$$

where

$$\Lambda_t=b-r\mathbf{1}_n-\Sigma_b\Sigma_b^\top\pi_t^{*\top}+\Sigma_b\varphi^\top(t)/M_t+\sum\nolimits_{k=1}^{n-d}\int_{A_k}\frac{(1+\psi_k(t,z)/M_t)\Sigma_{qk}z}{1+\pi_t^*\Sigma_{qk}z}\lambda_k\Phi_k(t,dz)$$

On the other hand, as π^* is an optimal portfolio strategy in $\mathcal{M}$,

$$\lim_{\varepsilon\downarrow 0}\frac{1}{\varepsilon}\mathbb{E}\left[U(W_T^{\pi^{(\varepsilon)}})-U(W_T^{\pi^*})\right]\leq 0$$

implying

$$\mathbb{E}\left[\int_0^{\tau_n}(\pi_t-\pi_t^*)M_t\Lambda_t dt\right]\leq 0$$

due to (B.2.3) and (B.2.5). By the same argument as that in Cvitanic and Karatzas (1992), it follows that

$$(\pi_t-\pi_t^*)M_t\Lambda_t\leq 0,$$

and hence,

$$\delta(-\Lambda_t)\leq -\pi_t^*(-\Lambda_t),$$

implying $\delta(-\Lambda_t)=-\pi_t^*(-\Lambda_t)$. Let

$$B_\delta(t)=\exp\left[\int_0^t\left(r+\delta(-\Lambda_s)\right)ds\right].$$

Next we show that there exists a $\nu^*=(\nu_1^*,...,\nu_n^*)\in\widetilde{K}$ and a positive local martingale ξ_t such that

$$U'(W_T^{\pi^*})=B_\delta^{-1}(T)\xi_T \tag{B.2.6}$$

$$B_\delta^{-1}(t)\xi_t W_t^{\pi^*}\text{ is a martingale} \tag{B.2.7}$$

and for any portfolio strategy π in $\mathcal{A}_{\upsilon^*}(w_0)$,

$$B_\delta^{-1}(t)\xi_t W_t^{\pi}(\nu^*)\text{ is a supermartingale} \tag{B.2.8}$$

Then from (B.2.6), (B.2.7) and (B.2.8) we have

$$W_T^{\pi^*}=U'^{-1}(B_\nu^{-1}(T)\xi_T),$$

which yields

$$\mathbb{E}[B_\delta^{-1}(T)\xi_T W_T^{\pi^*}] = B_\delta^{-1}(0)\xi_0 W_0 = \xi_0 W_0,$$

and

$$\mathbb{E}[B_\delta^{-1}(T)\xi_T W_T^{\pi}(\nu^*)] \leq B_\delta^{-1}(0)\xi_0 W_0 = \xi_0 W_0,$$

for any $\pi \in \mathcal{A}_{\upsilon^*}(w_0)$. Note that from (4.6) in Karatzas et al. (1991),

$$U(U'^{-1}(y)) \geq U(x) + y(U'^{-1}(y) - x),\ \forall x > 0,\ y > 0.$$

Hence it follows that for any arbitrary portfolio strategy π in $\mathcal{A}_{\upsilon^*}(w_0)$,

$$\begin{aligned} E[U(W_T^{\pi^*})] &= \mathbb{E}[U(U'^{-1}(B_\delta^{-1}(T)\xi_T))] \\ &\geq \mathbb{E}[U(W_T^{\pi}(\nu^*))] + \mathbb{E}\left\{B_\delta^{-1}(T)\xi_T \cdot [U'^{-1}(B_\delta^{-1}(T)\xi_T) - W_T^{\pi}(\nu^*)]\right\} \\ &\geq \mathbb{E}[U(W_T^{\pi}(\nu^*))]. \end{aligned}$$

Therefore, π^* is an optimal portfolio rule in $\mathcal{M}_{\nu^*}$, finishing the proof of the necessary condition.

Proof of (B.2.6) and (B.2.7): Applying Itō's Lemma to equation (3.3) of Section 3.2, we have

$$\begin{aligned} d\left(\frac{1}{B_\delta^{-1}(t)W_t^{\pi^*}}\right) = \frac{1}{B_\delta^{-1}(t)W_t^{\pi^*}} \Big\{ &\left[\delta(-\Lambda_t) - \pi_t^*(b - r\mathbf{1}_n) + \pi_t^*\Sigma_b\Sigma_b^\top \pi_t^{*\top}\right] dt - \pi_t^*\Sigma_b dB_t^S \\ &- \sum\nolimits_{k=1}^{n-d} \frac{\pi_t^*\Sigma_q Y_k}{1 + \pi_t^*\Sigma_q Y_k} dN_{k,t} \Big\} \end{aligned}$$

Hence, based on (B.2.2) and the equation above, an application of the product rule to

$\frac{M_t}{B_\delta^{-1}(t)W_t^{\pi^*}}$ leads to the following equation

$$
\begin{aligned}
&d\left(\frac{M_t}{B_\delta^{-1}(t)W_t^{\pi^*}}\right) \\
&= \frac{M_t}{B_\delta^{-1}(t)W_t^{\pi^*}}\left(-\pi_t^*\Sigma_b dB_t^S + \frac{\varphi(t)}{M_t}dB_t^S + \sum\nolimits_{k=1}^{n-d}\frac{\psi_k(t,z)/M_t - \pi_t^*\Sigma_{qk}Y_k}{1+\pi_t^*\Sigma_{qk}Y_k}dq_k(t)\right) \\
&\quad + \frac{M_t}{B_\delta^{-1}(t)W_t^{\pi^*}}\left[\delta(-\Lambda_t) + \pi_t^*\left(-(b-r\mathbf{1}_n)\Sigma_b\Sigma_b^\top\pi_t^{*\top} - \Sigma_b\varphi^\top(t)/M_t\right.\right. \\
&\quad \left.\left. - \sum\nolimits_{k=1}^{n-d}\int_{A_k}\frac{(1+\psi_k(t,z)/M_t)\Sigma_{qk}z}{1+\pi_t^*\Sigma_{qk}z}\lambda_k\Phi_k(t,dz)dt\right)\right] \\
&= \frac{M_t}{B_\delta^{-1}(t)W_t^{\pi^*}}\left(-\pi_t^*\Sigma_b dB_t^S + \varphi(t)/M_t dB_t^S + \sum\nolimits_{k=1}^{n-d}\frac{\psi_k(t,z)/M_t - \pi_t^*\Sigma_{qk}Y_k}{1+\pi^*(t)\Sigma_{qk}Y_k}dq_k(t)\right)
\end{aligned}
\tag{B.2.9}
$$

with the last equality following from that

$$
\begin{aligned}
&-(b-r\mathbf{1}_n) + \Sigma_b\Sigma_b^\top\pi_t^{*\top} - \Sigma_b\varphi^\top(t)/M_t - \sum\nolimits_{k=1}^{n-d}\int_{A_k}\frac{(1+\psi_k(t,z)/M_t)\Sigma_{qk}z}{1+\pi_t^*\Sigma_{qk}z}\lambda_k\Phi_k(t,dz)dt \\
&= -\Lambda_t,
\end{aligned}
$$

and $\delta(-\Lambda_t) = -\pi_t^*(-\Lambda_t)$. As a result, $\frac{M_t}{B_\delta^{-1}(t)W_t^{\pi^*}}$ is a positive local martingale. Letting $\xi_t = \frac{M_t}{B_\delta^{-1}(t)W_t^{\pi^*}}$, we complete the proof of (B.2.6) since $W_T^{\pi^*}U'(W_T^{\pi^*}) = M_T$ due to (B.2.1). In particular, $B_\delta^{-1}(t)\xi_t W_t^{\pi^*} = M_t$ and is a martingale from (B.2.1), proving (B.2.7).

Proof of (B.2.8): From (3.5), for any portfolio strategy π in $\mathcal{A}_{\upsilon^*}(w_0)$, the corresponding wealth process $W_t^\pi(\nu^*)$ satisfies the equation

$$
\begin{aligned}
W_t^\pi(\nu^*) = W_0 &+ \int_0^t (r+\delta(-\Lambda_s))W_s^\pi(\nu^*)ds + \int_0^t W_s^\pi(\nu^*)\pi_s(\widetilde{b}-r\mathbf{1}_n)ds \\
&+ \int_0^t W_{\nu^*}^\pi(s)\pi_s\Sigma_b dB_s^S + \int_0^t W_{s-}^\pi(\nu^*)\pi_{s-}\Sigma_q(Y\bullet dN_s)
\end{aligned}
\tag{B.2.10}
$$

where $\widetilde{b} = (b_1(X_t),...,b_n(X_t))^\top - \Lambda_t$. Applying Itō's Lemma to the product of $B_\delta^{-1}(t)\xi_t$

and $W_t^{\pi}(\nu^*)$, we have

$$
\begin{aligned}
d[B_\delta^{-1}(t)\xi_t W_t^{\pi}(\nu^*)] = B_\delta^{-1}(t)\xi_t W_t^{\pi}(\nu^*)\pi_t \Bigg(& \left[\widetilde{b} - r\mathbf{1}_n - \Sigma_b \Sigma_b^{\top} \pi_t^{*\top} + \frac{\Sigma_b \varphi^{\top}(t)}{M_t}\right] \\
& + \sum\nolimits_{k=1}^{n-d} \int_{A_k} \frac{(1+\psi_k(t,z)/M_t)\Sigma_{qk} z}{1+\pi^*(t)\Sigma_{qk}(t) z} \lambda_k \Phi_k(t,dz)dt \Bigg) \\
& + B_\delta^{-1}(t)\xi_t W_t^{\pi}(\nu^*) \Bigg(-\pi_t^* \Sigma_b dB_t^S + \frac{\varphi(t)}{M_t} dB_t^S + \pi_t \Sigma_b dB_t^S \\
& + \sum\nolimits_{k=1}^{n-d} \left(\int_{A_k} \frac{\psi_k(t,z)/M_t(1+\pi\Sigma_{qk}Y_k)}{1+\pi^*(t)\Sigma_{qk}(t)Y_k} + \frac{(\pi\Sigma_{qk} - \pi_t^*\Sigma_{qk})Y_k}{1+\pi^*(t)\Sigma_{qk}(t)Y_k} dq_k(t) \right) \Bigg)
\end{aligned}
$$

Note that the drift term of the equation above is

$$
e^{-rt}\xi_t W_t^{\pi} \pi(t)(-\Lambda_t + \Lambda_t) = 0.
$$

Hence, we have

$$
\begin{aligned}
& d\left[B_\delta^{-1}(t)\xi_t W_t^{\pi}(\nu^*)\right] \\
& \quad = B_\delta^{-1}(t)\xi_t W_t^{\pi}(\nu^*)(-\pi_t^* \Sigma_b dB_t^S + \frac{\varphi(t)}{M_t} dB_t^S + \pi_t \Sigma_b dB_t^S \\
& \qquad + \sum\nolimits_{k=1}^{n-d} \left(\int_{A_k} \frac{\psi_k(t,z)/M_t(1+\pi\Sigma_{qk}Y_k)}{1+\pi_t^*\Sigma_{qk} z} + \frac{(\pi\Sigma_{qk} - \pi_t^*\Sigma_{qk})Y_k}{1+\pi_t^*\Sigma_{qk} z} dq_k(t) \right) \Bigg)
\end{aligned}
$$

which is a positive local martingale and thus, a supermartingale, proving (B.2.8).

B.3 Proof of Proposition 3.3

Before proving Proposition 3.3, we first extend Propositions 1 and 2 in Jin and Zhang (2012) to the proposed model by incorporating the intermediate consumption, but without investment constraints.

Lemma B.3.1. *The optimal consumption c^* and portfolio π^**

$= (\pi_1^*, ..., \pi_n^*)$ are given by

$$c^* = W f(X_t, t)^{-1}$$

$$\pi^* = \left(\widetilde{\pi}_{b1}^*, ..., \widetilde{\pi}_{bd}^*, \widetilde{\pi}_{q1}^*, ..., \widetilde{\pi}_{q(n-d)}^*\right) \Sigma^{-1}$$

where

$$(\widetilde{\pi}_{b1}^*, ..., \widetilde{\pi} i_{bd}^*)^\top = \frac{\theta_t^b(\nu)}{\gamma} + \rho_t \sigma^{x\top} \frac{f_X}{f}$$

and $\widetilde{\pi}_{qk}^*$ solves the following optimization problem:

$$\sup_{\widetilde{\pi}_{qk} \in F_k} D_k(\widetilde{\pi}_{qk}) = \left[\widetilde{\pi}_{qk}(\theta_k^q(\nu, t) - \lambda_k a_k + \frac{1}{1-\gamma}\lambda_k \int_{E_k} [(\widetilde{\pi}_{qk} z + 1)^{1-\gamma} - 1]\Phi_k(dz)\right] \quad \text{(B.3.1)}$$

for $k = 1, ..., n-d$.

Proof: This can be proved in the same manner as proof of Proposition 1 in Jin and Zhang (2012) since the consumption rate and portfolio strategy are independent variables in the HJB equation (3.4). To save space, we omit the proof.

Lemma B.3.2. *The optimal value function, $J(t, W_t, X_t)$, is given by*

$$J^{(\nu)}(t, W_t, X_t) = \frac{W_t^{1-\gamma}}{1-\gamma} f^\gamma(X_t, t)$$

where

$$f(X_t, t) = \int_t^T g(t, s)ds + \alpha g(t, T) \quad \text{(B.3.2)}$$

and

$$g(t,s) = E_t\left\{\exp\left[\frac{1-\gamma}{\gamma}(g_1(X_t,s)+g_2(X_t,s))\right]\right\}$$

with

$$g_1(X_t,s) = \int_t^s \theta_s^b(\nu)dB(s) + \frac{1}{2}\int_t^T ||\theta_s^b(\nu)||^2 ds$$
$$g_2(X_t,s) = \frac{1}{1-\gamma}\int_t^s [(1-\gamma)(r+\delta(\nu)+D(\widetilde{\pi}_q^*)) - \beta]ds$$

where $D(\widetilde{\pi}_q^*) = \sum_{k=1}^{n-d} D_k(\widetilde{\pi}_{qk}^*)$.

Proof. We follow the proof of Propositions 2 and 3 of Jin and Zhang (2012). For notational convenience, we consider the unconstrained portfolio choice problem, since the results for the constrained one can be obtained by modifying the interest rate and the drift terms of stock prices as in Section 3.2. Let $\mathbf{0}_d$ denote the $d \times 1$ vector with each element being zero, and let $\mathbf{1}_{n-d}$ denote the $(n-d)\times 1$ vector with each element being one. Note that

$$\Sigma^{-1}\Sigma^q = \begin{pmatrix} \mathbf{0}_d \\ \mathbf{1}_{n-d} \end{pmatrix}$$

and

$$\begin{aligned}\Sigma^{-1}(b - r\mathbf{1}_n) =& \Sigma^{-1}\left[b - r\mathbf{1}_n + \Sigma_q(\lambda \bullet a)\right] - \Sigma^{-1}\Sigma_q(\lambda \bullet a) \\ =& \begin{pmatrix} \theta^b \\ \theta^q \end{pmatrix} - \begin{pmatrix} \mathbf{0}_d \\ \mathbf{1}_{n-d} \end{pmatrix}(\lambda \bullet a) \\ =& \begin{pmatrix} \theta^b \\ \theta^q - \lambda \bullet a \end{pmatrix}\end{aligned}$$

Hence,

$$\begin{aligned}\pi(b - r\mathbf{1}) &= \pi\Sigma\Sigma^{-1}(b - r\mathbf{1}_n) \\ &= (\pi\Sigma_b, \pi\Sigma_q)\begin{pmatrix}\theta^b \\ \theta^q - \lambda \bullet a\end{pmatrix} \\ &= \pi\Sigma_b\theta^b + \pi\Sigma_q(\theta^q - \lambda \bullet a)\end{aligned}$$

Plugging the equation above and $WJ_W = (1-\gamma)J$ into (3.4) gives

$$\begin{aligned}\beta J =& \max_{c,\pi}\left\{\frac{c^{1-\gamma}}{1-\gamma} + J_t + \frac{1}{2}W^2\pi\Sigma_b\Sigma_b^\top\pi^\top J_{WW} + \left[W(\pi\Sigma_b\theta^b + r) - c\right]J_W + b^x J_X\right. \\ &+ W\pi\Sigma_b\rho_t\sigma^{x\top}J_{WX} + \frac{1}{2}Tr(\sigma^x\sigma^{x\top}J_{XX^\top}) + W\pi\mathbf{\Sigma}_q\,(\theta^q - \lambda\bullet\alpha)J_W \\ &\left.+ \sum_{k=1}^{n-d}\lambda_k\int_{A_k}[J(W + W\pi\mathbf{\Sigma}_{qk}z) - J(W)]\Phi_k(dz)\right\} \\ =& \max_{c,\widetilde{\pi}_b}\left\{\frac{c^{1-\gamma}}{1-\gamma} + J_t + \frac{1}{2}W^2\widetilde{\pi}_b\widetilde{\pi}_b^\top J_{WW} + [W(\widetilde{\pi}_b\theta^b + r) - c]J_W + b^x J_X\right. \\ &+ W\widetilde{\pi}_b\rho_t\sigma^{x\top}J_{WX} + \frac{1}{2}Tr(\sigma^x\sigma^{x\top}J_{XX^\top}) \\ &\left.+ \left[(1-\gamma)\sum_{k=1}^{n-d}\widetilde{\pi}_{qk}^*(\theta_k^q - \lambda_k\alpha_k) + \lambda_k\int_{A_k}[(1+\widetilde{\pi}_{qk}^*z)^{1-\gamma} - 1]\Phi_k(dz)\right]J\right. \\ =& \max_{c,\widetilde{\pi}_b}\left\{\frac{c^{1-\gamma}}{1-\gamma} + J_t + \frac{1}{2}W^2\widetilde{\pi}_b\widetilde{\pi}_b^\top J_{WW} + \left[W(\widetilde{\pi}_b\theta^b(\nu) + r) - c\right]J_W + b^x J_X\right. \\ &\left.+W\widetilde{\pi}_b\rho_t\sigma^{x\top}J_{WX} + \frac{1}{2}Tr(\sigma^x\sigma^{x\top}J_{XX^\top}) + (1-\gamma)D(\widetilde{\pi}_q^*)J\right\}\end{aligned}$$

This is the HJB equation of the indirect value function of the portfolio choice problem with the expected utility function given by

$$E\left[\int_0^T e^{\int_0^t[(1-\gamma)D(\widetilde{\pi}_q^*)-\beta]du}\frac{c_t^{1-\gamma}}{1-\gamma}dt + \alpha\exp\left\{\int_0^T[(1-\gamma)D(\widetilde{\pi}_q^*) - \beta]dt\right\}\frac{W_T^{1-\gamma}}{1-\gamma}\right],$$

and stock prices given by Proposition 2 in Jin and Zhang (2012).

We will use a result in Karatzas et al. (1987) in the proof. To this end, define the Radon-Nikodym martingale Z as

$$Z_t = \exp\left\{-\int_0^t \theta^b dB_s^S - \frac{1}{2}\int_0^t ||\theta^b||^2 ds\right\}$$

As in Karatzas et al. (1987), we define a process ζ related to Z, which determines the optimal wealth in the pure-diffusion economy. The process ζ is given by:

$$\zeta_t = Z_t \exp\left\{-\int_0^t [(1-\gamma)D(\widetilde{\pi}_q^*) - \beta + r]ds\right\}$$

Let $Z_{t,T} = Z_T/Z_t$ and $\zeta_{t,T} = \zeta_T/\zeta_t$. By Theorem 5.2 in Karatzas et al. (1987), given $t \in [0,T]$, the optimal consumption and terminal wealth in the pure-diffusion economy are

$$c_{t,s}^* = y^{-\frac{1}{\gamma}}\zeta_{t,s}^{-\frac{1}{\gamma}}, \qquad W_{t,T}^* = \alpha^{\frac{1}{\gamma}} y^{-\frac{1}{\gamma}}\zeta_{t,T}^{-\frac{1}{\gamma}}$$

where $s \in [t,T]$ and y satisfies

$$\mathbb{E}_t\left(\int_t^T e^{-r(s-t)} Z_{t,s} c_{t,s}^* ds + e^{-r(T-t)} Z_{t,T} W_{t,T}^*\right) = W_t$$

From the equation above, we can obtain y as

$$\begin{aligned} y =& W_t^{-\gamma}\left[\mathbb{E}_t\left(\int_t^T e^{\frac{1}{\gamma}\int_t^s [(1-\gamma)D(\widetilde{\pi}_q^*) - \beta + (1-\gamma)r]du} Z_{t,s}^{1-\frac{1}{\gamma}} ds\right.\right. \\ &\left.\left. + \alpha^{\frac{1}{\gamma}} e^{\frac{1}{\gamma}\int_t^T [(1-\gamma)D(\widetilde{\pi}_q^*) - \beta + (1-\gamma)r]ds} Z_{t,T}^{1-\frac{1}{\gamma}}\right)\right]^{\gamma} \\ =& W_t^{-\gamma} f^{\gamma}(t, X_t) \end{aligned}$$

so the optimal consumption and terminal wealth can be rewritten as

$$c_{t,s}^* = W_t \zeta_{t,s}^{-\frac{1}{\gamma}} f(t,X_t)^{-1}, \quad W_{t,T}^* = W_t \zeta_{t,T}^{-\frac{1}{\gamma}} f(t,X_t)^{-1}$$

As a result, the optimal expected utility function can be evaluated as

$$\begin{aligned}
&J(t,W_t,X_t)\\
&\quad=\mathbb{E}_t\left[\int_t^T e^{\int_t^s[(1-\gamma)D(\widetilde{\pi}_q^*)-\beta]du}\frac{(c_{t,s}^*)^{1-\gamma}}{1-\gamma}ds\right.\\
&\qquad\left.+\alpha\exp\left\{\int_t^T[(1-\gamma)D(\widetilde{\pi}_q^*)-\beta]ds\right\}\frac{(W_{t,T}^*)^{1-\gamma}}{1-\gamma}\right]\\
&\quad=\frac{W_t^{1-\gamma}}{1-\gamma}f^\gamma(t,X_t).
\end{aligned}$$

Therefore, (B.3.2) follows from the definition of $Z_{t,T}$, completing the proof. ■

We now turn to the proof of Propositions 3.3. In the current model, there is no intermediate consumption and no state variables X_t by assumption. According to Lemma B.3.2, the indirect value function in the market $\mathcal{M}_v$ is given by

$$\begin{aligned}
J^{(\nu)}(t,W_t)=&\frac{W_t^{1-\gamma}}{1-\gamma}\left[E_t\left(\exp\left\{\frac{1}{\gamma}\int_t^T[(1-\gamma)(r+\delta(v))\right.\right.\\
&\left.\left.+\ (1-\gamma)D(\widetilde{\pi}_q)-\beta]ds\right\}\exp\left[\frac{1-\gamma}{\gamma}g_1\right]\right)\right]^\gamma. \qquad \text{(B.3.3)}
\end{aligned}$$

Note that $\exp\left[\frac{1-\gamma}{\gamma}g_1\right]$ can be rewritten as

$$\begin{aligned}
\exp\left[\frac{1-\gamma}{\gamma}g_1\right]&=\exp\left\{-\left(1-\frac{1}{\gamma}\right)\int_t^T\theta_s^b(\nu)dB_s^S-\frac{1}{2}\left(1-\frac{1}{\gamma}\right)\int_t^T||\theta_s^b(\nu)||^2ds\right\}\\
&=\exp\left\{-\left(1-\frac{1}{\gamma}\right)\int_t^T\theta_s^b(\nu)dB_s^S-\frac{1}{2}\left(1-\frac{1}{\gamma}\right)^2\int_t^T||\theta_s^b(\nu)||^2ds\right.\\
&\qquad\left.-\frac{1}{2\gamma}\left(1-\frac{1}{\gamma}\right)\int_t^T||\theta_s^b(\nu)||^2ds\right\},
\end{aligned}$$

and

$$E_t\left[\exp\left\{-\left(1-\frac{1}{\gamma}\right)\int_t^T\theta_s^b(\nu)dB_s^S-\frac{1}{2}\left(1-\frac{1}{\gamma}\right)^2\int_t^T||\theta_s^b(\nu)||^2ds\right\}\right]=1.$$

Hence,

$$J^{(\nu)}(t,W_t)=\frac{W_t^{1-\gamma}}{1-\gamma}\exp\left\{-\frac{1}{2}\left(1-\frac{1}{\gamma}\right)\int_t^T||\theta_s^b(\nu)||^2ds \right.$$
$$\left.+\int_t^T(1-\gamma)\left[(r+\delta(v))+\sum_{k=1}^d D_k(\widetilde{\pi}_{qk}^*)\right]ds-\beta(T-t)\right\}.$$

since there are no state variables. According to Proposition 3.2, the optimal ν^* solves the following minimization problem

$$\inf_{\nu\in\widetilde{K}} J^{(\nu)}(t,W_t),$$

which is equivalent to

$$\inf_{\nu\in\widetilde{K}}\left[\frac{1}{2\gamma}||\theta_s^b(\nu)||^2+\delta(\nu)+\sum_{k=1}^d D_k(\widetilde{\pi}_{qk}^*)\right].$$

On the other hand, by Lemma B.3.1, in the market M_ν, $\widetilde{\pi}_{qk}^*$ solves the maximization problem given below,

$$\max_{\widetilde{\pi}_{qk}\in F_k} D_k(\widetilde{\pi}_{qk}),$$

implying $\widetilde{\pi}_q^*=(\widetilde{\pi}_{q1}^*,...,\widetilde{\pi}_{q(n-d)}^*)$ maximizes $\sum_{k=1}^d D_k(\widetilde{\pi}_{qk})$. As a result, we have

$$\inf_{\nu\in\widetilde{K}}\left[\frac{1}{2\gamma}||\theta_s^b(\nu)||^2+\delta(\nu)+\sum_{k=1}^d D_k(\widetilde{\pi}_{qk}^*)\right]$$
$$=\inf_{\nu\in\widetilde{K}}\sup_{\widetilde{\pi}_{qk}\in F_k,k=1,...,n-d}\left[\frac{1}{2\gamma}||\theta_s^b(\nu)||^2+\delta(\nu)+\sum_{k=1}^{n-d} D_k(\widetilde{\pi}_{qk})\right].$$

completing the proof.

B.4 Proof of Proposition 3.4

We now rewrite the relative risk premium defined in Section 3.3 as

$$\begin{aligned}\theta_t(\nu) &= \begin{pmatrix} \theta_t^b(\nu) \\ \\ \theta_t^q(\nu) \end{pmatrix} \\ &= \Sigma^{-1}[b - r\mathbf{1_n} + \Sigma_q(\lambda \bullet a)] + \Sigma^{-1}\mathbf{1_n}\nu_1 \\ &= \begin{pmatrix} \theta_t^b \\ \\ \theta_t^q + \lambda \bullet a \end{pmatrix} + \begin{pmatrix} a^b(t) \\ \\ a^q(t) \end{pmatrix} \nu_1. \end{aligned} \tag{B.4.1}$$

Thus, (3.11) can be obtained by applying Proposition 3.3 with $\theta_t^b(\nu)$ and $\theta_t^q(\nu)$ given by (B.4.1), completing the proof.

B.5 Solving the optimization problem

We apply Proposition 3.1 to solve the portfolio choice problems in the numerical example in Section 3.4. For this, we define

$$\begin{aligned}\mu &= (\mu_1, \mu_2, \mu_3, \mu_4)' \\ &= (0.2683, 0.2956, 0.4661, 0.6317)\end{aligned}$$

$$\Sigma^z = \begin{pmatrix} \sigma^z_{11} & \sigma^z_{12} & \sigma^z_{13} & \sigma^z_{14} \\ \sigma^z_{21} & \sigma^z_{22} & \sigma^z_{23} & \sigma^z_{24} \\ \sigma^z_{31} & \sigma^z_{32} & \sigma^z_{33} & \sigma^z_{34} \\ \sigma^z_{41} & \sigma^z_{42} & \sigma^z_{43} & \sigma^z_{44} \end{pmatrix} = \begin{pmatrix} 0.0427 & 0.0431 & 0.0336 & 0.0735 \\ 0.0626 & 0.0380 & 0.0437 & 0.0850 \\ 0.1331 & 0.0490 & 0.0412 & 0.0866 \\ 0.1304 & 0.1317 & 0.0540 & 0.1084 \end{pmatrix}$$

$$\Sigma^q = \begin{pmatrix} \sigma^q_{11} & \sigma^q_{12} \\ \sigma^q_{21} & \sigma^q_{22} \\ \sigma^q_{31} & \sigma^q_{32} \\ \sigma^q_{41} & \sigma^q_{42} \end{pmatrix} = \begin{pmatrix} 0.5592 & 0.6893 \\ 0.9385 & 0.7668 \\ 0.5509 & 0.5677 \\ 0.6787 & 0.8168 \end{pmatrix}.$$

The values of Σ^z, Σ^q and μ are given according to Table 3.1. We can also compute the correlation matrix of all assets as

$$\widetilde{\Sigma} = \begin{pmatrix} 1.0000 & 0.9884 & 0.0336 & 0.0735 \\ 0.9884 & 1.0000 & 0.0437 & 0.0850 \\ 0.8984 & 0.9389 & 0.0412 & 0.0866 \\ 0.9398 & 0.9281 & 0.0540 & 0.1084 \end{pmatrix}.$$

In fact, Table 3.1 provides all the 32 parameters used in the numerical example. We introduce two fictitious stocks with prices driven by the positive and negative jumps

respectively. Therefore, there are six risky assets in the new market while the investor is prohibited to trade the two fictitious stocks. The coefficient matrix of diffusions and jumps and its inverse can be written as

$$\Sigma = \begin{pmatrix} \Sigma^z & \Sigma^q \\ 0_{4\times 2} & I_{2\times 2} \end{pmatrix}$$

$$\Sigma^{-1} = \begin{pmatrix} (\Sigma^z)^{-1} & -(\Sigma^z)^{-1}\Sigma^q \\ 0_{4\times 2} & I_{2\times 2} \end{pmatrix}$$

We let $\nu = (\nu_1, ..., \nu_6)'$ where $\widetilde{\nu}_1 = (\nu_1, \nu_2, \nu_3, \nu_4) \geq 0$ are the variables associated with the short-selling constraints and $\widetilde{\nu}_2 = (\nu_5, \nu_6)$ are the variables associated with the no-trading constraint of the two fictitious stocks. The optimal portfolio weight $\pi = (\pi_1, ..., \pi_6)'$, optimal diffusion exposure $\widetilde{\pi}^b = (\widetilde{\pi}^b_1, \widetilde{\pi}^b_2, \widetilde{\pi}^b_3, \widetilde{\pi}^b_4)'$ and jump exposure $\widetilde{\pi}^q = (\widetilde{\pi}^q_1, \widetilde{\pi}^q_2)'$ in the market $\mathcal{M}_\nu$ are given by Lemma B.3.1 in Appendix B.3. In particular,

$$\widetilde{\pi}_b = (\Sigma^z)^{-1}(\mu + \widetilde{\nu}_1 - r\mathbf{1}_4 - \Sigma^q(\widetilde{\nu}_2 - r\mathbf{1}_2))/\gamma \tag{B.5.1}$$

$$(\pi_1, \pi_2, \pi_3, \pi_4) = \widetilde{\pi}'_b(\Sigma^z)^{-1}. \tag{B.5.2}$$

In order to solve the optimal portfolio in the original market, we present some conditions. First, the no-trading constraint $\pi_5 = \pi_6 = 0$ leads to the condition

$$\widetilde{\pi}_q = (\widetilde{\pi}_{q1}, \widetilde{\pi}_{q2}) = \widetilde{\pi}'_b(\Sigma^z)^{-1}\Sigma^q. \tag{B.5.3}$$

Second, the condition $\delta(\nu) + \pi'\nu = 0$ in Proposition 3.1 and (B.5.2) implies

$$\widetilde{\pi}'_b(\Sigma^z)^{-1}\widetilde{v}'_1 = 0, \tag{B.5.4}$$

since $\delta(\nu) = 0, \pi_5 = \pi_6 = 0$. Third, we have the short-selling constraint

$$(\pi_1, \pi_2, \pi_3, \pi_4) = \widetilde{\pi}_b'(\Sigma^z)^{-1} \geq 0. \tag{B.5.5}$$

Fourth, the optimization problem in Lemma B.3.1 of Appendix B.3 gives two first-order conditions below

$$\nu_5 - r + \frac{\lambda_u}{\eta_u} \int_0^\infty z(1 + \widetilde{\pi}_{q1} z)^{-\gamma} (1+z)^{-\frac{1}{\eta_u}-1} dz = 0. \tag{B.5.6}$$

$$\nu_6 - r + \frac{\lambda}{\eta_d} \int_{-1}^0 z(1 + \widetilde{\pi}_{q2} z)^{-\gamma} (1+z)^{\frac{1}{\eta_d}-1} dz = 0. \tag{B.5.7}$$

By setting $\widetilde{\nu}_1 = 0$ in (B.5.1), the short-selling constraint is removed. It seems that we need to use a numerical algorithm to solve the constrained optimization problem stated above; however, conditions $(B.5.3)$ to $(B.5.7)$ together are equivalent to a system of equations. More precisely, the i-th element of $\widetilde{\nu}_1$ must be zero if the corresponding element of $\widetilde{\pi}_b'(\Sigma^z)^{-1}$ is non-zero. Hence, all the parameters including $\widetilde{\nu}_1$ and $\widetilde{\pi}_q$ can be seen as inexplicit functions of λ, which are easily solvable in a numerical sense. For example, we use the Trust-Region Dogleg Method and the detail of this algorithm can be found in Nocedal and Wright (2006). When dealing with the case without the short-selling constraint, π_q can be solved by using (B.5.1) to (B.5.5) given $\widetilde{\nu}_1 = 0$.

Appendix C

C.1 Estimation method and the optimal estimates

Table 5.1: *The optimal estimates of the Size portfolios*

μ	0.2531	0.2547	0.2437	0.2394	0.1948
Σ_b^0	0.0254	0.0664	0.0249	0.0669	0.1042
	0.0392	0.0749	0.0555	0.0899	0.0676
	0.0745	0.0786	0.0446	0.0632	0.0631
	0.0588	0.0740	0.0788	0.0476	0.0546
	0.0812	0.0154	0.0869	0.0396	0.0498
Σ_q^0	0.6249	0.6674	0.6411	0.6893	0.6244
	1.0460	1.0256	0.9686	0.9704	0.8350
η	0.0878	0.0210			
λ	0.0540	8.8976			

Table 5.2: *The optimal estimates of the Book-to-Market portfolios*

μ	0.2363	0.2306	0.2455	0.2559	0.2858
Σ_b^0	0.0662	0.0527	0.0286	0.0315	0.1059
	0.0597	0.0478	0.0750	0.0397	0.0609
	0.0420	0.0293	0.0574	0.0789	0.0496
	0.0266	0.0751	0.0441	0.0643	0.0294
	0.0865	0.0662	0.0231	0.0738	0.0066
Σ_q^0	0.9437	0.8712	1.0042	1.0826	1.1040
	1.1117	1.0286	1.1086	1.0921	1.1704
η	0.0366	0.0130			
λ	0.6500	15.1344			

Table 5.3: *The optimal estimates of the Industry portfolios*

μ	0.2344	0.2668	0.2630	0.2745	0.2478
Σ_b^0	0.0186	0.0406	0.0826	0.0387	0.1057
	0.0199	0.0333	0.0173	0.1119	0.0629
	0.1136	0.0078	0.0947	0.0783	0.0383
	0.0044	0.1109	0.0908	0.0677	0.0078
	0.0868	0.1012	0.0275	0.0394	0.1104
Σ_q^0	1.0369	0.9077	1.0675	0.9625	1.4203
	1.4300	1.7977	1.8122	1.7398	1.5387
η	0.1207	0.0067			
λ	0.0035	17.3857			

Table 5.4: *The optimal estimates of the International portfolios*

μ	0.2849	0.2242	0.3944	0.3860	0.4599
Σ_b^0	0.0397	0.0575	0.0220	0.1323	0.0173
	0.0129	0.0164	0.0712	0.0055	0.1536
	0.1554	0.0455	0.0598	0.0759	0.0295
	0.1060	0.1192	0.0298	0.0428	0.0110
	0.0505	0.0677	0.1532	0.0339	0.0070
Σ_q^0	0.5578	0.4160	0.6462	0.7672	0.7738
	0.6068	0.5321	0.8042	0.7938	0.8054
η	0.1012	0.0317			
λ	0.1057	15.0044			

Table 5.5: *Comparison of moments for the Size portfolios*

	data	model		data	model					
mean	0.0012	0.0012	kurtosis	9.1567	9.1853					
	0.0014	0.0014		8.4552	8.4310					
	0.0013	0.0014		7.9922	8.0219					
	0.0013	0.0013		9.3103	9.3036					
	0.0009	0.0009		7.8203	7.8258					
			data			model				
covariance (1e-3)	0.5891	0.5860	0.5391	0.5049	0.4017	0.5950	0.5802	0.5427	0.5070	0.4007
	0.5860	0.6314	0.5890	0.5583	0.4565	0.5802	0.6365	0.5940	0.5557	0.4611
	0.5391	0.5890	0.5766	0.5506	0.4615	0.5427	0.5940	0.5813	0.5487	0.4569
	0.5049	0.5583	0.5506	0.5532	0.4733	0.5070	0.5557	0.5487	0.5587	0.4723
	0.4017	0.4565	0.4615	0.4733	0.4743	0.4007	0.4611	0.4569	0.4723	0.4790

Table 5.6: *Comparison of moments for the Book-to-Market portfolios*

	data	model		data	model					
mean	0.0008	0.0008	kurtosis	6.8551	6.8034					
	0.0010	0.0010		6.9999	6.8986					
	0.0011	0.0011		10.1411	10.1178					
	0.0014	0.0014		12.2853	12.3028					
	0.0017	0.0017		9.8706	9.9028					
			data					model		
covariance (1e-3)	0.5784	0.4795	0.4452	0.4157	0.4451	0.5837	0.4814	0.4496	0.4196	0.4411
	0.4795	0.4753	0.4439	0.4153	0.4452	0.4814	0.4773	0.4483	0.4194	0.4496
	0.4452	0.4439	0.4733	0.4288	0.4551	0.4496	0.4483	0.4780	0.4331	0.4596
	0.4157	0.4153	0.4288	0.4499	0.4602	0.4196	0.4194	0.4331	0.4540	0.4648
	0.4451	0.4452	0.4551	0.4602	0.5519	0.4411	0.4496	0.4596	0.4648	0.5575

Table 5.7: *Comparison of moments for the Industry portfolios*

	data	model		data	model					
mean	0.0013	0.0013	kurtosis	10.0408	10.0399					
	0.0011	0.0011		9.6528	9.6382					
	0.001	0.001		7.1687	7.1722					
	0.0014	0.0014		7.1045	7.1063					
	0.0013	0.0013		14.1856	14.187					
			data					model		
covariance	0.4926	0.3802	0.4426	0.4045	0.4954	0.4975	0.3765	0.4467	0.4005	0.4905
	0.3802	0.4775	0.4229	0.3811	0.4435	0.3765	0.4728	0.4271	0.378	0.4391
	0.4426	0.4229	0.7088	0.4234	0.516	0.4467	0.4271	0.7098	0.4193	0.5108
	0.4045	0.3811	0.4234	0.6133	0.4459	0.4005	0.378	0.4193	0.6194	0.4415
	0.4954	0.4435	0.516	0.4459	0.7137	0.4905	0.4391	0.5108	0.4415	0.7208

Table 5.8: *Comparison of moments for the International portfolios*

	data	model		data	model					
mean	0.0002	0.0002	kurtosis	10.2485	10.2345					
	-0.0003	-0.0003		5.3548	5.6195					
	0.0006	0.0006		10.0359	10.052					
	0.0006	0.0006		15.1055	15.0732					
	0.0019	0.0019		14.2540	14.1950					
				data				model		
covariance	0.0007	0.0004	0.0008	0.0007	0.0006	0.0007	0.0004	0.0007	0.0007	0.0006
	0.0004	0.0008	0.0005	0.0005	0.0006	0.0004	0.0008	0.0005	0.0004	0.0006
	0.0008	0.0005	0.0012	0.0011	0.0009	0.0007	0.0005	0.0012	0.0011	0.0009
	0.0007	0.0005	0.0010	0.0011	0.0009	0.0007	0.0004	0.0010	0.0010	0.0009
	0.0006	0.0006	0.0009	0.0009	0.0011	0.0006	0.0006	0.0009	0.0009	0.0011